Science
AAAS

Supplementary Materials for

Chemical remodeling of a cellular chaperone to target the active state of mutant KRAS

Christopher J. Schulze[1†], Kyle J. Seamon[1†], Yulei Zhao[2†], Yu C. Yang[1], Jim Cregg[4], Dongsung Kim[2], Aidan Tomlinson[4], Tiffany J. Choy[1], Zhican Wang[5], Ben Sang[2], Yasin Pourfarjam[2], Jessica Lucas[2], Antonio Cuevas-Navarro[2], Carlos Ayala Santos[2], Alberto Vides[2], Chuanchuan Li[2], Abby Marquez[4], Mengqi Zhong[4], Vidyasiri Vemulapalli[1], Caroline Weller[1], Andrea Gould[1], Daniel M. Whalen[4], Anthony Salvador[4], Anthony Milin[4], Mae Saldajeno-Concar[4], Nuntana Dinglasan[1], Anqi Chen[4], Jim Evans[1], John E. Knox[4], Elena S. Koltun[4], Mallika Singh[1], Robert Nichols[1], David Wildes[1], Adrian L. Gill[4], Jacqueline A. M. Smith[1*], Piro Lito[2,3,6*]

Correspondence to:
Jacqueline A. M. Smith, Jan@revmed.com (J.S); Piro Lito, litop@mskcc.org (P.L.)

This PDF file includes:

Other Supplementary Materials for this manuscript include the following:

Materials and Methods

Cell lines

Cell lines obtained from ATCC were: NCI-H358 [H358] (ATCC CRL-5807), NCI-H23 [H23] (ATCC CRL-5800), NCI-H2030 (ATCC CRL-5914), MIA PaCa-2 (ATCC CRM-CRL-1420), NCI-H1975 [H1975] (ATCC CRL-5908), SW837 [SW-837] (ATCC CCL-235), U-2 OS [U2OS] (ATCC HTB-96), 293 [HEK-293] (ATCC CRL-1573). Lu65 was provided by the RIKEN BRC through the National BioResource Project of the MEXT, Japan. Cells were grown in either RPMI-1640 or DMEM supplemented with 10% FBS and 1% Penicillin/Streptomycin.

Antibodies

The antibodies used for immunoblots were: KRAS (Millipore Sigma, WH0003845M1), pan-RAS (Abcam, 108602), pERK (T202/Y204) (Cell Signaling Technology, 9101), ERK (Cell Signaling Technology, 4696), pRSK (T359) (Cell Signaling Technology, 8753), RSK (Cell Signaling Technology, 9355), pS6K (Cell Signaling Technology, 2211L), S6K (Cell Signaling Technology, 2217L), pAKT (4060L, Cell Signaling Technology,), AKT (Cell Signaling Technology, 9272S), CYPA (Abcam, ab58144), β-Actin (Cell Signaling Technology, 4970)

Protein production

His_6-TEV-KRAS4B^{G12C}[residues 1-169], His_6-TEV-AviTag-KRAS4B^{G12C}[residues 1-169], His_6-TEV-CYPA[full-length], His_6-TEV-AviTag-CYPA[full-length], and GST-TEV-BRAF[residues 155-229] were expressed from a pET28 vector in BL21(DE3) *E. coli*. Cell pellets were lysed by sonication in lysis buffer (50 mM Tris-HCl pH 8.0, 500 mM NaCl, 1 mM PMSF, 1 mM TCEP) and the recombinant proteins were isolated with Ni-NTA affinity chromatography. For KRAS^{G12C}, the His_6 tag was cleaved by overnight dialysis (50 mM Tris-HCl pH 8.0, 500 mM NaCl) at 4 °C in the presence of His-tagged TEV protease (1:20 w/w). The cleaved tag and protease were removed by Ni-NTA chromatography, and the KRAS^{G12C} was further purified by size exclusion chromatography on a Superdex 75 (26/600) column (20 mM Tris-HCl pH 8.0, 200 mM NaCl). Where indicated, the His_6 tag was left intact on KRAS^{G12C} by omitting the TEV protease incubation and the second Ni-NTA column. For CYPA, the His_6 tag was cleaved by overnight dialysis (50 mM Tris-HCl pH 8.0, 300 mM NaCl) at 4 °C in the presence of His-tagged TEV protease (1:10 w/w). The cleaved tag and protease were removed by Ni-NTA chromatography, and the KRAS^{G12C} was further purified by size exclusion chromatography on a Superdex 75 (26/600) column (PBS pH 7.4). For avi-tagged KRAS^{G12C}, the His_6 tag was cleaved by overnight dialysis (50 mM Tris-HCl pH 8.0, 100 mM NaCl, 7.5 mM $MgCl_2$) at 4 °C in the presence of His-tagged TEV protease (1:10 w/w). The Avi-tag was biotinylated by the addition of 1 mM ATP, 0.5 mM Biotin and 200 nM BirA followed by incubation at 18 ℃ for 4 hours. The cleaved tag and protease were removed by Ni-NTA chromatography, and the avi-KRAS^{G12C} was further purified by size exclusion chromatography on a Superdex 75 (26/600) column (20 mM Tris-HCl pH 8.0, 200 mM NaCl). For avi-tagged CYPA, the His_6 tag was removed by overnight dialysis (50 mM Tris-HCl pH 8.0, 100 mM NaCl, 7.5 mM $MgCl_2$) at 4 °C in the presence of His-tagged TEV protease (1:10 w/w). The Avi-tag was biotinylated by the addition of 1 mM ATP, 0.5 mM Biotin and 200 nM BirA followed by incubation at 18 ℃ for 4 hours. The cleaved tag and protease were removed by Ni-NTA chromatography, and avi-CYPA was further purified by Q anion exchange chromatography (20 mM Tris-HCl pH 8, 100 to 1000 mM NaCl) and size exclusion chromatography on a Superdex 75 (26/600) column (10 mM HEPES-NaOH pH 7.5, 150 mM

NaCl, 1mM $MgCl_2$). GST-TEV-BRAF was purified by GSH affinity chromatography, followed by size exclusion chromatography on a Superdex 75 (26/600) column (20 mM Tris-HCl pH 8.0, 200 mM NaCl).

For KRAS proteins, the nucleotide was exchanged to guanosine-5'-[(β-γ)-imido]triphosphate (GMPPNP) by incubation in exchange buffer (40 mM Tris-HCl pH 7.5, 5 mM DTT, 150 mM $(NH_4)_2SO_4$, 4 µM $ZnCl_2$) with 20 U of alkaline phosphatase per mg KRAS protein and a 5-fold molar excess of GMPPNP. After 4 hours of incubation at 30°C, $MgCl_2$ was added to 5 mM and the excess nucleotide was removed using a HiTrap 5 mL desalting column pre-equilibrated in storage buffer (10 mM HEPES-NaOH pH 7.5, 150 mM NaCl, 1mM $MgCl_2$).

Crystallography

Purified human CYPA and $KRAS^{G12C}$ bound to GMPPNP were combined in a 2:1 CYPA:KRAS molar ratio in a buffer solution consisting of 12.5 mM HEPES-NaOH pH 7.3, 75 mM NaCl, 1 mM $MgCl_2$. Compound-1 or RMC-4998 was added from a 10 mM DMSO stock to give a solution of 100 µM $KRAS^{G12C}$, 200 µM CYPA, and 300 µM compound in 1 mL total volume. This mixture was incubated for 1 hour at 25°C and the tricomplex was purified via gel filtration using a Superdex 75 10/300 GL column pre-equilibrated with a buffer consisting of 12.5 mM HEPES-NaOH pH 7.3, 75 mM NaCl, 1 mM $MgCl_2$. Fractions containing the tri-complex were pooled and concentrated to 15 mg/mL using an Amicon Ultra-4 30K centrifugal filter (Millipore Sigma). 80 µL of a screen composed of 0.1 M MES, 18-29% PEG 3350 (increasing by 1% increments), and 0-0.14 M NaCl (increasing by 0.02 M increments) was dispensed into the wells of an MRC-2 crystallization plate. 0.3 µL of well solution was mixed with 0.3 µL of the concentrated tricomplex in a sitting drop and the plate was incubated at 18°C. Crystals grew overnight and were vitrified following cryoprotection via mother liquor supplemented with 25% glycerol.

Crystallography data collection and refinement

X-ray diffraction datasets were collected at the Advances Photon Source (APS-23-ID-B, Lemont, Illinois, USA) at 100K. Data were processed with XDS (*32*), and initial structures were determined via Phaser (*33*) using previously solved KRAS and CYPA as molecular replacement search models. Ligand restraints were generated using AceDRG (*34*). The final structures were determined through iterative rounds of model building using Coot (*35*) and refinement using REFMAC5 from the CCP4 suite (*36*) and phenix.refine (*37*). Final processing and refinement statistics can be found in **Supplementary Table 1**.

RAS-RAF, RAS-CYPA, and RAS-RAL TR-FRET

Disruption of the interactions between wild-type KRAS or $KRAS^{G12C}$ and the RAS-binding domain of BRAF or the RAS-interaction domain of RALGDS were assessed by TR-FRET in reactions consisting of 12.5 nM His_6- $KRAS^{G12C}$[1-169], 50 nM GST-BRAF[155-229] or GST-RALGDS[789-914], 10 nM LANCE Eu-W1024 anti-6xHis antibody (Perkin Elmer AD0111) and 50 nM Allophycocyanin-anti-GST antibody (Perkin Elmer AD0059G), 25 µM CYPA in reaction buffer (25 mM HEPES-NaOH pH 7.3, 0.002% Tween20, 0.1% bovine serum albumin, 100 mM NaCl, 5 mM $MgCl_2$). Compounds or DMSO control (1% v/v) were added and incubated for 1.5 hours, and then TR-FRET was measured on a Perkin Elmer Envision plate reader (excitation at 320 nm, 20 µsec delay, 100 µsec window, 2000 µsec time between flashes; Emission at 665 nm and 615 nm in separate channels). The FRET ratio (665/615 nM emission) was used to calculate

% Inhibition as: (1 – (FRET Ratio of Sample – Average FRET Ratio of Positive Controls)/(Average FRET Ratio of DMSO Control – Average FRET Ratio of Positive Controls)) x 100%.

Induction of interactions between $KRAS^{G12C}$ and CYPA were assessed by TR-FRET in reactions consisting of 50 nM His_6- $KRAS^{G12C}$[1-169], 20 μM Avi-CYPA, 2 nM Anti-His Terbium (PV5863, ThermoFisher), and 1:100 dilution of Streptavidin-XL655 (610SAXLA, Cisbio/ Perkin Elmer) in buffer (20 mM HEPES-NaOH pH 7.5, 150 mM NaCl, 5 mM $MgCl_2$, 0.05% Tween20, 0.1% BSA, 10 μM GMPPNP). Compounds or DMSO control (1% v/v) were added and incubated for 4 hours, and then TR-FRET was measured on a BMG Labtech Pherastar plate reader. The FRET ratio (665/615 nM emission) was used to calculate the KRAS-CYPA interaction as a % of the signal change (calculated as the difference of the maximal (highest compound concentration) minimal (DMSO control) signals.

CYPA binding affinity

The binding affinity of compounds for CYPA was assessed by surface plasmon resonance (SPR) on Biacore 8K instrument. AviTag-CYPA was immobilized on a streptavidin sensor chip, and varying compound concentrations were flowed over the chip in assay buffer (10 mM HEPES-NaOH pH 7.4, 150 mM NaCl, 0.005% v/v Surfactant P20, 2% v/v DMSO). The SPR sensograms were fit using either a steady state affinity model or a 1:1 binding (kinetic) model to assess the K_D for CYPA binding.

Biochemical RMC-4998 tri-complex dissociation kinetics

The dissociation of RMC-4998 tri-complexes was assessed by surface plasmon resonance (SPR) on Biacore 8K instrument. AviTag-$KRAS^{G12C}$[1-169] was immobilized on a streptavidin sensor chip, and RMC-4998 (0.1 or 1 μM) and CYPA (25 μM) was flowed for 180 seconds of association in buffer (10 mM HEPES-NaOH pH 7.4, 150 mM NaCl, 0.005% v/v Surfactant P20, 5 mM MgCl2, 0.5 mM EDTA, 10 μM GMPPNP, 1% v/v DMSO). Dissociation of the complex was monitored during a continuous flow of buffer not containing RMC-4998 or CYPA for 8 hours.

Cellular tri-complex dissociation kinetics

U2OS cells with *PPIA* gene (encoding for CYPA) knockout were seeded at 500,000 cells per well in a 6-well plate and incubated overnight. Each well was transfected using FuGene HD reagent with pNLF1-N plasmid into which full-length $KRAS4B^{G12C}$ had been cloned and pHTN plasmid into which full-length CYPA had been cloned (Promega). The following day, the cells were trypsinized and reseeded in the wells of a white tissue culture treated 96-well plate in OptiMem phenol red-free media (Gibco) containing 4% FBS and a 1:1000 dilution of NanoBRET 618 HaloTag ligand (Promega). The following day, Endurazine nanoluciferase substrate was added to 1x concentration in OptiMem phenol red-free media with 4% FBS. 100 nM RMC-4998 or DMSO control (1% v/v) was added and the nanoBRET signal was measured using the appropriate filter cube in a Cytation5 multi-mode reader pre-equilibrated to 37 degrees and 5% CO_2. After one-hour of incubation, the media was washed out and replaced with the same media containing 0.1 mM cyclosporin A to block rebinding of any free compound to CYPA. The nanoBRET signal was measured every 5 minutes for the next 8 hours. The nanoBRET signal was taken as the difference between the compound-treated and DMSO-treated control wells and normalized as a percentage of the average milliBRET signal of the 30 minutes immediately prior to compound washout.

Covalent modification kinetics

The covalent modification of $KRAS^{G12C}$ was carried out at varying concentrations of inhibitor in the presence of 25 μM CYPA and 10 μM GMPPNP at ambient temperature in buffer (12.5 mM HEPES pH 7.4, 75 mM NaCl, 1 mM $MgCl_2$). Covalent modification was assessed by liquid-chromatography mass spectrometry on an Agilent 6230 TOF or by SDS PAGE followed by immunoblot detection. For LC-MS, samples were quenched by addition of formic acid to 10% and separated on a C4 column with a gradient of water to acetonitrile containing 0.1% formic acid and 0.1% 1 mM ammonium formate. The mass spectra were deconvoluted by the maximum entropy algorithm to determine the peak height corresponding to the unmodified and modified protein masses. The percent covalent modification was calculated from the ratio of the peak height of the covalently-modified protein to the sum of the covalently-modified and unmodified peak heights. For SDS PAGE analysis, the samples were quenched as described above and 4x LDS NuPage sample loading buffer (NP0007, Invitrogen) was added to 1x. Samples were separated on 10% or 12% NuPage Bis-Tris acrylamide gels, then transferred to a nitrocellulose membrane using the iBlot 2.0 system. After blocking, Avi-tagged $KRAS^{G12C}$ was detected by incubation with a 1:2500 dilution of streptavidin-IR800 Dye (LiCOR 926-32230). The membrane was washed then imaged on a LiCor Odyssey imager. The percent covalent modification was calculated from the ratio of the band intensity of the covalently-modified protein to the sum of the covalently-modified and unmodified band intensities. The covalently-modified protein had greater transfer efficiency so an experimental correction factor was calculated from unmodified and fully-modified $KRAS^{G12C}$ controls on each blot and applied to the quantification.

Native PAGE

His_6-$KRAS4B^{G12C}$ and His_6-CYPA purified proteins were mixed at the amount indicated in the figure, with or without addition of RMC-4998 or DMSO, and incubated with shaking at room temperature for 1 hour. 4x native gel loading dye (50 mM BisTris-HCl, 50 mM NaCl, 10% Glycerol, 0.001% Ponceau S, pH 7.2) was added to each sample before being loaded on a NativePAGE Gel (Novex 4-16%). The native gel was run according to the manufacturer's instructions. After electrophoresis, the gel was fixed (40% methanol, 10% acetic acid) and stained with Colloidal Blue Staining Kit (Invitrogen) according to the manufacturer's instructions.

For GDP or GTPγS loaded His_6-$KRAS4B^{G12C}$, the purified KRAS mutant protein first was loaded with GTPγS (Millipore) or GDP (Millipore) at 1mM in loading buffer (50 mM HEPES, 50 mM NaCl, 100 μM DTT, 10 mM EDTA and 50 μM EGTA). The samples were incubated at 30 °C for 2 hours then the reaction was stopped by adding 60 mM $MgCl_2$. Loaded KRAS mutant protein was then mixed with CYPA and DMSO or RMC-4998 and complex formation was assessed by native PAGE as described above.

Cyclophilin A peptide proline isomerase activity assay

Purified recombinant CYPA proteins were assessed for proline isomerase activity largely as described previously (*38*). The peptide substrate N-Suc-Ala-Ala-Pro-Phe-pNitroanilide was dissolved to 100 mM in trifluoroethanol containing 500 mM LiCl (Sigma Aldrich). CYPA proteins were diluted to 20 nM in buffer (50 mM HEPES, 100 mM NaCl, pH 8.0) containing 0.6 mg/mL of chymotrypsin in a 1 mL cuvette. The reaction solution was equilibrated to 4 °C in a temperature-controlled cell holder, then the reaction was initiated by addition of peptide substrate to 120 μM

with rapid mixing. The increase in absorbance at 400 nm was recorded with a Cary 60 UV-vis spectrophotometer. There was an initial burst of absorbance from the substrate already in the trans conformation. The second slow phase, corresponding to the isomerization of cis to trans proline, was fit to determine a k_{obs} for each mutant.

Live cell RAS-RAF and RAS-CYPA sensors

KRAS mutant proteins were cloned into NanoBIT vector 1.1 (Promega) and CYPA or CRAF were cloned into NanoBIT vector 2.1 (Promega). KRAS mutant vector and CYPA, SOS1, or CRAF vectors were co-transfected into HEK293 cells in equal amounts. 24 hours post-transfection, the cells were treated with RMC-4998 (0.1 μM) or DMSO for 2 hours, NanoGlo luciferase substrate (Promega, #N2011) was added, and the bioluminescence signal was detected in GloMax plate luminometer.

For kinetic tests, NanoBIT tagged $KRAS^{G12C}$ and CRAF or SOS1 catalytic domain (SOScat) were connected with P2A sequence and subcloned into pLIX_403 vector (a gift from David Root, Addgene plasmid # 41395; http://n2t.net/addgene:41395 ; RRID:Addgene_41395). H358 cells were transduced with the lentivirus derived from this vector and selected with puromycin (1 μg/mL) for 5 days. The puromycin resistant cells were plated into 96-well plates in triplicates. The expression of nanoBIT tagged $KRAS^{G12C}$ and CRAF or SOScat was induced by addition of doxycycline (2 μg/mL) for 1 day. NanoGlo luciferase substrate solution (Promega, #N2590) was added to these cells and bioluminescence was detected in plate reader SpectraMax iD5 (Molecular Devices). After recording the baseline of the signal, RMC-4998 (0.1 μM) or DMSO were added to cells and bioluminescence was continuously recorded for 5 hours.

Saturation mutagenesis

The saturation mutagenesis library was generated by mutating the DNA sequence of $KRAS^{G12C}$ (codon 2-188) to encode for all possible amino acids for each site. The DNA sequence was codon-optimized for expression in human cells and subcloned into the pLIX_403 vector (Addgene, #41395). Lentivirus was produced by transfecting the library DNA along with packaging (psPAX2) and envelope (pMD2.G) plasmid into HEK293T cells. The virus was collected 48 hrs after transfection to transduce NCI-H358 cell line at an MOI (multiplicity of infection) of 0.5 with polybrene (Millipore) at 0.8 μg/mL. After selection with puromycin (2 μg/mL), live cells were collected and separated into three equal fractions (4 million cells per fraction). One fraction was pelleted and frozen at -80°C (day 0). Another fraction was propagated in cell culture in the presence of doxycycline (dox, 1 μg/mL) and DMSO. The third fraction was propagated in the presence of dox and RMC-4998 (50 nM). The cells were passaged when reaching confluence. The media was refreshed every three days. The cells were collected and pelleted after 14 days of treatment. The screen was performed in biological triplicates. Genomic DNA (gDNA) from pelleted cells was extracted with the DNeasy blood and tissue kit (QIAGEN) and used as template to amplify the mutagenesis library with the primers as followings: F: 5'-tttagtgaaccgtcagatcgcctgg-3' and R: 5'-gaaagctgaaccgggatcccgtca-3'. The PCR products were purified with agarose gel electrophoresis and the QIAquick Gel Extraction kit (QIAGEN). Purified PCR products were fragmented, indexed with Nextera reactions according to the Illumina Nextera XT protocol before being subjected to Hiseq analysis at 2x150 bp. Count files were generated by using the ORFcall software (Broad Institute) and analyzed using edgeR to determine the $\log_2$ fold change between the reads at day 14 relative to day 0.

Cellular ERK phosphorylation assays
Cells were plated at a density of 25,000 cells per well in tissue culture-treated 96-well plates and incubated overnight. The following day, serial dilutions of compound were prepared in growth medium. Cells were treated with compound or DMSO control (0.1%) for 4 hours. Following the incubation period, cells were lysed and the levels of ERK phosphorylation were determined using the MesoScale Discovery (MSD) Multi-Array Assay System – Phospho/Total ERK1/2 Whole Cell Lysate Kit (K15107D), following the manufacturer's instructions. The assay was read in a Meso QuickPlex SQ120 reader. MSD signal from pERK1/2 was divided by MSD signal for total ERK1/2. The ratio was normalized to vehicle (% of pERK/total ERK= ((ratio $pERK_{treated}$/total $ERK_{treated}$)/ (ratio $pERK_{DMSO}$/total ERK_{DMSO}))*100).

2D cell proliferation
For 2D cellular proliferation assays, cells were plated in tissue culture-treated 96-well plates and incubated overnight. The following day, 10 serial dilutions of compound were prepared in growth medium. Cells were treated with compound or DMSO (0.1% v/v) for 120 hours. 50 µL of CellTiter-Glo 2.0 reagent (G9243, Promega) was added to each well. Plates were shaken at 450 rpm for 2 minutes at room temperature and then incubated for an additional 10 minutes without shaking at room temperature and protected from light. luminescence was detected using the SpectraMax M5 Plate Reader (Molecular Devices). Luminescence signal from the CellTiter-Glo 2.0 reagent was normalized to vehicle treated wells (% vehicle = ($lum_{treated}$/mean($lum_{vehicle}$))*100). Data were plotted as a function of log molar [inhibitor] and a 4-parameter sigmoidal concentration response model was fitted to the data to calculate the IC_{50}.

3D cell proliferation
For 3D cellular proliferation assays, cells were seeded in the wells of a round bottom ultra-low attachment 96-well plate (Corning 7007) and centrifuged at 1000x g for 10 minutes to pellet the cells. After 3 days incubation to allow for spheroid formation, cells were treated with compound or DMSO (0.1% v/v) for 120 hours. 50 µL of 3D CellTiter-Glo reagent (G9683, Promega) was added to each well. The solution was mixed by pipetting up-and-down 10 times, then transferred to a white flat-bottom 96-well plate. After 10 minutes shaking at 750 rpm, luminescence was detected using the SpectraMax M5 Plate Reader (Molecular Devices). Luminescence signal from the 3D CellTiter-Glo reagent was normalized to vehicle treated wells (% vehicle = ($lum_{treated}$/mean($lum_{vehicle}$))*100). Data were plotted as a function of log molar [inhibitor] and a 4-parameter sigmoidal concentration response model was fitted to the data to calculate the IC_{50}.

Target engagement by western blot
Cells were seeded at a density of 500,000 to 1 million cells in the wells of a 6-well plate. Compounds or DMSO (0.1% v/v) were added and incubated for the indicated time, then halted by removal of the media and addition of ice-cold PBS. The PBS was removed, and NP-40 lysis buffer (J60766, ThermoFisher Scientific) containing HALT™ protease phosphatase inhibitors (78441, ThermoFisher Scientific) was added. Cells were lysed and collected by scraping, and the lysate was clarified by centrifugation at 21,000 x g for 10 minutes at 4 °C. The protein-containing supernatant was quantified by BCA assay (23225, Pierce) and equal quantities of protein were prepared in 4x LDS sample buffer (NP0007, Invitrogen). Samples were resolved on 12% NuPage Bis-Tris acrylamide gels, then transferred to a nitrocellulose membrane using the iBlot 2.0 system.

Membranes were blocked in Intercept TBS buffer (927-60001, LiCor), then probed with the primary antibodies (RAS, Abcam 108602; ERK1/2, Cell Signaling Technologies 4696; pERK, Cell Signaling Technologies 9101; β-Actin, Cell Signaling Technologies 4970) overnight at 4° C. Goat anti-rabbit IR800-conjugated secondary (926-32211, LiCor) or anti-mouse IR680-conjugated (926-68070, LiCor) secondary antibodies were added, as appropriate, and the membranes were imaged on a LiCor Odyssey imager.

RAL activation assay

RALA activation was measured using the RAL G-LISA kit (cytoskeleton, #BK129) according to the manufacturer's protocol. In brief, 6.25 µg of total cell lysate was added to independent wells of a 96 well plate coated with the active RAL-binding domain followed by incubation for 20 min at 4°. The plate was then incubated with an anti-RAL primary antibody and an HRP-conjugated secondary antibody. At least three washes were performed between each antibody incubation step. The experiment was performed in biological triplicates. The absorbance was measured at 490 nM and the final measurement values were subtracted from background (wells without added lysate).

Caspase 3/7 activation assay

NCI-H358 cells were plated in tissue-culture 96-well plates at a density of 30,000 cells/well and incubated overnight. The following day, serial dilutions of compound were prepared in growth medium containing the Incucyte Caspase 3/7 Dye (diluted 1:1000, final concentration). Plates were incubated in the Incucyte S3 Live-Cell Analysis System. Imaging was performed every 4 hours for 48 hours. The number of green objects (apoptotic cells) was determined using the Incucyte S3 software and normalized to DMSO control wells. The fold-increase in green objects at 48 hours was plotted as a function of log molar [inhibitor] and a 4-parameter sigmoidal concentration response model was fitted to the data to calculate the IC_{50}.

CYPA knockout and rescue

H358 cells were transduced by lentivirus encoding Cas9, a guide RNA targeting the PPIA (CYPA) gene, and the puromycin resistance gene. Following puromycin selection, FLAG-CYPA was reintroduced under the control of a tet-inducible promoter by lentiviral transduction. Clones were isolated, and three clones with similar levels of expression were pooled. For experiments with FLAG-CYPA rescue, the expression of the transgene was induced by addition of 1 µg/mL of doxycycline.

Switch II pocket mutant library and assay

The nanoBRET assay was used to assess how switch II pocket mutations affect the potency of RMC-4998, adagrasib, and sotorasib. All possible protein mutations that arise from single nucleotide changes at residues R68, H95, or Y96 were introduced into pNLF1-N plasmid encoding $KRAS4B^{G12C}$ by Q5 Site-Directed Mutagenesis (E0554S, New England Biolabs) according to manufacturer instructions. U2OS cells were seeded at 500,000 cells in the wells of a 6-well plate and transfected with the pNLF1-N plasmid encoding each KRAS mutation and a pHTC plasmid into which the RAS-binding domain of RAF1 (RBD, residues 51-149) had been cloned. The following day, the cells were reseeded in the wells of a white 96-well plate in OptiMem phenol red-free media containing 4% FBS and a 1:1000 dilution of NanoBRET 618 halotag ligand. The following day, Vivazine nanoluciferase substrate was added to a 1x concentration in the same media. Serial dilutions of compounds, or DMSO control (1% v/v), were added to the wells and

incubated for five hours. The nanoBRET signal was measured on a PerkinElmer Envision plate reader equipped with the appropriate filters (Chroma Technology AT460/50m and AT600lp). The resulting nanoBRET data were plotted as a function of log molar [inhibitor] and a 4-parameter sigmoidal concentration response model was fitted to the data to calculate the IC_{50}. The fold-change IC_{50} loss relative to the $KRAS^{G12C}$ were determined from these fits.

Western blot and pull-down assays

Cells under certain treatments were harvested before being lysed with NP40 lysis buffer (50 mM Tris pH 7.5, 1% NP40, 150 mM NaCl, 10% glycerol and 1 mM EDTA) containing protease (Pierce Protease Inhibitor Mini Tablets, Thermo Fisher Scientific #88665) and phosphatase (Pierce Phosphatase Inhibitor Mini Tablets, Thermo Fisher Scientific #88667) inhibitors on ice for 10 min. After that, the lysates were centrifuged at 16,000 x g for 10 minutes before protein concentration was quantified with the BCA assay (Thermo Fisher Scientific). The proteins were resolved on 4-12% SDS-PAGE gels (Thermo Fisher Scientific) in 1X MOPS buffer (Thermo Fisher Scientific) at 90-120 constant voltage (V) and transferred to nitrocellulose membranes (GE Healthcare) with 1x Tris-Glycine Buffer (BioRad) at 100 V for 1 hour. Membranes were blocked in 5% nonfat milk for 1 hour and then probed with primary antibodies overnight at 4 °C and visualized using horseradish peroxidase (HRP)-conjugated secondary antibodies and ECL (Thermo Fisher Scientific). Immunoblots were quantified using ImageJ.

Cellular RAS-RAF binding was detected using the active Ras pull-down and detection kit (Thermo Fisher Scientific). Briefly, GST–RAF1 RAS-binding domain (RBD) and glutathione agarose resin were mixed with whole-cell lysates and incubated on a rotator for 1 h at 4 °C, followed by 3 washes and elution with 2x SDS–PAGE loading buffer. The samples were then analyzed by SDS-PAGE and western blotting with a KRAS-specific antibody (WH0003845M1).

Growth-factor shift assays

To assess the effects of growth factor stimulation on the potency of RMC-4998 and adagrasib, the EC_{95} concentration of EGF or HGF (236-EGF, 294-HG/CF; RND systems) was determined by incubation with a serial dilution of the appropriate growth factor followed by the measurement of pERK or cellular proliferation as described above. The data were fit to a 4-parameter sigmoidal concentration response model to calculate the EC_{95} for each growth factor. Growth factors were added immediately prior to the addition of compounds and the effects on cellular proliferation or cellular pERK were assessed as described above. For target engagement, 100 ng/mL of HGF or EGF was added immediately prior to the addition of compounds and the covalently modified protein was detected as described above.

Cysteinome profiling

NCI-H358 cells in 10 cm dishes at a density of 8 million cells/dish and incubated overnight. The following day, cells were treated with either vehicle (n = 5, DMSO, 0.1% final concentration) or 50 nM RMC-6291 (n = 5) for 4 hours. Cells were washed with cold PBS, lifted, pelleted and frozen at -80 °C. Frozen pellets were processed by IQ Proteomics, LLC. Briefly, cell pellets were lysed by probe sonication and treated with 200 µM desthiobiotin iodoacetamide (1 hr) followed by DTT (5 mM, 30 minutes) to label unreacted solvent exposed cysteines. Protein pellets were digested with trypsin and Lys-C and labeled with tandem-mass tags (TMT, 15-plex, ThermoFisher). Samples were mixed, desalted by reversed-phase SPE (C18 Sep Pak, 50 mg) and dried. Mixed

samples were enriched with streptavidin agarose. Enriched peptides were microfractionated using a high pH microfractionation kit (Pierce). Samples were analyzed using nano-LC-MS on an Orbitrap Lumos mass spectrometer using a C18 column (Sepax GP-C18 resin). LC-MS runs are searched using the SEQUEST algorithm. Desthiobiotinylated peptides are identified via searching for peptides with a fixed modification on cysteine residues of 57.02146 Da (Iodoacetamide), and variable modification on cysteine residues of 398.2529 Da (corresponding to the difference in mass between iodoacetamide and the desthiobiotin iodoacetamide modification). Raw TMT intensities for each sample are normalized to the summed intensities for that channel observed in the input sample. Normalized data are then expressed as proportions to facilitate data analysis. Log_2-fold changes were calculated between DMSO and RMC-4998 treated sample groups and statistical significance was assessed using a two-tailed t-test for each peptide assuming equal variance. Peptides with $p < .01$ were deemed significant and plotted in ascending order by log_2 fold-change.

Cell panel

A panel of 28 cancer cell lines was selected harboring either the $KRAS^{G12C}$ mutation or another mutation in the RAS pathways (non-$KRAS^{G12C}$). The list of cell lines and mutations can be found in **Table S2.** The experiment was conducted at Shanghai ChemPartner Co. To measure inhibition of cell proliferation/viability, cells were cultured as 3D spheroids in ultra-low adhesion (ULA) plates. RMC-4998, RMC-6291, or adagrasib (diluted in growth media) was added at increasing concentrations to wells. At the end of the 120-hour incubation period, cell viability in the culture was measured using the CellTiter-Glo Luminescent 3D Cell Viability Assay (CTG), a method of determining the number of viable cells based on quantitation of cellular adenosine triphosphate (ATP) as an indicator of metabolically active cells, according to the manufacturer's instructions. CTG readouts were normalized to vehicle control and plotted as a function of log molar [inhibitor]. A 4-parameter sigmoidal concentration response model was fitted to the data to calculate the inhibitor EC_{50}.

Animal studies

All procedures related to animal handling, care and treatment were conducted in compliance with all applicable regulations and guidelines of the relevant Institutional Animal Care and Use Committee (IACUC).

NCI-H358 xenograft studies

Studies were conducted at WuXi AppTec (Suzhou) Co., Ltd. (Jiangsu, China). The NCI-H358 tumor cells (ECACC-95111733) were maintained in vitro as a monolayer culture in RPMI-1640 medium supplemented with 10 % heat inactivated fetal bovine serum, 100 U/mL penicillin and 100 μg/mL streptomycin at 37ºC in an atmosphere of 5 % CO2 in air. The tumor cells were subcultured once every five days. The cells growing in an exponential growth phase were harvested and counted for tumor inoculation. Female BALB/c nude mice 6-8 weeks old from Shanghai Sino-British Sippr/BK Laboratory Animal Co., LTD. were used for these studies. Each mouse was inoculated subcutaneously at the right flank with NCI-H358 tumor cells (5×10^6) in 0.1 mL of PBS supplemented with Matrigel (3:1) for tumor development. **For efficacy study**, treatments started at the time of randomization when the average tumor volume of each group reached the ideal range (150-300 mm^3). RMC-4998 was administered daily at the indicated doses via oral gavage. Tumors were measured in two dimensions using a digital caliper, by an unblinded employee who was not involved in the design or analysis of study results. The tumor volume in

mm^3 was calculated using the formula: Volume = $((width)^2 \times length)/2$, where width and length are measured in mm. Mice on studies were weighed and tumor measurements collected 2 times a week. **For single-dose pharmacokinetic/pharmacodynamics (PK/PD) study**, mice were randomized into treatment groups when mean tumor volume reached 400-600 mm^3. At the indicated time points after a single dose of RMC-4998 at the indicated dose levels, plasma and tumor samples were collected for PK and PD analysis, respectively. RMC-4998 was formulated in 10/20/10/60 (%v/v/v/v) DMSO/PEG400/Solutol/2% HPMC in 50 mM sodium citrate buffer, pH=4), and the vehicle formulation was used for control group.

Mouse plasma sample bioanalysis

Plasma concentrations of RMC-4998 and RMC-6291 were determined using liquid chromatography-tandem mass spectrometry (LC-MS/MS) methods performed at WuXi AppTec (Suzhou, China). An aliquot of plasma (10 μL) was transferred to 96-well plates (or tubes) and quenched with a 20× volume of acetonitrile/methanol (1:1; v/v) containing a cocktail of internal standards (IS, each 100 ng/mL of labetalol, tolbutamide, verapamil, dexamethasone, glyburide and celecoxib). After thorough mixing and centrifugation, the supernatant was directly analyzed on a Sciex 6500+ triple quadrupole mass spectrometer equipped with an ACQUITY UPLC system. An ACQUITY UPLC BEH C18 1.7 μm (2.1 × 50 mm) column was used with gradient elution for compound separation. RMC-4998 or RMC-6291 and IS verapamil were detected by positive electrospray ionization using multiple reaction monitoring (RMC-4998: m/z 983.7/906.4; RMC-6291: m/z 506.8/633.3; verapamil: m/z 455.2/165.0). The lower limit of quantification was 2.0 ng/mL, and the calibration range was 2.0 to 3000 ng/mL.

***In vivo* pharmacodynamic analysis by *DUSP6* qPCR**

RNA was extracted from at least 20 mg of tumor tissue using RNeasy Mini Kit (Qiagen, 74104) using a High Throughput Tissue grinder and following manufacturer's protocol from the RNeasy Mini Kit. Reverse transcription was carried using High-Capacity cDNA Reverse Transcription Kit (ABI, 4368814) according to manufacturer's protocol. The cDNA product was used for qPCR analysis using TaqMan Gene Expression Master Mix (ABI, 4369016). TaqMan primer probes specific to human *DUSP6* and *18S* (used as an internal control gene) were used to detect the levels from each sample in duplicates using a 10 μL final reaction volume in a 384-well clear optical reaction plate. For qPCR, Ct value of *DUSP6* and *18S* were obtained for analysis. *DUSP6* Ct value was normalized to *18S*, and then the mean relative mRNA expression levels of each group were normalized to the vehicle control group.

Tumor target engagement

Tumor target engagement was measured by LC-MS at IQ Proteomics LLC. Snap-frozen tumor samples were were homogenized in 100 mM EPPS pH 8.1 and 8 M Urea, then fully denatured via addition of SDS (1% final (w/v)). Heavy $KRAS^{G12C}$ was spiked into each lysate as an internal control to account for sample recovery. Samples were reduced with dithiothreitol, and cysteines alkylated with iodoacetamide. Following alkylation, protein was isolated via SP3 cleanup. Isolated protein was resuspended in 100 mM EPPS pH 8.1. Samples were digested with LysC (overnight, room temperature), and Trypsin (6 hours, 37 degrees). Digested samples were analyzed via Orbitrap Lumos instrument (Thermo) using a PRM assay targeting KRAS peptides (including modified G12C peptides (iodoacetamide: Indirect (+57)). Relative engagement of the G12C peptide was determined as a percentage of the signal observed for that peptide compared to that of

each control peptide. For a given control peptide, G12C peptide signal was normalized across all samples using the median ratio to standard in the DMSO treated samples to set the stoichiometry of G12C for DMSO samples at 100%.

PDX studies

Studies were conducted at the following CROs: Charles River Discovery Research Services Germany GmbH (Freiburg, Germany), Champions Oncology, Inc. (Rockville, MD), GenenDesign (Shanghai, China), XenoSTART (San Antonio, TX). All PDX mouse studies were conducted in compliance with all applicable regulations and guidelines of the relevant Institutional Animal Care and Use Committee (IACUC). Tumor volumes and body weights were measured and weighed, respectively, twice a week during the study. RMC-6291 was administered via oral gavage daily at 200 mg/kg, using the formulation made of 10/20/10/60 (%v/v/v/v) DMSO/PEG400/Solutol/2% HPMC in 50 mM sodium citrate buffer, pH=4), and the vehicle formulation was used for control group. For all PDX studies, animals were randomized into vehicle control and RMC-6291 treatment groups. Tumor volumes were measured by an unblinded employee not involved in the design or analysis of this study. Percentage of tumor volume change from baseline was calculated as 100% X (Tumor volume$_{Day\text{-}x}$ – Initial tumor volume)/Initial tumor volume, where Day-x is treatment responses at 28 ± 2 days, or an earlier time if tumor burden reaches humane endpoint. Means ± SEM were plotted in the waterfall plots. Tumor regression in a model is defined as achieving mean tumor volume reduction of more than 10% from baseline.

Immunohistochemistry (IHC)

For the immunohistochemical detection of pERK 1/2, formalin fixed tumors were serially sectioned (4 μm) and stained on a Biocare IntelliPATH automation system. Heat induced epitope retrieval was carried out at pH 6.2 and sections were stained with the anti-pERK rabbit monoclonal antibody from Cell Signaling Technologies (4370, Clone: D13.14.4E). The primary antibody was detected with the MACH4 HRP-polymer Detection System (Biocare, MRH534). The chromogenic detection and counterstaining kits IntelliPATHFLX DAB chromogen (Biocare, IPK5010) and IntelliPATH Hematoxylin (Biocare Medical, XMF963) were used for final slide preparation. The ApopTag Plus Peroxidase In Situ Apoptosis Detection Kit (EMD Millipore, S7101) was used to detect apoptotic cells by TUNEL staining on 4μm tumor sections. Stained slides were scanned and digitized with a TissueScope LE whole slide scanner (Huron Digital Pathology) at 20x magnification.

Image analysis for pERK levels was performed only on regions classified as human tumor cells with the HALO Image Analysis software from Indica labs using the area quantification module.

Analysis of TUNEL staining was also measured only on regions classified as human tumor cells with the HALO Image Analysis software from Indica labs using the CytoNuclear module.

Supplementary Text

Chemical Syntheses

Definitions used in the following syntheses and elsewhere herein are:

CH_2Cl_2, DCM	Methylene chloride, Dichloromethane
CH_3CN, MeCN	Acetonitrile
CuI	Copper (I) iodide
DIPEA	Diisopropylethyl amine
DMF	N,N-Dimethylformamide
EtOAc	Ethyl acetate
h	hour
H_2O	Water
HCl	Hydrochloric acid
K_3PO_4	Potassium phosphate (tribasic)
MeOH	Methanol
Na_2SO_4	Sodium sulfate
NMP	N-methyl pyrrolidone
Pd(dppf)Cl_2	[1,1′-Bis(diphenylphosphino)ferrocene]dichloropalladium(II)

Instrumentation

Mass spectrometry data collection took place with a Shimadzu LCMS-2020, an Agilent 1260LC-6120/6125MSD, a Shimadzu LCMS-2010EV, or a Waters Acquity UPLC, with either a QDa detector or SQ Detector 2. Samples were injected in their liquid phase onto a C-18 reverse phase. The compounds were eluted from the column using an acetonitrile gradient and fed into the mass analyzer. Initial data analysis took place with either Agilent ChemStation, Shimadzu LabSolutions, or Waters MassLynx. NMR data was collected with either a Bruker AVANCE III HD 400MHz, a Bruker Ascend 500MHz instrument, or a Varian 400MHz, and the raw data was analyzed with either TopSpin or Mestrelab Mnova.

Synthesis and characterization of Compounds 1-4, RMC-4998 and RMC-6291

Synthesis of **Compound 1**

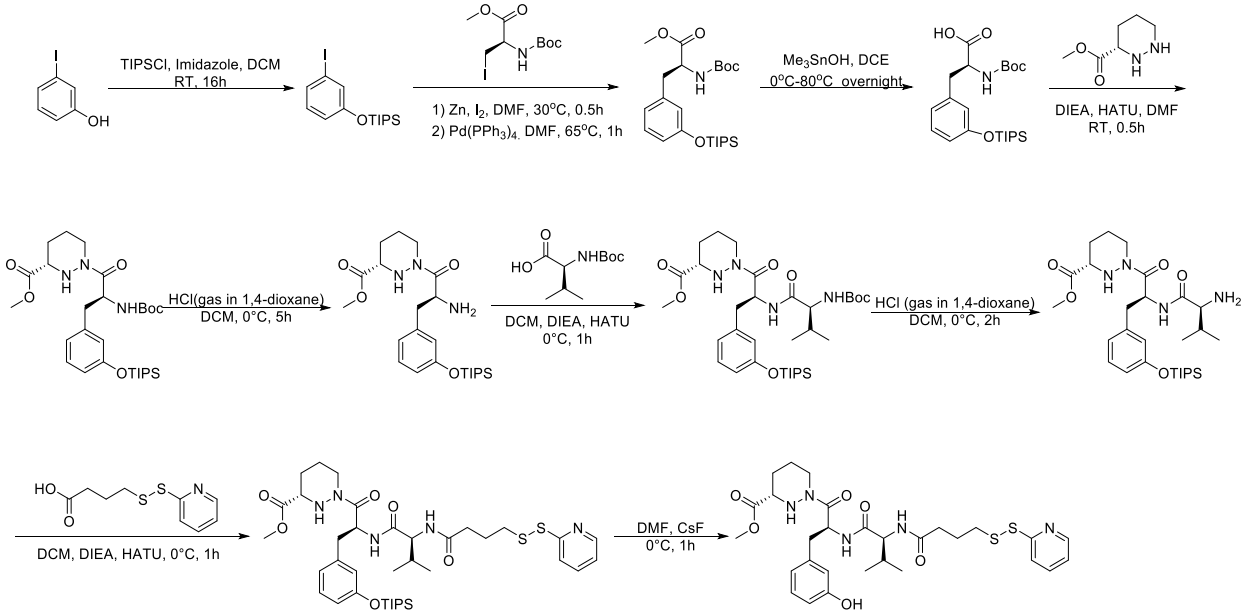

(3-iodophenoxy) triisopropylsilane (**T1**) To a 500 mL round-bottom flask was added 3-iodophenol (10 g, 45.45 mmol, 1 equiv), DCM (100 mL), Imidazole (6.19 g, 90.93 mmol, 2.00 equiv), and TIPSCl (10.5 g, 54.54 mmol, 1.2 equiv) at 0°C. The resulting mixture was stirred overnight then diluted with water (100 mL). The resulting mixture was extracted with EtOAc (3 x 100 mL) and dried over anhydrous Na_2SO_4. After filtration, the filtrate was concentrated under reduced pressure. The residue was purified by silica gel column chromatography, eluted with PE / EA (3:1) to afford (3-iodophenoxy) triisopropylsilane (8 g, 46% yield) as a yellow oil. ^{1}H NMR (300 MHz, DMSO-d6) δ 7.32 (ddd, J = 7.8, 1.6, 1.0 Hz, 1H), 7.22 (dd, J = 2.4, 1.6 Hz, 1H), 7.06 (t, J = 8.0 Hz, 1H), 6.89 (ddd, J = 8.2, 2.4, 1.0 Hz, 1H), 1.35 – 1.13 (m, 3H), 1.05 (d, J = 7.2 Hz, 18H). ^{13}C NMR (101 MHz, DMSO-d_6) δ 156.65, 131.90, 130.57, 128.80, 119.57, 95.21, 18.13, 12.47.

methyl (S)-2-((tert-butoxycarbonyl) amino)-3-(3-((triisopropylsilyl)oxy) phenyl) propanoate (**T2)** To a 100 mL 3-necked round-bottom flask was added Zn (0.69 g, 10.63 mmol, 2 equiv), I_2 (0.01 g, 0.04 mmol, 0.01 equiv), DMF (15 mL) and methyl (*R*)-2-((tert-butoxycarbonyl) amino)-3-iodopropanoate (1.75 g, 5.31 mmol, 1 equiv) at 0 °C. The resulting mixture was stirred for 0.5 h at 30 °C. This solution was canula transferred to a 100 mL 3-necked round-bottom flask containing (3-iodophenoxy) triisopropylsilane (2 g, 5.31 mmol, 1 equiv), DMF (15 mL), and $Pd(PPh_3)_4$ (0.12 g, 0.02 equiv) at 0 °C. The resulting mixture was stirred for 1 h at 65 °C under an argon atmosphere. The resulting mixture was diluted with 100 mL of NaCI(aq) then extracted with EtOAc (3 x 100 mL). The combined organic layers were washed with NaCI(aq) (2x100 mL) and dried over anhydrous Na_2SO_4. The resulting mixture was concentrated under reduced pressure. The crude product was purified by reverse phase flash with the following conditions (Column: C18 spherical 20-35um 100A 120 g; Mobile Phase A: Water(0.1%FA), Mobile Phase B: ACN; Flow rate: 60 mL/min; Gradient: 60% B to 100% B in 30 min.) This resulted in methyl (*S*)-2-((*tert*-butoxycarbonyl) amino)-3-(3-

((triisopropylsilyl)oxy) phenyl) propanoate (1.6 g, 66%yield) as a yellow oil. ^{1}H NMR (400 MHz, DMSO-d_6) δ 7.24 (d, J = 8.1 Hz, 1H), 7.14 (t, J = 7.8 Hz, 1H), 6.82 – 6.75 (m, 2H), 6.70 (dd, J = 8.0, 2.5 Hz, 1H), 4.21 – 4.00 (m, 1H), 3.61 (s, 3H), 2.99 – 2.73 (m, 2H), 1.38 – 1.15 (m, 13H), 1.06 (d, J = 7.4 Hz, 19H). ^{13}C NMR (101 MHz, DMSO-d_6) δ 173.01, 155.78, 155.70, 139.71, 129.67, 122.45, 120.89, 118.05, 78.59, 55.59, 52.19, 36.65, 28.53, 28.24, 18.19, 12.50. ESI-MS m/z = 452.3 $[M+H]^+$; calculated for $C_{24}H_{41}NO_5Si$: 451.3.

(S)-2-((tert-butoxycarbonyl) amino)-3-(3-((triisopropylsilyl)oxy) phenyl) propanoic acid (**T3)** To a 100 mL round-bottom flask was added methyl (S)-2-((tert-butoxycarbonyl) amino)-3-(3-((triisopropylsilyl)oxy) phenyl) propanoate (1.2 g, 2.66 mmol, 1 equiv), DCE (15 mL) and trimethylstannanol (2.40 g, 13.29 mmol, 5 equiv) at 0 °C. The resulting mixture was stirred overnight at 80 °C then filtered, the filter cake was washed with EtOAc (3x20 mL). The filtrate was concentrated under reduced pressure to afford (*S*)-2-((*tert*-butoxycarbonyl) amino)-3-(3-((triisopropylsilyl)oxy) phenyl) propanoic acid. The crude product was used in the next step directly without further purification. ^{1}H NMR (400 MHz, DMSO-d_6) δ 7.10 (t, J = 7.7 Hz, 1H), 6.79 – 6.70 (m, 2H), 6.66 (dd, J = 8.0, 2.5 Hz, 1H), 3.94 (s, 1H), 2.97 – 2.86 (m, 1H), 2.80 – 2.69 (m, 1H), 1.33 (s, 6H), 1.30 (s, 1H), 1.26 – 1.14 (m, 4H), 1.05 (d, J = 7.4 Hz, 19H), 0.39 (s, 5H). ^{13}C NMR (101 MHz, DMSO-d_6) δ 127.09, 120.56, 118.89, 115.41, 75.81, 54.01, 38.37, 38.16, 37.95, 37.74, 37.54, 37.33, 37.12, 35.20, 26.40, 26.17, 16.02, 10.34. ESI-MS m/z = 438.3 $[M+H]^+$; calculated for $C_{23}H_{39}NO_5Si$: 437.3

methyl (3S)-1-[(2S)-2-[(tert-butoxycarbonyl) amino]-3-{3-[(triisopropylsilyl) oxy] phenyl} propanoyl]-1,2-diazinane-3-carboxylate (**T4**) To a 100 mL round-bottom flask was added methyl (*S*)-hexahydropyridazine-3-carboxylate (0.69 g, 4.79 mmol, 3.49 equiv), DMF (8 mL), ethylbis(propan-2-yl) amine (1.77 g, 13.71 mmol, 10 equiv), (*S*)-2-((*tert*-butoxycarbonyl) amino)-3-(3-((triisopropylsilyl)oxy) phenyl) propanoic acid (0.6 g, 1.37 mmol, 1 equiv) and HATU (0.57 g, 1.508 mmol, 1.1 equiv) at 0 °C. The reaction was stirred for 0.5 h at room temperature and then diluted with 50 mL of NaCl(aq.). The resulting mixture was extracted with EtOAc (3x50 mL). The combined organic layers were washed with NaCl(aq.) (2x50 mL) and dried over anhydrous Na_2SO_4. After filtration, the filtrate was concentrated under reduced pressure. The crude product was purified by reverse phase flash with the following conditions (Column: C18 spherical 20-35um 100A 80 g; Mobile Phase A: Water(0.1%FA), Mobile Phase B: ACN; Flow rate: 60 mL/min; Gradient: 70% B to 100% B in 20 min) to afford methyl (3S*)*-1-[(2*S*)-2-[(*tert*-butoxycarbonyl) amino]-3-{3-[(triisopropylsilyl) oxy] phenyl} propanoyl]-1,2-diazinane-3-carboxylate (0.2 g, 25% yield) as a yellow oil. ^{1}H NMR (400 MHz, DMSO-d_6) δ 7.11 (t, J = 7.8 Hz, 1H), 6.81 – 6.72 (m, 2H), 6.67 (dd, J = 7.8, 2.7 Hz, 1H), 6.50 (d, J = 8.8 Hz, 1H), 5.27 (d, J = 10.1 Hz, 1H), 5.11 – 5.02 (m, 1H), 3.67 (s, 3H), 3.33 (s, 6H), 2.79 (dd, J = 13.3, 4.2 Hz, 1H), 2.63 – 2.54 (m, 1H), 1.87 – 1.79 (m, 1H), 1.77 – 1.44 (m, 4H), 1.31 (s, 7H), 1.29 – 1.16 (m, 6H), 1.05 (d, J = 7.4 Hz, 19H). ^{13}C NMR (101 MHz, DMSO-d_6) δ 172.63, 171.88, 155.59, 155.31, 140.57, 129.40, 122.76, 121.03, 117.69, 78.02, 52.38, 52.17, 40.96, 37.56, 28.62, 18.24, 12.51. ESI-MS m/z = 564.3 $[M+H]^+$; calculated for $C_{29}H_{49}N_3O_6Si$: 563.3

(3S)-1-[(2S)-2-amino-3-{3-[(triisopropylsilyl)oxy]phenyl}propanoyl]-1,2-diazinane-3-carboxylate (**T5**) To a 20mL vial was added methyl (3*S*)-1-[(2*S*)-2-[(*tert*-butoxycarbonyl)amino]-3-{3-[(triisopropylsilyl)oxy] phenyl}propanoyl]-1,2-diazinane-3-carboxylate (310 mg, 0.550 mmol, 1 equiv), DCM (3 mL) and HCl (gas) in 1,4-dioxane (1.5 mL)

at 0 °C. The reaction was stirred for 3h at 0 °C then diluted with DCM (50mL). The resulting mixture was washed with 3x50 mL of sat. NH_4Cl (aq.) and dried over anhydrous Na_2SO_4. After filtration, the filtrate was concentrated under reduced pressure to afford (3*S*)-1-[(2*S*)-2-amino-3-{3-[(triisopropylsilyl)oxy]phenyl}propanoyl]-1,2-diazinane-3-carboxylate (270 mg, crude) as a greenish solid. ^{1}H NMR (400 MHz, DMSO-d_6) δ 7.11 (t, *J* = 7.7 Hz, 1H), 6.86 – 6.63 (m, 3H), 5.08 (d, *J* = 9.8 Hz, 1H), 4.48 – 4.34 (m, 1H), 3.64 (s, 3H), 3.30 – 2.81 (m, 7H), 2.74 (dd, *J* = 12.9, 6.3 Hz, 1H), 2.51 – 2.38 (m, 2H), 1.81 – 1.73 (m, 1H), 1.70 – 1.53 (m, 2H), 1.49 – 1.37 (m, 1H), 1.30 – 1.15 (m, 4H), 1.05 (dd, *J* = 7.4, 2.6 Hz, 20H). ^{13}C NMR (101 MHz, DMSO-d_6) δ 175.75, 171.99, 155.65, 141.28, 129.40, 122.79, 120.90, 117.44, 58.14, 52.12, 51.73, 41.95, 40.97, 27.59, 22.78, 22.08, 18.28, 18.18, 16.30, 12.54. ESI-MS m/z = 464.3 $[M+H]^+$; calculated for $C_{24}H_{41}N_3O_4Si$: 463.3.

methyl (3S)-1-[(2S)-2-[(2S)-2-[(tert-butoxycarbonyl)amino]-3-methylbutanamido]-3-{3-[(triisopropylsilyl)oxy]phenyl}propanoyl]-1,2-diazinane-3-carboxylate (**T6**) To a 20mL vial was added methyl (3*S*)-1-[(2*S*)-2-amino-3-{3-[(triisopropylsilyl)oxy]phenyl}propanoyl]-1,2-diazinane -3-carboxylate (670 mg, 1.45 mmol, 1 equiv), DCM (6.7 mL), DIEA (2.52 mL, 14.45 mmol, 10 equiv), (2*S*)-2-[(*tert*-butoxycarbonyl)amino]-3-methylbutanoic acid (376.72 mg, 1.734 mmol, 1.2 equiv) and HATU (604.35 mg, 1.59 mmol, 1.1 equiv) at 0°C. The reaction was stirred for 1h at 0°C then quenched by the addition of sat. NH_4Cl (aq.). The resulting mixture was extracted with DCM (3x100 mL) and the combined organic layers were washed with water (3x50 mL) then dried over anhydrous Na_2SO_4. After filtration, the filtrate was concentrated under reduced pressure. The residue was purified by silica gel column chromatography, eluted with PE / EA (2:3) to afford methyl (3*S*)-1-[(2*S*)-2-[(2*S*)-2-[(*tert*-butoxycarbonyl)amino]-3-methylbutanamido]-3-{3-[(triisopropylsilyl)oxy]phenyl}propanoyl]-1,2-diazinane-3-carboxylate (640 mg, 58.13% yield) as a yellow solid. ^{1}H NMR (400 MHz, DMSO-d_6) δ 7.61 (d, *J* = 8.6 Hz, 1H), 7.09 (t, *J* = 7.8 Hz, 1H), 6.78 (d, *J* = 7.6 Hz, 1H), 6.72 – 6.64 (m, 3H), 5.55 – 5.47 (m, 1H), 5.26 (d, *J* = 10.1 Hz, 1H), 3.95 – 3.79 (m, 1H), 3.71 (dd, *J* = 9.3, 6.8 Hz, 1H), 3.65 (s, 3H), 3.17 – 2.92 (m, 2H), 2.84 (dd, *J* = 13.4, 5.3 Hz, 1H), 2.63 (dd, *J* = 13.3, 8.2 Hz, 1H), 1.92 – 1.74 (m, 2H), 1.72 – 1.63 (m, 1H), 1.62 – 1.42 (m, 2H), 1.38 (s, 8H), 1.33 (s, 1H), 1.27 – 1.16 (m, 4H), 1.05 (dd, *J* = 7.4, 1.1 Hz, 19H), 0.71 (t, *J* = 7.2 Hz, 6H). ^{13}C NMR (101 MHz, DMSO-d_6) δ 172.05, 171.86, 155.65, 139.80, 129.45, 122.82, 121.00, 117.72, 78.54, 60.50, 52.18, 50.05, 38.48, 31.04, 28.63, 19.68, 18.53, 18.22, 12.53. ESI-MS m/z = 663.4 $[M+H]^+$; calculated for $C_{34}H_{58}N_4O_7Si$: 662.4.

methyl (3S)-1-[(2S)-2-[(2S)-2-amino-3-methylbutanamido]-3-{3-[(triisopropylsilyl)oxy]phenyl}propanoyl]-1,2-diazinane-3-carboxylate (**T7**) To a 20mL vial was added methyl (3*S*)-1-[(2*S*)-2-[(2*S*)-2-[(*tert*-butoxycarbonyl)amino]-3-methylbutanamido]-3 -{3-[(triisopropylsilyl)oxy]phenyl}propanoyl]-1,2-diazinane-3-carboxylate (610 mg, 0.92 mmol, 1 equiv), DCM (6 mL) and 4M HCl (gas)in 1,4-dioxane (3 mL) at 0°C. The reaction was stirred for 2h at 0°C then concentrated under reduced pressure to afford methyl (3*S*)-1-[(2*S*)-2-[(2*S*)-2-amino-3-methylbutanamido]-3-{3-[(triisopropylsilyl)oxy]phenyl}propanoyl]-1,2-diazinane-3-carboxylate (600 mg, crude) as a yellow solid. ^{1}H NMR (400 MHz, DMSO-d_6) δ 7.95 (d, *J* = 8.8 Hz, 1H), 7.14 – 7.06 (m, 1H), 6.75 (d, *J* = 7.6, 1H), 6.70 – 6.63 (m, 2H), 5.54 – 5.45 (m, 1H), 5.28 (d, *J* = 10.0 Hz, 1H), 3.66 (s, 3H), 3.12 (s, 1H), 2.94 (d, *J* = 4.5 Hz, 1H), 2.83 (dd, *J* = 13.3, 5.7 Hz, 1H), 2.70 (dd, *J* = 13.3, 7.5 Hz, 1H), 1.98 – 1.87 (m, 1H), 1.79 (dd, *J* = 13.0, 4.5 Hz, 1H), 1.68 (s, 1H), 1.47 (d, *J* = 10.4 Hz, 1H), 1.29 – 1.17 (m, 4H), 1.07 – 1.03 (m, 18H), 0.99 (d,

J = 6.3 Hz, 1H), 0.83 (d, *J* = 6.8 Hz, 3H), 0.66 (d, *J* = 6.9 Hz, 3H). ^{13}C NMR (101 MHz, DMSO-d_6) δ 173.88, 172.08, 171.88, 139.75, 129.43, 122.82, 121.07, 117.70, 60.17, 58.19, 52.17, 49.79, 40.95, 38.75, 31.34, 27.41, 22.70, 20.05, 18.22, 16.95, 12.53. ESI-MS m/z = 563.4 $[M+H]^+$; calculated for $C_{29}H_{50}N_4O_5Si$: 562.4.

methyl (S)-1-((S)-2-((S)-3-methyl-2-(4-(pyridin-2-yldisulfaneyl)butanamido)butanamido)-3-(3-((triisopropylsilyl)oxy)phenyl)propanoyl)hexahydropyridazine-3-carboxylate (**T8**) To a 20mL vial was added methyl (3*S*)-1-[(2*S*)-2-[(2*S*)-2-amino-3-methylbutanamido]-3-{3-[(triisopropylsilyl)oxy]phenyl}propanoyl]-1,2-diazinane-3-carboxylate (570 mg, 1.01 mmol, 1 equiv), DCM (6 mL), DIEA (1.76 mL, 10.13 mmol, 10 equiv), 4-(pyridin-2-yldisulfanyl)butanoic acid (278.68 mg, 1.216 mmol, 1.2 equiv) and HATU (423.59 mg, 1.11 mmol, 1.1 equiv) at 0°C. The reaction was stirred for 1.5h at 0°C then quenched by the addition of sat. NH_4Cl (aq.) at 0°C. The resulting mixture was extracted with DCM (3x100 mL). The combined organic layers were washed with water (3x50 mL) and dried over anhydrous Na_2SO_4. After filtration, the filtrate was concentrated under reduced pressure. The residue was purified by silica gel column chromatography, eluted with PE / EA (1:1) to afford methyl (*S*)-1-((*S*)-2-((*S*)-3-methyl-2-(4-(pyridin-2-yldisulfaneyl)butanamido)butanamido)-3-(3-((triisopropylsilyl)oxy)phenyl)propanoyl)hexahydropyridazine-3-carboxylate (320 mg, 38.78% yield) as a white solid. ^{1}H NMR (400 MHz, DMSO-d_6) δ 8.44 (d, *J* = 4.8 Hz, 1H), 7.87 – 7.73 (m, 3H), 7.60 (d, *J* = 8.3 Hz, 1H), 7.25 – 7.20 (m, 1H), 7.11 – 7.06 (m, 1H), 6.76 (d, *J* = 7.6 Hz, 1H), 6.69 – 6.64 (m, 2H), 5.45 (q, *J* = 7.6 Hz, 1H), 5.22 (d, *J* = 10.1 Hz, 1H), 4.11 (dd, *J* = 9.0, 6.8 Hz, 1H), 3.97 – 3.76 (m, 1H), 3.65 (s, 3H), 3.06 (s, 2H), 2.81 (t, *J* = 7.3 Hz, 3H), 2.70 – 2.62 (m, 1H), 2.36 – 2.18 (m, 2H), 2.01 – 1.63 (m, 6H), 1.51 (dd, *J* = 46.4, 11.1 Hz, 2H), 1.28 – 1.14 (m, 4H), 1.04 (d, *J* = 7.3 Hz, 20H), 0.75 (dd, *J* = 6.8, 3.0 Hz, 6H). ^{13}C NMR (101 MHz, DMSO-d_6) δ 171.93, 171.64, 170.78, 155.66, 149.99, 138.19, 129.43, 122.83, 121.53, 121.00, 119.54, 117.72, 58.22, 52.16, 50.17, 40.97, 38.29, 37.99, 34.19, 30.78, 27.45, 25.35, 22.70, 19.78, 18.55, 18.22, 12.54. ESI-MS m/z = 774.3 $[M+H]^+$; calculated for $C_{38}H_{59}N_5O_6S_2Si$: 773.4

methyl (S)-1-((S)-3-(3-hydroxyphenyl)-2-((S)-3-methyl-2-(4-(pyridin-2-yldisulfaneyl)butanamido)butanamido)propanoyl)hexahydropyridazine-3-carboxylate (**Compound-1**) To an 8mL vial was added methyl (3*S*)-1-[(2*S*)-2-[(2*S*)-3-methyl-2-[4-(pyridin-2-yldisulfanyl)butanamido]butanamido]-3-{3-[(triisopropylsilyl)oxy]phenyl}propanoyl]-1,2-diazinane-3-carboxylate (102 mg, 0.13 mmol, 1 equiv), DMF (1 mL) and CsF (100.08 mg, 0.66 mmol, 5 equiv) at 0°C. The reaction was stirred for 1h at 0°C then filtered and the filter cake was washed with DMF. After concentration of the filtrate, the crude product was purified by Prep-HPLC with the following conditions: (Column: XBridge Prep OBD C18 Column, 30*150 mm, 5μm; Mobile Phase A: 10mmolNH_4HCO_3+0.05%NH_3H_2O, Mobile Phase B: ACN; Flow rate: 60 mL/min; Gradient: 37% B to 49% B in 8 min, 49% B; Wave Length: 254/220 nm; RT1(min): 4.45; Number Of Runs: 0) to afford (**Compound-1**) (22 mg, 26.54% yield, 98.2% purity @ 254nm, 96.9% purity @ 220nm) as a white solid. ^{1}H NMR (400 MHz, DMSO-d_6) δ 9.22 (s, 1H), 8.53 – 8.34 (m, 1H), 7.89 – 7.73 (m, 3H), 7.62 (d, *J* = 8.2 Hz, 1H), 7.26 – 7.21 (m, 1H), 7.07 – 6.93 (m, 1H), 6.57 (d, *J* = 6.4 Hz, 3H), 5.46 (q, *J* = 7.3 Hz, 1H), 5.10 (d, *J* = 10.4 Hz, 1H), 4.12 (dd, *J* = 9.0, 6.8 Hz, 1H), 3.95 (s, 1H), 3.65 (s, 3H), 3.01 – 2.71 (m, 5H), 2.70 – 2.61 (m, 1H), 2.37 – 2.19 (m, 2H), 1.99 – 1.80 (m, 3H), 1.79 – 1.63 (m, 2H), 1.55 – 1.32 (m, 2H), 0.76 (dd, *J* = 6.8, 3.1 Hz, 6H). ^{13}C NMR (101 MHz, DMSO-d_6) δ 172.04, 171.94, 170.86, 159.74, 157.61, 149.98, 139.29, 138.26, 129.38, 121.58, 120.45, 119.59, 116.75, 113.80, 58.29, 58.09, 52.18,

50.03, 41.02, 38.65, 37.93, 34.17, 30.64, 27.42, 25.32, 22.78, 19.73, 18.50. ESI-MS m/z = 618.20 $[M+H]^+$; calculated for $C_{29}H_{39}N_5O_6S_2$: 617.2.

Synthesis of **Intermediate 1**

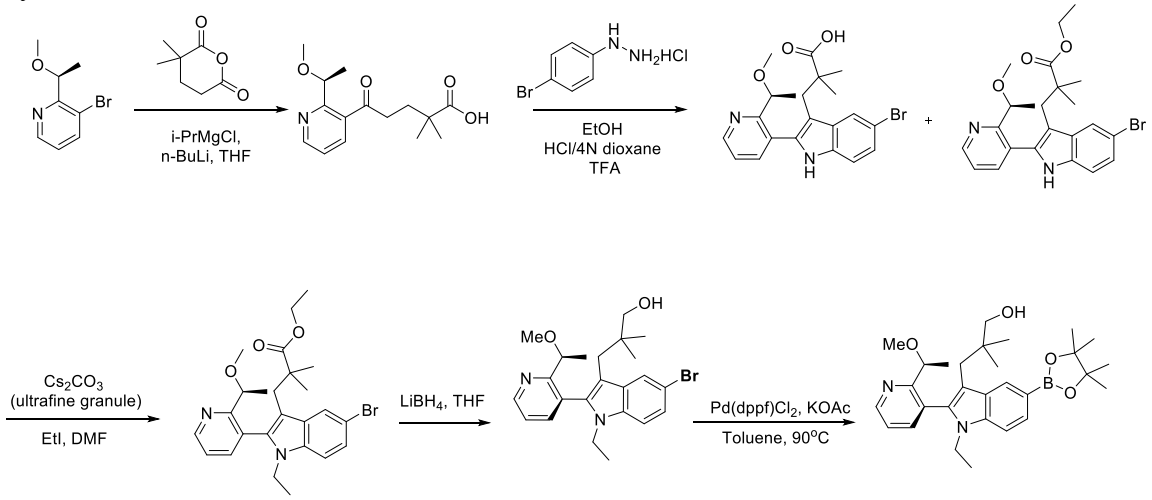

5-[2-[(1S)-1-methoxyethyl]pyridin-3-yl]-2,2-dimethyl-5-oxopentanoic acid (**T9**) To a mixture of *i*-PrMgCl (2M in in THF, 0.5 L) at -10 °C under an atmosphere of N_2 was added *n*-BuLi, 2.5 M in hexane (333 mL, 833 mmol) dropwise over 15 min. The mixture was stirred for 30 min at -10 °C then 3-bromo-2-[(1*S*)-1-methoxyethyl]pyridine (180 g, 833 mmol) in THF (0.5 L) added dropwise over 30 min at -10 °C. The resulting mixture was warmed to -5 °C and stirred for 1 h, then 3,3-dimethyloxane-2,6-dione (118 g, 833 mmol) in THF (1.2 L) was added dropwise over 30 min at -5 °C. The mixture was warmed to 0 °C and stirred for 1.5 h, then quenched with the addition of pre-cooled 4M HCl in 1,4-dioxane (0.6 L) at 0 °C to adjust pH ~5. The mixture was diluted with ice-water (3 L) and extracted with EtOAc (3 x 2.5 L). The combined organic layers were dried over anhydrous Na_2SO_4, filtered, the filtrate was concentrated under reduced pressure, and the residue was purified by silica gel column chromatography to give 5-[2-[(1*S*)-1-methoxyethyl]pyridin-3-yl]-2,2-dimethyl-5-oxopentanoic acid (87 g, 34% yield) as a solid. ^{1}H NMR (400 MHz, DMSO-d_6) δ 12.22 (s, 1H), 8.60 (dd, J = 4.8, 1.7 Hz, 1H), 7.89 (dd, J = 7.7, 1.7 Hz, 1H), 7.39 (dd, J = 7.7, 4.8 Hz, 1H), 4.56 (q, J = 6.5 Hz, 1H), 3.12 (s, 3H), 2.82 – 2.80 (m, 2H), 1.86 – 1.75 (m, 2H), 1.43 (d, J = 6.5 Hz, 3H), 1.13 (s, 6H); ^{13}C NMR (101 MHz, DMSO) δ 204.46, 178.94, 158.72, 149.90, 135.99, 134.91, 122.55, 78.17, 56.70, 41.03, 39.08, 34.12, 25.35, 25.29, 19.88. LCMS (ESI): m/z [M+H] calc'd for $C_{15}H_{21}NO_4$ 279.2; found 280.1.

3-(5-bromo-2-[2-[(1S)-1-methoxyethyl]pyridin-3-yl]-1H-indol-3-yl)-2,2-dimethylpropanoic acid and ethyl (S)-3-(5-bromo-2-(2-(1-methoxyethyl)pyridin-3-yl)-1H-indol-3-yl)-2,2-dimethylpropanoate (**T10**) To a mixture of 5-[2-[(1*S*)-1-methoxyethyl]pyridin-3-yl]-2,2-dimethyl-5-oxopentanoic acid (78 g, 279 mmol) in EtOH (0.78 L) at rt under an atmosphere of N_2 was added (4-bromophenyl)hydrazine HCl salt (68.7 g, 307 mmol) in portions. The mixture was heated to 85 °C and stirred for 2 h, cooled to rt, then 4M HCl in 1,4-dioxane (69.8 mL, 279 mmol) added dropwise. The mixture was heated to 85 °C and stirred for an additional 3 h, then concentrated under reduced pressure, and the residue was dissolved in TFA (0.78 L). The mixture was heated to 60 °C and stirred for 1.5 h, concentrated under reduced pressure, and the

residue adjusted to pH ~5 with saturated $NaHCO_3$, then extracted with EtOAc (3 x 1.5 L). The combined organic layers were dried over anhydrous Na_2SO_4, filtered, the filtrate concentrated under reduced pressure, and the residue was purified by silica gel column chromatography to give 3-(5-bromo-2-[2-[(1*S*)-1-methoxyethyl]pyridin-3-yl]-1*H*-indol-3-yl)-2,2-dimethylpropanoic acid and ethyl (S)-3-(5-bromo-2-(2-(1-methoxyethyl)pyridin-3-yl)-1H-indol-3-yl)-2,2-dimethylpropanoate (78 g, crude). ^{1}H NMR (400 MHz, DMSO-d_6) δ 11.41 (s, 1H), 8.72 (dd, *J* = 4.8, 1.7 Hz, 1H), 7.81 (dd, *J* = 7.7, 1.8 Hz, 1H), 7.67 (d, *J* = 1.9 Hz, 1H), 7.47 (dd, *J* = 7.7, 4.7 Hz, 1H), 7.32 (d, *J* = 8.6 Hz, 1H), 7.22 (dd, *J* = 8.6, 1.9 Hz, 1H), 4.24 (q, *J* = 6.3 Hz, 1H), 3.84 – 3.78 (m, 2H), 2.92 (d, *J* = 21.6 Hz, 4H), 2.78 (d, *J* = 34.5 Hz, 1H), 1.39 (d, *J* = 6.3 Hz, 3H), 1.04 (t, *J* = 7.1 Hz, 3H), 0.92 (d, *J* = 2.7 Hz, 6H); ^{13}C NMR (101 MHz, DMSO) δ 177.11, 150.04, 139.80, 135.34, 135.04, 130.65, 128.40, 124.25, 122.73, 122.01, 113.58, 111.97, 109.55, 75.78, 60.40, 56.02, 43.78, 36.21, 34.70, 31.21, 25.67, 25.58, 14.16. LCMS (ESI): m/z [M+H] calc'd for $C_{21}H_{23}BrN_2O_3$ 430.1 and $C_{23}H_{27}BrN_2O_3$ 458.1; found 431.1 and 459.1. ^{1}H NMR (400 MHz, DMSO-d_6) δ 11.49 (d, *J* = 2.8 Hz, 1H), 8.75 (dd, *J* = 4.9, 1.7 Hz, 1H), 7.95 (d, *J* = 7.7 Hz, 1H), 7.79 (d, *J* = 1.9 Hz, 1H), 7.56 (dd, *J* = 7.8, 4.9 Hz, 1H), 7.36 – 7.20 (m, 2H), 4.26 (q, *J* = 6.3 Hz, 1H), 2.99 (s, 3H), 2.94 – 2.69 (m, 2H), 1.36 (d, *J* = 6.3 Hz, 3H), 0.90 (d, *J* = 4.0 Hz, 6H); ^{13}C NMR (101 MHz, DMSO) δ 179.26, 158.47, 148.83, 141.67, 135.17, 134.45, 130.74, 128.94, 124.44, 123.41, 122.50, 113.67, 112.11, 110.25, 75.53, 56.38, 43.57, 34.47, 25.90, 25.63, 21.19.

ethyl 3-(5-bromo-1-ethyl-2-[2-[(1S)-1-methoxyethyl]pyridin-3-yl]indol-3-yl)-2,2-dimethylpropanoate (**T11**) To a mixture of 3-(5-bromo-2-[2-[(1*S*)-1-methoxyethyl]pyridin-3-yl]-1*H*-indol-3-yl)-2,2-dimethylpropanoic acid and ethyl (S)-3-(5-bromo-2-(2-(1-methoxyethyl)pyridin-3-yl)-1*H*-indol-3-yl)-2,2-dimethylpropanoate (198 g, 459 mmol) in DMF (1.8 L) at 0 °C under an atmosphere of N_2 was added Cs_2CO_3 (449 g, 1.38 mol) in portions. EtI (215 g, 1.38 mmol) in DMF (200 mL) was then added dropwise at 0 °C. The mixture was warmed to rt and stirred for 4 h then diluted with brine (5 L) and extracted with EtOAc (3 x 2.5 L). The combined organic layers were washed with brine (2 x 1.5 L), dried over anhydrous Na_2SO_4, and filtered. The filtrate was concentrated under reduced pressure and the residue was purified by silica gel column chromatography to give ethyl 3-(5-bromo-1-ethyl-2-[2-[(1*S*)-1-methoxyethyl]pyridin-3-yl]indol-3-yl)-2,2-dimethylpropanoate (160 g, 57% yield) as a solid. ^{1}H NMR (400 MHz, Chloroform-*d*) δ 8.84 – 8.82 (m, 1H), 7.73 (dd, *J* = 7.3, 1.9 Hz, 1H), 7.72–7.65 (m, 1H), 7.41 – 7.29 (m, 2H), 7.24 – 7.22 (m, 1H), 4.17 – 3.92 (m, 4H), 3.90 – 3.75 (m, 1H), 3.29 – 3.04 (m, 4H), 2.60 (dd, *J* = 63.6, 14.4 Hz, 1H), 1.48 (d, *J* = 6.3 Hz, 1.6H), 1.27 (d, *J* = 6.4 Hz, 1.8H), 1.23 – 1.14 (m, 6H), 1.06 – 0.99 (m, 6H); ^{13}C NMR (101 MHz, DMSO) δ 177.27, 177.08, 160.05, 159.57, 150.70, 150.46, 140.89, 140.72, 136.91, 136.51, 134.70, 130.17, 130.10, 126.64, 126.05, 124.37, 124.33, 122.92, 122.66, 122.33, 122.24, 112.44, 112.26, 112.24, 110.05, 109.83, 75.84, 75.76, 60.48, 56.23, 56.03, 43.61, 43.54, 38.88, 35.19, 34.81, 26.55, 26.14, 25.31, 25.13, 18.79, 17.86, 15.46, 15.15, 14.19, 14.16. LCMS (ESI): m/z [M+H] calc'd for $C_{25}H_{31}BrN_2O_3$ 486.2; found 487.2.

3-(5-bromo-1-ethyl-2-(2-((S)-1-methoxyethyl)pyridin-3-yl)-1H-indol-3-yl)-2,2-dimethylpropan-1-ol (**T12**) To a mixture of ethyl 3-(5-bromo-1-ethyl-2-[2-[(1*S*)-1-methoxyethyl]pyridin-3-yl]indol-3-yl)-2,2-dimethylpropanoate (160 g, 328 mmol) in THF (1.6 L) at 0 °C under an atmosphere of N_2 was added $LiBH_4$ (28.6 g, 1.3 mol). The mixture was heated to 60 °C for 16 h, cooled, and quenched with pre-cooled (0 °C) aqueous NH_4Cl (5 L). The mixture was extracted with EtOAc (3 x 2 L) and the combined organic layers were washed with

brine (2 x 1 L), dried over anhydrous Na_2SO_4, and filtered. The filtrate was concentrated under reduced pressure and the residue was purified by silica gel column chromatography to give to two atropisomers (as single atropisomers) of 3-(5-bromo-1-ethyl-2-(2-((*S*)-1-methoxyethyl)pyridin-3-yl)-1*H*-indol-3-yl)-2,2-dimethylpropan-1-ol (60 g, 38% yield) and (40 g, 26% yield) both as solids. ^{1}H NMR (400 MHz, DMSO-d_6) δ 8.74 (dd, *J* = 4.8, 1.7 Hz, 1H), 7.93 – 7.80 (m, 2H), 7.55 – 7.45 (m, 2H), 7.28 (dd, *J* = 8.7, 1.8 Hz, 1H), 4.50 (t, *J* = 5.2 Hz, 1H), 4.18 – 3.98 (m, 2H), 3.84 – 3.80 (m, 1H), 3.05 (dd, *J* = 10.2, 5.3 Hz, 1H), 2.96 (dd, *J* = 10.2, 5.2 Hz, 1H), 2.85 (d, *J* = 0.6 Hz, 3H), 2.65 (d, *J* = 13.9 Hz, 1H), 2.12 (d, *J* = 14.0 Hz, 1H), 1.39 (d, *J* = 6.3 Hz, 3H), 1.10 (t, *J* = 7.1 Hz, 3H), 0.58 (d, *J* = 9.9 Hz, 6H); ^{13}C NMR (101 MHz, DMSO) δ 159.64, 150.30, 140.81, 136.55, 134.67, 131.00, 127.09, 124.21, 122.84, 122.72, 112.21, 112.13, 111.28, 75.83, 70.30, 56.03, 38.82, 38.16, 33.20, 25.37, 25.03, 17.90, 15.21. LCMS (ESI): m/z [M+H] calc'd for $C_{23}H_{29}BrN_2O_2$ 444.1; found 445.2.

(S)-3-(1-ethyl-2-(2-(1-methoxyethyl)pyridin-3-yl)-5-(4,4,5,5-tetramethyl-1,3,2-dioxaborolan-2-yl)-1H-indol-3-yl)-2,2-dimethylpropan-1-ol (**Intermediate 1**) To a stirred solution of (S)-3-(5-bromo-1-ethyl-2-(2-(1-methoxyethyl)pyridin-3-yl)-1*H*-indol-3-yl)-2,2-dimethylpropan -1-ol (16.00 g, 35.92 mmol, 1.00 equiv) in toluene (160.00 mL) was added 4,4,4',4',5,5,5',5'-octamethyl-2,2'-bi (1,3,2-dioxaborolane) (13.68 g, 53.88 mmol, 1.50 equiv), KOAc (7.76 g, 79.03 mmol, 2.20 equiv) and Pd(dppf)Cl_2 (2.63 g, 3.59 mmol, 0.10 equiv) at room temperature under argon atmosphere. The resulting mixture was stirred for 3 h at 90 °C under argon atmosphere. After filtration, the filtrate was concentrated under reduced pressure. The residue was purified by silica gel column chromatography to afford (*S*)-3-(1-ethyl-2-(2-(1-methoxyethyl)pyridin-3-yl)-5-(4,4,5,5-tetramethyl-1,3,2-dioxaborolan-2-yl)-1*H*-indol-3-yl)-2,2-dimethylpropan-1-ol (13 g, 66% yield) as a light yellow solid. ^{1}H NMR (400 MHz, DMSO-d_6) δ 8.75 – 8.73 (m, 1H), 8.03 (s, 1H), 7.86 (dd, *J* = 7.7, 1.8 Hz, 1H), 7.54 – 7.47 (m, 3H), 4.46 (t, *J* = 5.4 Hz, 1H), 4.11 – 4.01 (m, 2H), 3.81 (dd, *J* = 14.7, 7.3 Hz, 1H), 3.06 (dd, *J* = 10.3, 5.5 Hz, 1H), 2.97 (dd, *J* = 10.3, 5.4 Hz, 1H), 2.83 (s, 3H), 2.69 (d, *J* = 14.1 Hz, 1H), 2.18 (d, *J* = 14.0 Hz, 1H), 1.39 (d, *J* = 6.2 Hz, 3H), 1.32 (d, *J* = 1.9 Hz, 12H), 1.11 (t, *J* = 7.1 Hz, 3H), 0.64 (s, 3H), 0.54 (s, 3H); ^{13}C NMR (101 MHz, DMSO) δ 170.66, 159.70, 150.13, 140.88, 138.01, 135.20, 128.89, 127.93, 127.44, 122.80, 112.05, 109.60, 83.50, 75.75, 71.14, 60.16, 56.00, 38.60, 38.32, 33.54, 25.41, 25.23, 25.09, 25.07, 25.02, 21.14, 17.92, 15.17, 14.50. LCMS (ESI): m/z [M+H] calc'd for $C_{29}H_{41}BN_2O_4$ 492.3; found 493.2.

Synthesis of **Intermediate Macrocycle 1**

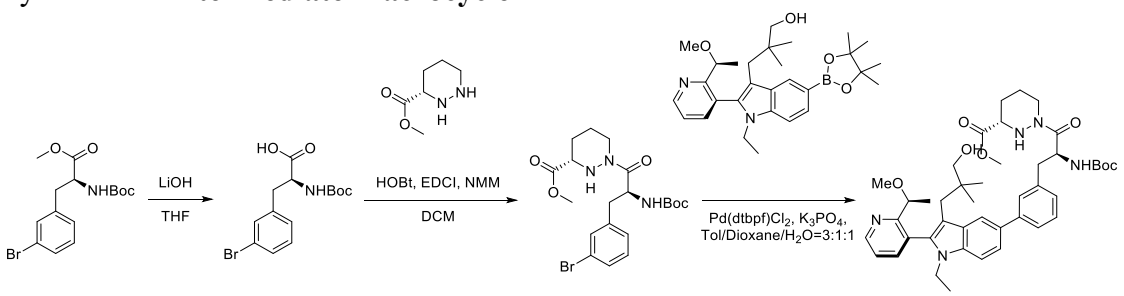

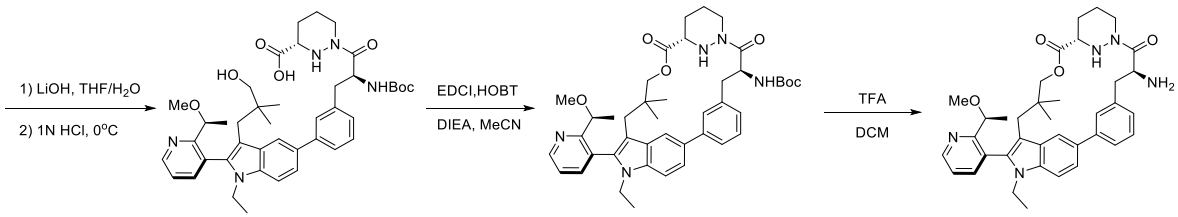

(2S)-3-(3-bromophenyl)-2-[(tert-butoxycarbonyl)amino]propanoic acid (**T13**) To a stirred solution of methyl (2*S*)-3-(3-bromophenyl)-2-[(*tert*-butoxycarbonyl)amino]propanoate (2 g, 5.58 mmol, 1 equiv) in THF (5 mL) was added LiOH.H2O (702.78 mg, 16.75 mmol, 3 equiv) in H_2O (5 mL) dropwise at 0 °C. The resulting reaction was stirred overnight at room temperature then acidified to pH 5~6 with HCl (aq.). The resulting mixture was extracted with EtOAc (3 x 5 mL). The combined organic layers were dried over anhydrous Na_2SO_4. After filtration, the filtrate was concentrated under reduced pressure to afford (2*S*)-3-(3-bromophenyl)-2-[(*tert*-butoxycarbonyl)amino]propanoic acid (2.2 g, crude) as a white solid.^{1}H NMR (400 MHz, DMSO-d_6) δ 7.46 – 7.36 (m, 2H), 7.24 (d, *J* = 6.2 Hz, 2H), 6.98 (d, *J* = 8.3 Hz, 1H),4.10 – 4.07 (m, 1H), 3.04 (dd, *J* = 13.7, 4.5 Hz, 1H), 2.81 (dd, *J* = 13.7, 10.2 Hz, 1H), 1.32 (s, 9H); ^{13}C NMR (101 MHz, DMSO) δ 173.79, 155.81, 141.36, 132.37, 130.61, 129.62, 128.65, 121.85, 78.53, 55.26, 36.56, 28.57.; LCMS (ESI): m/z [M+H] calc'd for $C_{14}H_{18}BrNO_4$ 343.3; found 344.2.

methyl (3S)-1-[(2S)-3-(3-bromophenyl)-2-[(tert-butoxycarbonyl)amino]propanoyl]-1,2-diazinane-3-carboxylate (**T14**) To a stirred solution of methyl (3*S*)-1,2-diazinane-3-carboxylate (942.44 mg, 6.53 mmol, 1.5 equiv) in DCM (15 mL) was added NMM (1.44 mL, 13.07 mmol, 3 equiv) dropwise at 0 °C and stirred for 5 min. To the above mixture was added (2S)-3-(3-bromophenyl)-2-[(*tert*-butoxycarbonyl)amino]propanoic acid (1.5 g, 4.36 mmol, 1 equiv), HOBt (176.66 mg, 1.307 mmol, 0.3 equiv), and EDCI (1.67 g, 8.716 mmol, 2 equiv) at 0 °C. The resulting mixture was stirred for additional 1 h at room temperature then concentrated under reduced pressure to remove the majority of the DCM. The desired product was purified by trituration with DCM (5 mL). The precipitated solids were collected by filtration and washed with DCM (3 x 5 mL). This resulted in methyl (3*S*)-1-[(2*S*)-3-(3-bromophenyl)-2-[(*tert*-butoxycarbonyl)amino]propanoyl]-1,2-diazinane-3-carboxylate (1.5 g, 73.18% yield) as a white solid. ^{1}H NMR (400 MHz, DMSO-d_6) δ 7.41 – 7.39 (m, 2H), 7.26 – 7.23 (m, 2H), 6.69 (d, *J* = 8.8 Hz, 1H), 5.28 (d, *J* = 10.3 Hz, 1H), 5.09 – 5.04 (m, 1H), 3.91 (d, *J* = 22.3 Hz, 1H), 3.70 (s,

3H), 3.36 – 3.35 (m, 1H), 2.99 (s, 1H), 2.85 (dd, *J* = 13.3, 4.0 Hz, 1H), 2.63 (dd, *J* = 13.4, 9.4 Hz, 1H), 1.89 – 1.80 (m, 1H), 1.72 (d, *J* = 11.7 Hz, 1H), 1.61 (d, *J* = 11.3 Hz, 1H), 1.51 (s, 1H), 1.31 (s, 9H); ^{13}C NMR (101 MHz, DMSO) δ 172.48, 171.84, 155.42, 141.91, 132.29, 130.63, 129.56, 128.76, 121.84, 78.32, 58.45, 52.33, 41.02, 37.54, 28.58, 28.21, 27.27, 22.80.; LCMS (ESI): m/z [M+H] calc'd for $C_{20}H_{28}BrN_3O_5$ 469.3; found 470.3.

(S)-1-((S)-2-((tert-butoxycarbonyl)amino)-3-(3-(1-ethyl-3-(3-hydroxy-2,2-dimethylpropyl)-2-(2-((S)-1-methoxyethyl)pyridin-3-yl)-1H-indol-5-yl)phenyl)propanoyl)hexahydropyridazine-3-carboxylate (**T15**) A mixture of methyl (3*S*)-1-[(2*S*)-3-(3-bromophenyl)-2-[(*tert*-butoxycarbonyl)amino]propanoyl]-1,2-diazinane-3-carboxylate (867 mg, 1.84 mmol, 1.00 equiv), 3-[(2M)-1-ethyl-2-{2-[(1*S*)-1-methoxyethyl]pyridin-3-yl}-5-(4,4,5,5-tetramethyl-1,3,2-dioxaborolan-2-yl)indol-3-yl]-2,2-dimethylpropan-1-ol (1.00 g, 2.03 mmol, 1.1 equiv), Pd(dtbpf)Cl_2 (240.27 mg, 0.37 mmol, 0.2 equiv) and K_3PO_4 (0.12 g, 0.55 mmol, 0.3 equiv) in toluene (9 mL), dioxane (3 mL) and H_2O (3 mL) was stirred for 1 h at 80 °C under nitrogen atmosphere. The reaction was cooled to 0 °C and quenched by the addition of Water (10 mL). The resulting mixture was extracted with EtOAc (3 x 8 mL). The combined organic layers were dried over anhydrous Na_2SO_4. After filtration, the filtrate was concentrated under reduced pressure. The residue was purified by reverse phase flash to afford methyl (*S*)-1-((*S*)-2-((*tert*-butoxycarbonyl)amino)-3-(3-(1-ethyl-3-(3-hydroxy-2,2-dimethylpropyl)-2-(2-((S)-1-methoxyethyl)pyridin-3-yl)-1*H*-indol-5-yl)phenyl)propanoyl)hexahydropyridazine-3-carboxylate (312 mg, 22.39% yield) as a white solid. ^{1}H NMR (400 MHz, DMSO-d_6) δ 8.76 – 8.74 (m, 1H), 7.98 – 7.80 (m, 2H), 7.62 – 7.48 (m, 4H), 7.47 – 7.30 (m, 2H), 7.15 (d, *J* = 7.5 Hz, 1H), 6.65 (s, 1H), 5.32 – 5.09 (m, 2H), 4.46 (d, *J* = 5.4 Hz, 1H), 4.20 – 3.92 (m, 3H), 3.89 – 3.72 (m, 1H), 3.59 (s, 3H), 3.25 – 3.06 (m, 2H), 3.04 – 2.90 (m, 3H), 2.88 (s, 3H), 2.77 (dd, *J* = 24.6, 11.4 Hz, 2H), 2.20 (d, *J* = 14.1 Hz, 1H), 1.80 (s, 1H), 1.67 (s, 1H), 1.58 (s, 1H), 1.41 (d, *J* = 6.3 Hz, 4H), 1.31 (s, 7H), 1.21 (s, 1H), 1.15 (t, *J* = 7.2 Hz, 3H), 0.63 (d, *J* = 23.6 Hz, 6H); ^{13}C NMR (101 MHz, DMSO) δ 172.86, 171.91, 159.76, 155.45, 150.26, 142.39, 140.94, 139.20, 135.67, 132.19, 129.74, 129.04, 128.50, 127.74, 125.29, 122.90, 121.32, 118.80, 112.08, 110.52, 78.27, 75.82, 70.71, 58.43, 56.09, 52.14, 38.77, 38.38, 33.54, 28.68, 27.48, 25.39, 25.22, 22.93, 18.16, 15.39.; LCMS (ESI): m/z [M+H] calc'd for $C_{43}H_{57}N_5O_7$ 755.3; found 756.3.

(S)-1-((S)-2-((tert-butoxycarbonyl)amino)-3-(3-(1-ethyl-3-(3-hydroxy-2,2-dimethylpropyl)-2-(2-((S)-1-methoxyethyl)pyridin-3-yl)-1H-indol-5-yl)phenyl)propanoyl)hexahydropyridazine-3-carboxylic acid (**T16**) To a stirred solution of methyl (*S*)-1-((*S*)-2-((*tert*-butoxycarbonyl)amino)-3-(3-(1-ethyl-3-(3-hydroxy-2,2-dimethylpropyl)-2-(2-((*S*)-1-methoxyethyl)pyridin-3-yl)-1*H*-indol-5-yl)phenyl)propanoyl)hexahydropyridazine-3-carboxylate (200 mg, 0.27 mmol, 1 equiv) in THF (4 mL) was added $LiOH{\cdot}H_2O$ (33.30 mg, 0.78 mmol, 3 equiv) in H_2O (4 mL) dropwise at 0 °C. The resulting reaction was stirred for 1 h at room temperature then acidified to pH 5~6 with HCl (aq.). The resulting mixture was extracted with EtOAc (3 x 5 mL). The combined organic layers were dried over anhydrous Na_2SO_4. After filtration, the filtrate was concentrated under reduced pressure to afford (*S*)-1-((*S*)-2-((*tert*-butoxycarbonyl)amino)-3-(3-(1-ethyl-3-(3-hydroxy-2,2-dimethylpropyl)-2-(2-((*S*)-1-methoxyethyl)pyridin-3-yl)-1*H*-indol-5-yl)phenyl)propanoyl)hexahydropyridazine-3-carboxylic acid (228 mg, crude) as a yellow solid. The crude product was used in the next step directly without further purification. ^{1}H NMR (400 MHz, DMSO-d_6) δ 12.72 (s, 1H), 8.75 (dd, *J* = 4.7, 1.7 Hz, 1H), 7.93 (s, 1H), 7.86 (dd, *J* = 7.7,

1.8 Hz, 1H), 7.57 (d, *J* = 8.6 Hz, 1H), 7.54 – 7.48 (m, 3H), 7.44 (dd, *J* = 8.6, 1.7 Hz, 1H), 7.34 (t, *J* = 7.7 Hz, 1H), 7.16 (d, *J* = 7.6 Hz, 1H), 6.64 (d, *J* = 8.7 Hz, 1H), 5.27 – 5.15 (m, 1H), 5.04 (d, *J* = 11.2 Hz, 1H), 4.49 (s, 1H), 4.15 – 4.12 (m, 3H), 3.83 (dd, *J* = 14.6, 7.3 Hz, 1H), 3.10 (d, *J* = 10.4 Hz, 2H), 3.04 – 2.92 (m, 2H), 2.89 (s, 3H), 2.84 – 2.69 (m, 2H), 2.21 (d, *J* = 14.1 Hz, 1H), 1.86 (d, *J* = 11.2 Hz, 1H), 1.70 (d, *J* = 11.9 Hz, 1H), 1.41 (d, *J* = 6.2 Hz, 5H), 1.31 (s, 7H), 1.29 – 1.17 (m, 4H), 0.66 (s, 3H), 0.60 (s, 3H); ^{13}C NMR (101 MHz, DMSO) δ 173.21, 172.70, 159.73, 155.45, 150.25, 142.27, 140.92, 139.19, 135.62, 135.58, 132.12, 129.68, 129.03, 128.44, 127.65, 127.48, 125.24, 122.85, 121.30, 118.76, 112.06, 110.56, 78.24, 75.74, 70.69, 58.60, 56.04, 52.27, 41.00, 38.72, 38.31, 38.19, 33.47, 28.64, 28.33, 27.96, 25.34, 25.19, 23.31, 18.19, 15.37.; LCMS (ESI): m/z [M+H] calc'd for $C_{42}H_{55}N_5O_7$ 741.3; found 742.3.

tert-butyl ((6^{3}S,4S)-11-ethyl-1^2-(2-((S)-1-methoxyethyl)pyridin-3-yl)-10,10-dimethyl-5,7-dioxo-6^1,6^2,6^3,6^4,6^5,6^6-hexahydro-1^{1}H-8-oxa-1(5,3)-indola-6(1,3)-pyridazina-2(1,3)-benzenacycloundecaphane-4-yl)carbamate (**T17**) To a stirred solution of (*S*)-1-((*S*)-2-((*tert*-butoxycarbonyl)amino)-3-(3-(1-ethyl-3-(3-hydroxy-2,2-dimethylpropyl)-2-(2-((*S*)-1-methoxyethyl)pyridin-3-yl)-1*H*-indol-5-yl)phenyl)propanoyl)hexahydropyridazine-3-carboxylic acid (40 g, 53.91 mmol, 1.00 equiv) and DIEA (209.04 g, 1617.39 mmol, 30 equiv) in DCM (3 L) was added HOBT (36.42 g, 269.565 mmol, 5 equiv) and EDCI (289.39 g, 1509.564 mmol, 28 equiv) in portions at 0 °C. The resulting mixture was stirred for 16 h at room temperature then washed with 3 x 1 L of water. The combined organic layers were concentrated under reduced pressure and purified by silica gel column chromatography to afford *tert*-butyl ((6^3*S*,4*S*)-11-ethyl-1^2-(2-((*S*)-1-methoxyethyl)pyridin-3-yl)-10,10-dimethyl-5,7-dioxo-6^1,6^2,6^3,6^4,6^5,6^6-hexahydro-1^1*H*-8-oxa-1(5,3)-indola-6(1,3)-pyridazina-2(1,3)-benzenacycloundecaphane-4-yl)carbamate (30 g, 73.79%) as a yellow solid. ^{1}H NMR (400 MHz, DMSO-*d*$_6$) δ 8.78 – 8.76 (m, 1H), 8.00 (s, 1H), 7.92 – 7.81 (m, 2H), 7.75 – 7.65 (m, 2H), 7.61 (d, *J* = 8.7 Hz, 1H), 7.54 (dd, *J* = 7.7, 4.7 Hz, 1H), 7.32 (t, *J* = 7.7 Hz, 1H), 7.16 (d, *J* = 7.5 Hz, 1H), 7.07 (d, *J* = 8.7 Hz, 1H), 5.38 (d, *J* = 12.2 Hz, 1H), 5.07 (dd, *J* = 9.9, 7.6 Hz, 1H), 4.36 – 4.13 (m, 3H), 4.07 – 3.88 (m, 2H), 3.74 – 3.57 (m, 2H), 3.44 (s, 4H), 2.88 – 2.78 (m, 4H), 2.01 (d, *J* = 12.0 Hz, 1H), 1.82 (d, *J* = 12.4 Hz, 1H), 1.73 – 1.50 (m, 2H), 1.40 (d, *J* = 6.2 Hz, 3H), 1.33 (s, 7H), 1.15 (s, 2H), 0.98 (t, *J* = 7.1 Hz, 3H), 0.74 (s, 3H), 0.58 (s, 3H); ^{13}C NMR (101 MHz, DMSO) δ 173.42, 171.97, 159.31, 155.85, 150.06, 141.28, 140.99, 140.18, 136.61, 135.79, 130.36, 130.15, 129.50, 129.09, 128.03, 127.36, 125.46, 123.78, 123.49, 120.06, 115.97, 111.51, 111.19, 110.23, 78.14, 75.96, 70.98, 59.51, 56.16, 53.92, 38.45, 38.29, 35.96, 32.77, 31.76, 28.71, 25.91, 25.37, 17.24, 15.14.; LCMS (ESI): m/z [M+H] calc'd for $C_{42}H_{53}N_5O_6$ 723.3; found 724.3.

((6^{3}S,4S)-4-amino-1^1-ethyl-1^2-(2-((S)-1-methoxyethyl)pyridin-3-yl)-10,10-dimethyl-6^1,6^2,6^3,6^4,6^5,6^6-hexahydro-1^{1}H-8-oxa-1(5,3)-indola-6(1,3)-pyridazina-2(1,3)-benzenacycloundecaphane-5,7-dione (**Intermediate Macrocycle 1**) To a solution of *tert*-butyl ((6^3*S*,4*S*)-11-ethyl-1^2-(2-((*S*)-1-methoxyethyl)pyridin-3-yl)-10,10-dimethyl-5,7-dioxo-6^1,6^2,6^3,6^4,6^5,6^6-hexahydro-1^1*H*-8-oxa-1(5,3)-indola-6(1,3)-pyridazina-2(1,3)-benzenacycloundecaphane-4-yl)carbamate (5 g, 6.907 mmol, 1 equiv) in dioxane (20 mL) was added HCl(gas) in 1,4-dioxane (30 mL) at 0 °C. The reaction was stirred for 1 h at 0 °C then the resulting mixture was concentrated under reduced pressure to afford **Intermediate Macrocycle 1** (5 g, 98.64% yield)) which was used in the next step directly without further purification. ^{1}H NMR (400 MHz, DMSO-*d*$_6$) δ 8.78 – 8.76 (m, 1H), 8.46 (s, 2H), 7.87 –7.84 (m, 2H), 7.70 – 7.52 (m, 4H), 7.41 (t, *J* = 7.6 Hz, 1H), 7.17 (d, *J* = 7.5 Hz, 1H), 5.49 (d, *J* = 11.9 Hz, 1H), 4.81 (dd, *J*

= 7.9, 3.6 Hz, 1H), 4.34 – 4.15 (m, 2H), 4.22 – 4.00 (m, 1H), 3.66 – 3.56 (m, 2H), 3.21 – 3.12 (m, 1H), 3.07 (s, 2H), 2.99 (dd, *J* = 14.7, 7.9 Hz, 1H), 2.90 – 2.69 (m, 3H), 2.57 (d, *J* = 13.8 Hz, 1H), 1.96 (d, *J* = 7.9 Hz, 1H), 1.87 – 1.77 (m, 1H), 1.57 (d, *J* = 9.9 Hz, 2H), 1.48 – 1.33 (m, 5H), 1.22 (d, *J* = 9.8 Hz, 1H), 1.21 – 1.00 (m, 3H), 0.90 – 0.76 (m, 2H), 0.72 (s, 2H), 0.59 (s, 2H); ^{13}C NMR (101 MHz, DMSO) δ 171.50, 169.64, 163.53, 159.37, 150.27, 141.81, 140.62, 137.81, 136.49, 135.64, 131.08, 129.93, 129.45, 127.89, 127.27, 126.45, 125.21, 123.35, 120.44, 117.26, 111.39, 111.01, 76.02, 71.25, 58.87, 56.10, 51.85, 41.18, 38.50, 37.48, 35.83, 32.80, 29.48, 28.60, 28.48, 25.74, 25.56, 23.04, 19.83, 18.99, 17.36, 15.16, 14.37, 1.60.; LCMS (ESI): m/z [M+H] calc'd for $C_{37}H_{45}N_5O_4$ 623.3; found 624.3.

Synthesis of **Intermediate Macrocycle 2**

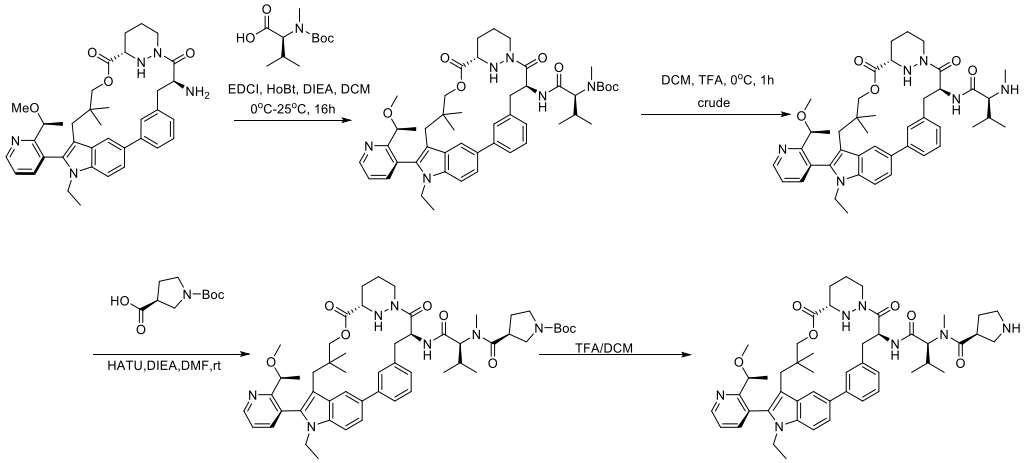

tert-butyl ((2S)-1-(((6^{3}S,4S)-1^1-ethyl-1^2-(2-((S)-1-methoxyethyl) pyridin-3-yl)-10,10-dimethyl-5,7-dioxo-6^1,6^2,6^3,6^4,6^5,6^6-hexahydro-1^{1}H-8-oxa-1(5,3)-indola-6(1,3)-pyridazina-2(1,3)-benzenacycloundecaphane-4-yl) amino)-3-methyl-1-oxobutan-2-yl) (methyl)carbamate (**T18**) To a stirred solution of (6^3*S*,4*S*)-4-amino-1^1-ethyl-1^2-(2-((*S*)-1-methoxyethyl) pyridin-3-yl)-10,10-dimethyl-6^1,6^2,6^3,6^4,6^5,6^6-hexahydro-1^1*H*-8-oxa-1(5,3)-indola-6(1,3)-pyridazina-2(1,3)-benzenacycloundecaphane-5,7-dione (5 g, 8.02 mmol, 1 equiv) and (2S)-2-[(*tert*-butoxycarbonyl)(methyl)amino]-3-methylbutanoic acid (2.22 g, 9.62 mmol, 1.2 equiv) in DMF (50.00 mL) was added HATU (6.10 g, 16.03 mmol, 2 equiv) followed by DIEA (10.36 g, 80.15 mmol, 10 equiv) dropwise at 0 °C. The resulting reaction was stirred for 1 h then quenched with water (50 mL). The resulting mixture was extracted with EtOAc (2 x 50 mL). The combined organic layers were washed with brine (3 x 100 mL) and dried over anhydrous Na_2SO_4. After filtration, the filtrate was concentrated under reduced pressure. The residue was purified by silica gel column chromatography, eluted with CH_2Cl_2 / MeOH (10:1) to afford *tert*-butyl ((2*S*)-1-(((6^3*S*,4*S*)-1^1-ethyl-1^2-(2-((*S*)-1-methoxyethyl) pyridin-3-yl)-10,10-dimethyl-5,7-dioxo-6^1,6^2,6^3,6^4,6^5,6^6-hexahydro-1^1*H*-8-oxa-1(5,3)-indola-6(1,3)-pyridazina-2(1,3)-benzenacycloundecaphane-4-yl) amino)-3-methyl-1-oxobutan-2-yl) (methyl)carbamate (5 g, 67.07%) as a white solid. ^{1}H NMR (400 MHz, DMSO-d_6) δ 8.77 (dd, *J* = 4.7, 1.7 Hz, 1H), 8.14 (s, 1H), 8.00 (s, 1H), 7.83 (dd, *J* = 7.7, 1.8 Hz, 2H), 7.72 (d, *J* = 8.7 Hz, 1H), 7.67 (d, *J* = 7.8 Hz, 1H), 7.62 (d, *J* = 8.6 Hz, 1H), 7.53 (dd, *J* = 7.7, 4.7 Hz, 1H), 7.23 (t, *J* = 7.7 Hz, 1H), 7.15 (d, *J* = 7.5 Hz, 1H), 5.32 (s, 2H), 4.34 – 4.18 (m, 4H), 4.08 (s, 1H), 3.69 (d, *J* = 10.9 Hz, 1H), 3.61 (d, *J* = 10.9 Hz, 1H), 3.15 (s, 3H), 2.88 (d, *J* = 11.1 Hz, 2H), 2.77 (s, 2H), 2.65 (s, 4H), 2.05 (s, 1H), 1.83 (d, *J* = 12.3 Hz, 1H), 1.69 (d, *J* = 12.1 Hz, 1H), 1.56 (d, *J* = 13.2 Hz, 1H), 1.47 (s, 9H), 1.39

(d, *J* = 6.1 Hz, 3H), 0.93 (dd, *J* = 15.7, 8.0 Hz, 6H), 0.79 (s, 6H), 0.50 (s, 3H); ^{13}C NMR (101 MHz, DMSO) δ 170.79, 170.63, 169.99, 168.29, 157.36, 153.98, 153.35, 148.15, 138.97, 138.55, 138.27, 134.89, 133.77, 128.36, 128.20, 126.98, 125.21, 124.88, 123.77, 121.86, 121.37, 118.07, 116.34, 113.98, 109.45, 109.13, 77.39, 77.23, 74.05, 68.79, 62.22, 61.15, 54.05, 49.85, 33.89, 30.71, 27.97, 27.55, 27.19, 26.53, 25.27, 24.79, 24.02, 23.07, 21.39, 17.77, 17.32, 17.06, 14.85, 13.01.; LCMS (ESI): m/z [M+H] calc'd for $C_{48}H_{64}N_6O_7$ 836.3; found 837.2.

Step 2

(2S)-N-((6^{3}S,4S)-1^1-ethyl-1^2-(2-((S)-1-methoxyethyl) pyridin-3-yl)-10,10-dimethyl-5,7-dioxo-6^1,6^2,6^3,6^4,6^5,6^6-hexahydro-1^{1}H-8-oxa-1(5,3)-indola-6(1,3)-pyridazina-2(1,3)-benzenacycloundecaphane-4-yl)-3-methyl-2-(methylamino) butanamide (**T19**) To a solution of *tert*-butyl ((2*S*)-1-(((6^3*S*,4*S*)-1^1-ethyl-1^2-(2-((*S*)-1-methoxyethyl) pyridin-3-yl)-10,10-dimethyl-5,7-dioxo-6^1,6^2,6^3,6^4,6^5,6^6-hexahydro-1^{1}H-8-oxa-1(5,3)-indola-6(1,3)-pyridazina-2(1,3)-benzenacycloundecaphane-4-yl) amino)-3-methyl-1-oxobutan-2-yl) (methyl)carbamate (5 g, 5.97 mmol, 1 equiv) in DCM (30 mL) was added TFA (10 mL, 134.63 mmol, 22.54 equiv) dropwise and the reaction stirred for 1 h at 0°C. The resulting mixture was concentrated under reduced pressure. The residue was dissolved in EtOAc (50 mL) and neutralized to pH 9 with saturated $NaHCO_3$ (100 mL). The resulting mixture was extracted with EtOAc (3 x 30 mL). The combined organic layers were washed with brine (1 x 100 mL) and dried over anhydrous Na_2SO_4. After filtration, the filtrate was concentrated under reduced pressure. This resulted in (2*S*)-N-((6^3*S*,4*S*)-1^1-ethyl-1^2-(2-((*S*)-1-methoxyethyl) pyridin-3-yl)-10,10-dimethyl-5,7-dioxo-6^1,6^2,6^3,6^4,6^5,6^6-hexahydro-1^1*H*-8-oxa-1(5,3)-indola-6(1,3)-pyridazina-2(1,3)-benzenacycloundecaphane-4-yl)-3-methyl-2-(methylamino) butanamide (5 g, crude) as a white solid. The crude product was used in the next step directly without further purification. ^{1}H NMR (400 MHz, DMSO-*d*$_6$) δ 8.77 (dd, *J* = 4.7, 1.7 Hz, 1H), 8.51 (s, 1H), 8.02 (s, 1H), 7.91 (s, 1H), 7.84 (dd, *J* = 7.7, 1.8 Hz, 1H), 7.72 (dd, *J* = 8.8, 1.7 Hz, 1H), 7.67 (d, *J* = 8.0 Hz, 1H), 7.62 (d, *J* = 8.7 Hz, 1H), 7.53 (dd, *J* = 7.8, 4.7 Hz, 1H), 7.28 (t, *J* = 7.7 Hz, 1H), 7.13 (d, *J* = 7.6 Hz, 1H), 5.59 – 5.40 (m, 2H), 4.34 – 4.19 (m, 3H), 4.02 – 4.01 (m, 1H), 3.65 (q, *J* = 11.0 Hz, 2H), 3.11 (s, 3H), 2.99 (d, *J* = 13.7 Hz, 1H), 2.85 – 2.75 (m, 2H), 2.72 (d, *J* = 8.7 Hz, 2H), 2.21 (s, 2H), 2.03 (d, *J* = 12.9 Hz, 1H), 1.92 – 1.78 (m, 2H), 1.68 (d, *J* = 12.6 Hz, 1H), 1.56 (d, *J* = 16.2 Hz, 1H), 1.40 (d, *J* = 6.0 Hz, 3H), 1.00 – 0.90 (m, 5H), 0.90 – 0.72 (m, 6H), 0.55 (s, 3H); ^{13}C NMR (101 MHz, DMSO) δ 172.50, 172.03, 170.77, 169.98, 159.40, 150.22, 140.65, 140.31, 136.82, 135.78, 130.34, 130.18, 129.02, 127.27, 127.10, 125.75, 123.93, 123.36, 120.02, 116.07, 111.43, 111.15, 76.08, 70.92, 68.54, 60.20, 56.07, 52.06, 38.42, 35.97, 33.80, 32.76, 30.72, 29.26, 25.92, 25.28, 23.40, 21.13, 19.21, 19.18, 17.08, 15.07, 14.48.; LCMS (ESI): m/z [M+H] calc'd for $C_{43}H_{56}N_6O_5$ 736.3; found 737.2.

tert-butyl (3S)-3-(((2S)-1-(((6^{3}S,4S)-1^1-ethyl-1^2-(2-((S)-1-methoxyethyl) pyridin-3-yl)-10,10-dimethyl-5,7-dioxo-6^1,6^2,6^3,6^4,6^5,6^6-hexahydro-1^{1}H-8-oxa-1(5,3)-indola-6(1,3)-pyridazina-2(1,3)-benzenacycloundecaphane-4-yl) amino)-3-methyl-1-oxobutan-2-yl) (methyl)carbamoyl) pyrrolidine-1-carboxylate (**T20**) To a stirred solution of (2*S*)-N-((6^3*S*,4*S*)-1^1-ethyl-1^2-(2-((*S*)-1-methoxyethyl) pyridin-3-yl)-10,10-dimethyl-5,7-dioxo-6^1,6^2,6^3,6^4,6^5,6^6-hexahydro-1^1*H*-8-oxa-1(5,3)-indola-6(1,3)-pyridazina-2(1,3)-benzenacycloundecaphane-4-yl)-3-methyl-2-(methylamino) butanamide (3 g, 4.07 mmol, 1 equiv) and (S)-1-(*tert*-butoxycarbonyl)pyrrolidine-3-carboxylic acid (1.75 g, 8.14 mmol, 2 equiv) in DMF (30 mL) was added HATU (2.32 g, 6.106 mmol, 1.5 equiv) and DIEA (2.63 g, 20.36 mmol, 5 equiv) dropwise

at 0 °C. The resulting mixture was stirred for 1 h at 0 °C then quenched by the addition of water (50 mL). The resulting mixture was extracted with EtOAc (3 x 30 mL). The combined organic layers were washed with brine (3 x 50 mL) and dried over anhydrous Na_2SO_4. After filtration, the filtrate was concentrated under reduced pressure. The residue was purified by silica gel column chromatography, eluted with CH_2Cl_2 / MeOH (10:1) to afford *tert*-butyl (3*S*)-3-(((2*S*)-1-(((6^3*S*,4*S*)-1^1-ethyl-1^2-(2-((*S*)-1-methoxyethyl) pyridin-3-yl)-10,10-dimethyl-5,7-dioxo-6^1,6^2,6^3,6^4,6^5,6^6-hexahydro-1^1*H*-8-oxa-1(5,3)-indola-6(1,3)-pyridazina-2(1,3)-benzenacycloundecaphane-4-yl) amino)-3-methyl-1-oxobutan-2-yl) (methyl)carbamoyl) pyrrolidine-1-carboxylate (3 g, 71.00%) as a white solid. ^{1}H NMR (400 MHz, DMSO-d_6) δ 8.77 (dd, *J* = 4.8, 1.7 Hz, 1H), 8.77 – 8.21 (m, 1H), 8.00 (s, 1H), 7.91 – 7.80 (m, 2H), 7.77 – 7.59 (m, 3H), 7.54 – 7.53 (m, 1H), 7.50 – 7.25 (m, 1H), 7.14 – 6.99 (m, 1H), 5.34 – 5.32 (m, 2H), 4.71 – 4.68 (m, 1H), 4.26 (dd, *J* = 6.2, 3.3 Hz, 3H), 3.99 (d, *J* = 13.7 Hz, 1H), 3.72 – 3.51 (m, 3H), 3.51 – 3.37 (m, 2H), 3.28 (s, 1H), 3.12 (d, *J* = 5.3 Hz, 3H), 3.06 – 2.89 (m, 1H), 2.76 (t, *J* = 17.9 Hz, 7H), 2.04 – 1.94 (m, 3H), 1.93 (d, *J* = 11.1 Hz, 1H), 1.83 (d, *J* = 12.1 Hz, 1H), 1.69 (s, 1H), 1.57 (s, 1H), 1.50 – 1.26 (m, 13H), 1.25 (d, *J* = 9.1 Hz, 1H), 1.02 – 0.92 (m, 4H), 0.91 – 0.66 (m, 8H), 0.54 (s, 3H); ^{13}C NMR (101 MHz, DMSO) δ 171.11, 170.64, 170.52, 169.99, 168.24, 167.80, 157.40, 151.89, 151.77, 148.18, 138.99, 138.60, 138.41, 138.21, 134.85, 133.82, 133.77, 128.19, 126.91, 125.24, 123.58, 122.00, 121.34, 118.00, 116.35, 113.94, 109.42, 109.16, 76.85, 76.75, 76.62, 74.03, 68.87, 62.79, 59.56, 54.07, 47.60, 46.73, 43.78, 36.37, 33.93, 30.71, 28.76, 27.84, 27.51, 27.24, 26.62, 26.56, 25.96, 24.62, 23.98, 23.89, 23.27, 23.14, 21.41, 18.07, 17.52, 17.42, 16.91, 14.96, 13.03.; LCMS (ESI): m/z [M+H] calc'd for $C_{53}H_{71}N_7O_8$ 933.5; found 934.5.

(3S)-N-((2S)-1-(((6^{3}S,4S)-1^1-ethyl-1^2-(2-((S)-1-methoxyethyl) pyridin-3-yl)-10,10-dimethyl-5,7-dioxo-6^1,6^2,6^3,6^4,6^5,6^6-hexahydro-1^{1}H-8-oxa-1(5,3)-indola-6(1,3)-pyridazina-2(1,3)-benzenacycloundecaphane-4-yl) amino)-3-methyl-1-oxobutan-2-yl)-N-methylpyrrolidine-3-carboxamide (**Intermediate Macrocycle 2**) To a solution of *tert*-butyl (3*S*)-3-(((2*S*)-1-(((6^3*S*,4*S*)-1^1-ethyl-1^2-(2-((*S*)-1-methoxyethyl) pyridin-3-yl)-10,10-dimethyl-5,7-dioxo-6^1,6^2,6^3,6^4,6^5,6^6-hexahydro-1^1*H*-8-oxa-1(5,3)-indola-6(1,3)-pyridazina-2(1,3)-benzenacycloundecaphane-4-yl) amino)-3-methyl-1-oxobutan-2-yl) (methyl)carbamoyl) pyrrolidine-1-carboxylate (3 g, 3.21 mmol, 1 equiv) in DCM (24 mL) was added TFA (8 mL, 107.71 mmol, 33.54 equiv) and the reaction stirred for 1 h at 0°C. The resulting mixture was concentrated under reduced pressure. The residue was dissolved in EtOAc (20 mL) and neutralized to pH 9 with saturated $NaHCO_3$ (100 mL). The resulting mixture was extracted with EtOAc (3 x 30 mL). The combined organic layers were washed with brine (1 x 100 mL) and dried over anhydrous Na_2SO_4. After filtration, the filtrate was concentrated under reduced pressure. This resulted in **Intermediate Macrocycle 2** (3 g, crude) as a white solid. The crude product was used in the next step directly without further purification. ^{1}H NMR (400 MHz, DMSO-d_6) δ 8.77 (dd, *J* = 4.7, 1.8 Hz, 1H), 8.77 – 8.21 (m, 1H), 8.00 (s, 1H), 7.94 – 7.81 (m, 2H), 7.75 – 7.59 (m, 3H), 7.58 – 7.47 (m, 1H), 7.28 (dt, *J* = 20.3, 7.7 Hz, 1H), 7.08 (dd, *J* = 15.9, 7.5 Hz, 1H), 5.37 (d, *J* = 9.0 Hz, 2H), 4.69 – 4.43 (m, 1H), 4.37 – 4.14 (m, 3H), 3.96 – 3.95(m, 1H),3.70 – 3.61 (m, 2H), 3.54 – 3.42 (m, 2H), 3.25 – 3.13 (m, 3H), 3.10 (d, *J* = 8.0 Hz, 3H), 3.00 (d, *J* = 13.6 Hz, 1H), 2.90 – 2.67 (m, 7H), 2.25 – 2.15 (m, 3H), 1.83 – 1.75 (m, 2H), 1.74 – 1.48 (m, 3H), 1.40 (d, *J* = 6.1 Hz, 3H), 1.25 (d, *J* = 9.2 Hz, 1H), 0.98 (d, *J* = 6.7 Hz, 4H), 0.92 (d, *J* = 6.4 Hz, 2H), 0.81 – 0.68 (m, 6H), 0.57 (d, *J* = 11.3 Hz, 3H); ^{13}C NMR (101 MHz, DMSO) δ 172.67, 172.62, 172.38, 172.01, 170.12, 169.73, 159.98, 159.66, 159.41, 159.35, 159.03, 150.25, 140.95, 140.76, 140.67, 140.31, 140.21, 136.83, 136.77, 135.81, 135.78, 130.27, 130.16, 129.09,

128.97, 127.23, 127.09, 125.61, 123.83, 123.35, 122.05, 119.99, 119.09, 116.13, 115.93, 113.17, 111.43, 111.18, 76.03, 70.95, 64.88, 61.74, 56.09, 48.05, 47.63, 45.47, 45.23, 39.30, 38.42, 38.19, 35.95, 32.74, 30.98, 29.85, 29.60, 29.25, 28.94, 28.12, 26.86, 25.91, 25.82, 25.39, 25.25, 23.41, 20.13, 19.43, 19.38, 18.98, 17.24, 17.10, 15.07, 1.51.; LCMS (ESI): m/z [M+H] calc'd for $C_{48}H_{63}N_7O_6$ 833.5; found 834.5.

Synthesis of **Compound-2**

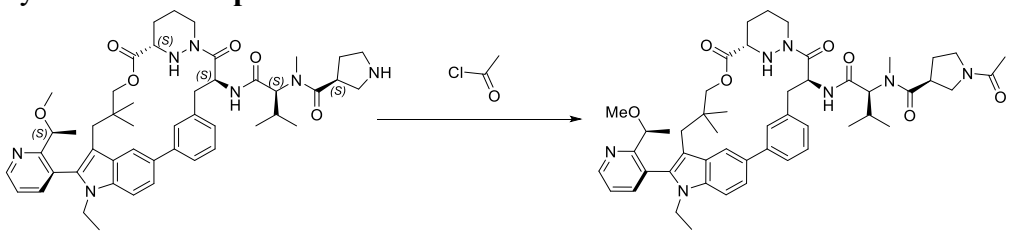

(3S)-1-acetyl-N-((2S)-1-(((6³S,4S)-1¹-ethyl-1²-(2-((S)-1-methoxyethyl)pyridin-3-yl)-10,10-dimethyl-5,7-dioxo-6¹,6²,6³,6⁴,6⁵,6⁶-hexahydro-1¹H-8-oxa-1(5,3)-indola-6(1,3)-pyridazina-2(1,3)-benzenacycloundecaphane-4-yl)amino)-3-methyl-1-oxobutan-2-yl)-N-methylpyrrolidine-3-carboxamide (**Compound-2**) To a stirred solution of (3*S*)-N-((2*S*)-1-(((6³*S*,4*S*)-1¹-ethyl-12-(2-((S)-1-methoxyethyl)pyridin-3-yl)-10,10-dimethyl-5,7-dioxo-6¹,6²,6³,6⁴,6⁵,6⁶-hexahydro-1¹*H*-8-oxa-1(5,3)-indola-6(1,3)-pyridazina-2(1,3)-benzenacycloundecaphane-4-yl)amino)-3-methyl-1-oxobutan-2-yl)-*N*-methylpyrrolidine-3-carboxamide (290 mg, 0.35 mmol, 1 equiv) and TEA (105.55 mg, 1.04 mmol, 3 equiv) in DCM (5 mL) was added acetyl chloride (30.02 mg, 0.38 mmol, 1.1 equiv) dropwise at 0 °C under nitrogen atmosphere. The resulting mixture was stirred for 2 h at 0 °C then quenched with water (10 mL). The resulting mixture was extracted with EtOAc (2 x 10 mL). The combined organic layers were washed with brine (2 x 10 mL) and dried over anhydrous Na_2SO_4. After filtration, the filtrate was concentrated under reduced pressure. The residue was purified by Prep-TLC ($CH2Cl_2$ / MeOH 15:1) to afford (3*S*)-1-acetyl-N-((2*S*)-1-(((6³*S*,4*S*)-1¹-ethyl-1²-(2-((*S*)-1-methoxyethyl)pyridin-3-yl)-10,10-dimethyl-5,7-dioxo-6¹,6²,6³,6⁴,6⁵,6⁶-hexahydro-1¹*H*-8-oxa-1(5,3)-indola-6(1,3)-pyridazina-2(1,3)-benzenacycloundecaphane-4-yl)amino)-3-methyl-1-oxobutan-2-yl)-*N*-methylpyrrolidine-3-carboxamide (80 mg) as a light yellow crude solid. This was further purified by Prep-HPLC with the following conditions (Column: XBridge Prep OBD C18 Column, 30*150 mm, 5μm; Mobile Phase A: Water(10 mmol/L NH_4HCO_3), Mobile Phase B: ACN; Flow rate: 60 mL/min; Gradient: 36% B to 58% B in 8 min, 58% B; Wave Length: 254/220 nm; RT1(min): 7.95) to afford **Compound-2** (28.5 mg, 10%yield) as a white solid. ^{1}H NMR (400 MHz, DMSO-d_6) δ 8.81 – 8.74 (m, 1H), 8.72 – 8.18 (m, 1H), 8.00 (s, 1H), 7.92 – 7.81 (m, 2H), 7.77 – 7.58 (m, 3H), 7.54 (dd, *J* = 7.7, 4.8 Hz, 1H), 7.36 – 7.18 (m, 1H), 7.09 (q, *J* = 7.5 Hz, 1H), 5.47 – 5.25 (m, 2H), 4.36 – 4.19 (m, 3H), 4.03 – 4.01 (m, 3H), 3.73 – 3.49 (m, 7H), 3.13 – 3.11 (m, 3H), 2.97 – 2.66 (m, 8H), 2.22 – 1.92 (m, 7H), 1.87 – 1.53 (m, 4H), 1.40 (d, *J* = 6.1 Hz, 3H), 1.02 – 0.87 (m, 6H), 0.86 – 0.70 (m, 6H), 0.54 (s, 3H); ^{13}C NMR (101 MHz, DMSO) δ 172.76, 172.52, 172.03, 170.37, 169.82, 159.29, 150.11, 140.88, 140.25, 136.74, 135.83, 135.78, 130.15, 128.99, 127.31, 127.02, 125.64, 123.90, 123.51, 120.07, 115.91, 111.49, 75.99, 70.89, 70.27, 64.73, 61.57, 56.16, 49.66, 49.18, 48.39, 47.03, 46.84, 45.44, 45.22, 35.95, 32.72, 30.86, 30.19, 29.30, 26.00, 25.92, 25.20, 22.77, 22.62, 20.10, 19.55, 19.01, 17.10, 15.10.; HRMS(ESI$^+$, m/z) calc'd for $(C_{50}H_{66}N_7O_7)^+$: 876.50182 $[M+H]^+$, found 876.49890

Synthesis of **Compound-3**

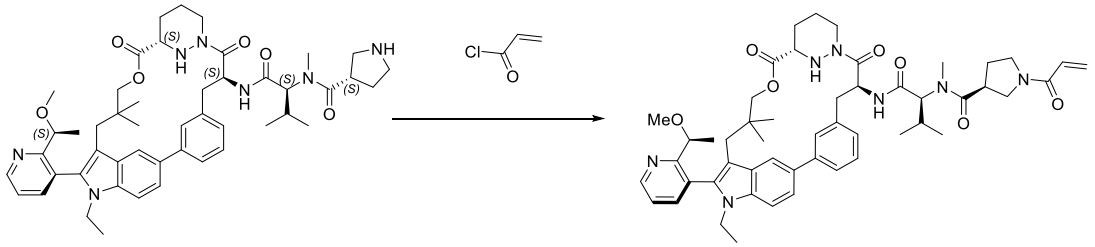

(3S)-1-acryloyl-N-((2S)-1-(((6³S,4S)-1¹-ethyl-1²-(2-((S)-1-methoxyethyl)pyridin-3-yl)-10,10-dimethyl-5,7-dioxo-6¹,6²,6³,6⁴,6⁵,6⁶-hexahydro-1¹H-8-oxa-1(5,3)-indola-6(1,3)-pyridazina-2(1,3)-benzenacycloundecaphane-4-yl)amino)-3-methyl-1-oxobutan-2-yl)-N-methylpyrrolidine-3-carboxamide (**Compound-3**) To a stirred solution of (3*S*)-N-((2*S*)-1-(((6³*S*,4*S*)-1¹-ethyl-12-(2-((S)-1-methoxyethyl)pyridin-3-yl)-10,10-dimethyl-5,7-dioxo-6¹,6²,6³,6⁴,6⁵,6⁶-hexahydro-1¹*H*-8-oxa-1(5,3)-indola-6(1,3)-pyridazina-2(1,3)-benzenacycloundecaphane-4-yl)amino)-3-methyl-1-oxobutan-2-yl)-*N*-methylpyrrolidine-3-carboxamide (300 mg, 0.36 mmol, 1 equiv) and TEA (109.19 mg, 1.08 mmol, 3 equiv) in DCM (3 mL) was added acryloyl chloride (48.83 mg, 0.54 mmol, 1.5 equiv) dropwise at 0 °C under nitrogen atmosphere. The resulting mixture was stirred for 2 h at room temperature then washed with brine (2 x 10 mL), the organic layer was dried over anhydrous Na_2SO_4. After filtration, the filtrate was concentrated under reduced pressure. The residue was purified by Prep-TLC (CH_2Cl_2 / MeOH 15:1) to afford (3*S*)-1-acryloyl-*N*-((2*S*)-1-(((6³*S*,4*S*)-1¹-ethyl-1²-(2-((S)-1-methoxyethyl)pyridin-3-yl)-10,10-dimethyl-5,7-dioxo-6¹,6²,6³,6⁴,6⁵,6⁶-hexahydro-1¹*H*-8-oxa-1(5,3)-indola-6(1,3)-pyridazina-2(1,3)-benzenacycloundecaphane-4-yl)amino)-3-methyl-1-oxobutan-2-yl)-*N*-methylpyrrolidine-3-carboxamide (190 mg, crude) as a yellow solid. This was further purified by reversed-phase flash chromatography with the following conditions: column, C18 silica gel; mobile phase, MeCN in Water (10mmol/L NH_4HCO_3), 0% to 100% gradient in 30 min; detector, UV 254 nm. This resulted in **Compound-3** (130 mg, 36.63%) as a white solid. ^{1}H NMR (400 MHz, DMSO-d_6) δ 8.77 (dd, *J* = 4.9, 1.7 Hz, 1H), 8.00 (s, 1H), 7.83 (dd, *J* = 7.9, 1.8 Hz, 2H), 7.77 – 7.60 (m, 3H), 7.57 – 7.50 (m, 1H), 7.36 – 7.22 (m, 1H), 7.08 (dd, *J* = 13.6, 7.5 Hz, 1H), 6.73 – 6.54 (m, 1H), 6.17 (ddd, *J* = 16.7, 5.8, 2.6 Hz, 1H), 5.80 – 5.63 (m, 1H), 5.48 – 5.29 (m, 2H), 4.75 – 4.74 (m, 1H), 4.39 – 4.20 (m, 3H), 4.02 (dt, *J* = 17.2, 9.0 Hz, 3H), 3.81 (t, *J* = 9.0 Hz, 1H), 3.73 – 3.52 (m, 5H), 3.12 (t, *J* = 4.5 Hz, 3H), 2.97 (t, *J* = 14.3 Hz, 1H), 2.85 (s, 1H), 2.82 (s, 1H), 2.76 (s, 2H), 2.73 – 2.65 (m, 1H), 2.23 – 1.96 (m, 4H), 1.94 – 1.76 (m, 2H), 1.76 – 1.51 (m, 2H), 1.40 (d, *J* = 6.1 Hz, 3H), 1.00 – 0.93 (m, 4H), 0.90 (t, *J* = 6.6 Hz, 2H), 0.83 – 0.70 (m, 6H), 0.54 (s, 3H); ^{13}C NMR (101 MHz, DMSO) δ 173.41, 172.79, 172.62, 171.97, 170.44, 169.95, 164.01, 159.41, 150.10, 136.73, 135.79, 130.19, 129.58, 127.27, 120.06, 115.98, 111.50, 76.04, 61.76, 55.92, 48.73, 48.61, 48.52, 48.39, 48.31, 48.18, 48.10, 47.97, 47.89, 47.76, 47.68, 47.55, 47.46, 47.34, 46.08, 45.49, 35.79, 30.63, 29.21, 27.94, 26.56, 25.74, 24.96, 23.23, 19.71, 19.23, 18.59, 16.76, 14.76.; HRMS(ESI$^+$, m/z) calc'd for $(C_{51}H_{66}N_7O_7)^+$: 888.50182 $[M+H]^+$, found 888.49915

Synthesis of **Compound-4**

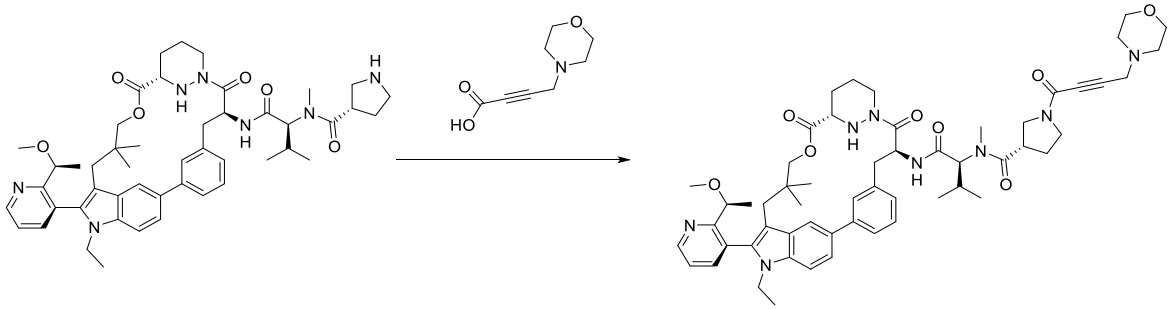

(3S)-N-((2S)-1-(((6³S,4S)-1¹-ethyl-1²-(2-((S)-1-methoxyethyl)pyridin-3-yl)-10,10-dimethyl-5,7-dioxo-6¹,6²,6³,6⁴,6⁵,6⁶-hexahydro-1¹H-8-oxa-1(5,3)-indola-6(1,3)-pyridazina-2(1,3)-benzenacycloundecaphane-4-yl)amino)-3-methyl-1-oxobutan-2-yl)-N-methyl-1-(4-morpholinobut-2-ynoyl)pyrrolidine-3-carboxamide (**Compound-4**) To a stirred solution of (3S)-N-((2S)-1-(((6³S,4S)-1¹-ethyl-1²-(2-((S)-1-methoxyethyl)pyridin-3-yl)-10,10-dimethyl-5,7-dioxo-6¹,6²,6³,6⁴,6⁵,6⁶-hexahydro-1¹H-8-oxa-1(5,3)-indola-6(1,3)-pyridazina-2(1,3)-benzenacycloundecaphane-4-yl)amino)-3-methyl-1-oxobutan-2-yl)-N-methylpyrrolidine-3-carboxamide (300 mg, 0.360 mmol, 1 equiv) and 4-(morpholin-4-yl)but-2-ynoic acid (73.02 mg, 0.432 mmol, 1.20 equiv) in DMF (5 mL) was added DIEA (232.44 mg, 1.800 mmol, 5 equiv) and COMU (231.06 mg, 0.540 mmol, 1.5 equiv) at 0°C. The reaction was stirred at 0°C for 2 h then quenched with water (20 mL) at 0 °C. The resulting mixture was extracted with EtOAc (3 x 30 mL). The combined organic layers were washed with brine (3x50 mL), then dried over anhydrous Na_2SO_4. After filtration, the filtrate was concentrated under reduced pressure. The residue was purified by silica gel column chromatography, eluted with CH_2Cl_2 / MeOH (10:1) to afford **Compound-4** (160 mg, 33.77%) as a white solid. ^{1}H NMR (400 MHz, Methanol-d_4) δ 8.82 – 8.81 (t, J = 5.8 Hz, 1H), 8.15 (dd, J = 30.6, 8.1 Hz, 1H), 8.04 (d, J = 14.3 Hz, 1H), 7.89 (d, J = 33.0 Hz, 1H), 7.77 – 7.68 (m, 2H), 7.67 – 7.52 (m, 2H), 7.30 (dt, J = 15.0, 7.6 Hz, 1H), 7.09 (dd, J = 27.3, 7.6 Hz, 1H), 5.69 – 5.42 (m, 2H), 4.72 (dd, J = 11.2, 5.7 Hz, 1H), 4.45 (d, J = 13.3 Hz, 1H), 4.39 – 4.20 (m, 4H), 4.16 (d, J = 2.2 Hz, 1H), 3.91 (d, J = 18.5 Hz, 4H), 3.84 – 3.65 (m, 8H), 3.55 (td, J = 12.4, 6.1 Hz, 2H), 3.40 (s, 3H), 3.28 – 3.19 (m, 3H), 3.12 – 2.70 (m, 10H), 2.37 – 2.05 (m, 5H), 1.90 (s, 1H), 1.64 (s, 3H), 1.46 (dd, J = 6.3, 1.9 Hz, 3H), 1.14 – 0.92 (m, 7H), 0.92 – 0.77 (m, 7H), 0.67 (d, J = 38.3 Hz, 3H); ^{13}C NMR (101 MHz, DMSO) δ 173.00, 172.65, 172.39, 172.23, 172.01, 170.22, 169.92, 169.81, 159.15, 158.94, 150.51, 150.38, 149.61, 141.69, 140.99, 140.73, 140.28, 136.27, 135.85, 130.33, 130.13, 128.96, 127.53, 127.04, 125.55, 123.77, 120.10, 117.95, 115.99, 115.05, 111.75, 111.22, 82.61, 79.25, 79.02, 78.95, 75.81, 70.95, 63.91, 61.63, 56.17, 51.23, 47.53, 45.20, 35.93, 32.64, 30.81, 29.10, 25.86, 25.16, 23.38, 20.06, 19.40, 18.83, 17.16, 15.02. HRMS(ESI$^+$, m/z) calculated for $(C_{56}H_{73}N_8O_8)^+$: 985.55459 $[M+H]^+$, found 985.55096

Synthesis of **RMC-4998**

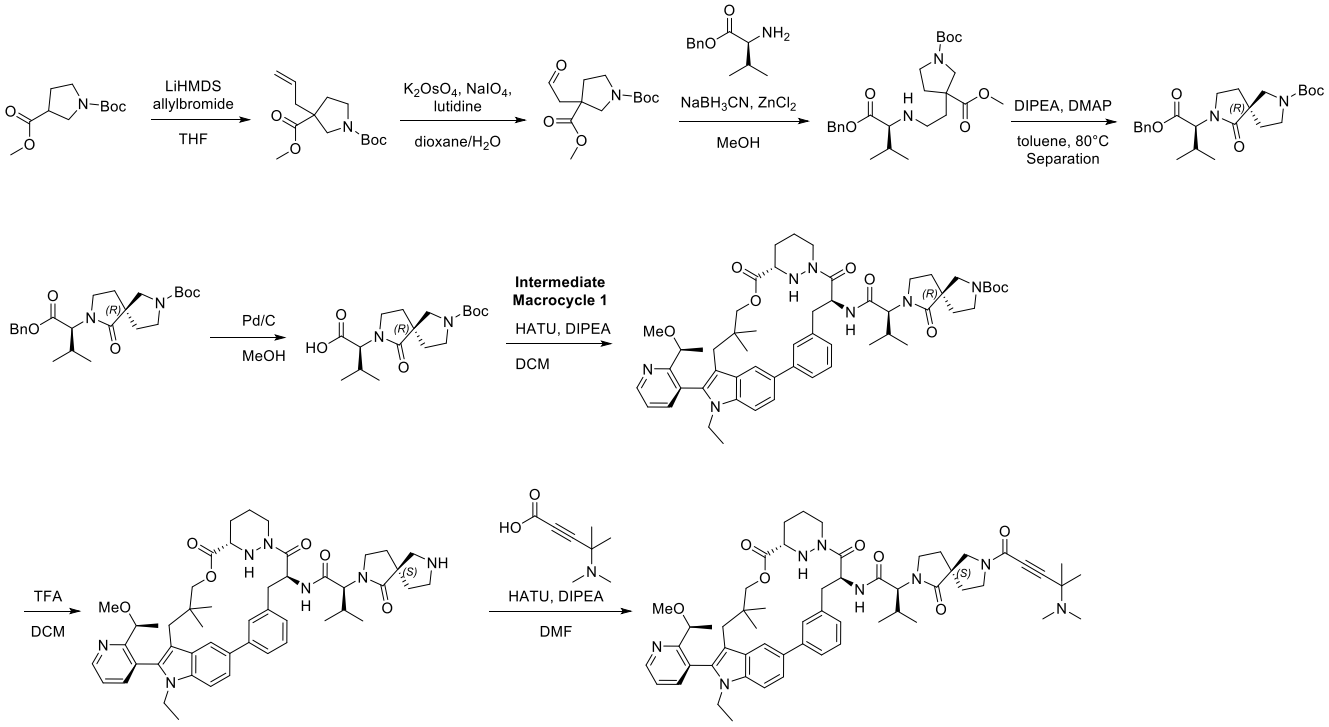

1-(tert-butyl) 3-methyl 3-allylpyrrolidine-1,3-dicarboxylate (**T21**) To a mixture of 1-*tert*-butyl 3-methyl pyrrolidine-1,3-dicarboxylate (20.0 g, 87.2 mmol) in THF (150 mL) at -78 °C under an atmosphere of nitrogen was added 1M LiHMDS in THF (113.4 mL, 113.4 mmol). After stirring at -78 °C for 40 min, allyl bromide (13.72 g, 113.4 mmol) was added and the mixture was allowed to warm to room temperature and stirred for 4 h. The mixture was cooled to 0 °C, saturated NaCl (30 mL) was added and the mixture extracted with EtOAc. The combined organic layers were dried over anhydrous Na_2SO_4 and filtered. The filtrate was concentrated under reduced pressure and the residue was purified by silica gel column chromatography to give 1-(*tert*-butyl) 3-methyl 3-allylpyrrolidine-1,3-dicarboxylate (17 g, 72% yield) as an oil. ^{1}H NMR (300 MHz, $CDCl_3$) δ 5.80 - 5.60 (m, 1H), 5.16 - 5.02 (m, 2H), 3.71 (s, 4H), 3.42 (d, J = 9.3 Hz, 2H), 3.27 (t, J = 11.2 Hz, 1H), 2.42 (d, J = 7.6 Hz, 2H), 2.38 - 2.24 (m, 1H), 2.05 (s, 1H), 1.85 (dt, J = 14.3, 7.5 Hz, 1H), 1.46 (s, 10H), 1.27 (t, J = 7.1 Hz, 1H). ^{13}C NMR (75 MHz, DMSO-d_6) δ 174.5, 153.8, 134.0, 118.6, 78.7, 53.0, 52.9, 52.3, 44.8, 44.6, 40.3, 33.7, 32.8, 28.5; LCMS (ESI): m/z [M+H] calc'd for $C_{11}H_{19}NO_4$ 269.3; found 270.2.

1-(tert-butyl) 3-methyl 3-allylpyrrolidine-1,3-dicarboxylate To a mixture of 1-(*tert*-butyl) 3-methyl 3-allylpyrrolidine-1,3-dicarboxylate (**T22**) (4.0 g, 14.9 mmol) and 2,6-dimethylpyridine (3.18 g, 29.7 mmol) in 1,4-dioxane (200 mL) and H_2O (100 mL) at 0 °C was added K_2OsO_4•$2H_2O$ (0.11 g, 0.3 mmol) in portions. The mixture was stirred for 15 min at 0 °C, then $NaIO_4$ (6.35 g, 29.7 mmol) was added in portions. The mixture was stirred at room temperature for 3 h at room temperature, then cooled to 0 °C and saturated aqueous $Na_2S_2O_3$ (50 mL) added. The mixture was extracted with EtOAc (3 x 100 mL) and the combined organic layers were washed with 2 M HCl, then dried over anhydrous Na_2SO_4 and filtered. The filtrate was concentrated under reduced pressure to give 1-(*tert*-butyl) 3-methyl 3-(2-oxoethyl)pyrrolidine-1,3-dicarboxylate (4 g, 52% yield) as an oil. ^{1}H NMR (300 MHz, $CDCl_3$) δ

5.80 - 5.60 (m, 1H), 5.16 - 5.04 (m, 2H), 3.72 (s, 3H), 3.41 (s, 3H), 3.28 (d, J = 11.0 Hz, 1H), 2.44 (s, 2H), 2.31 (d, J = 9.1 Hz, 1H), 1.85 (dt, J = 12.7, 7.5 Hz, 1H), 1.69 (s, 1H), 1.47 (s, 10H). ^{13}C NMR (101 MHz, DMSO-d_6) δ 201.7, 201.6, 174.7, 153.8 (2C), 153.8, 79.0, 53.7, 52.6, 49.5, 48.8, 47.9, 44.7, 44.5, 34.8, 34.1, 28.6; LCMS (ESI): m/z [M+H] calc'd for $C_{13}H_{21}NO_5$ 271.3; found 272.2.

1-(tert-butyl) 3-methyl 3-(2-(((S)-1-(benzyloxy)-3-methyl-1-oxobutan-2-yl)amino)ethyl)pyrrolidine-1,3-dicarboxylate (**T23**) To a mixture of 1-(*tert*-butyl) 3-methyl 3-(2-oxoethyl)pyrrolidine-1,3-dicarboxylate (6.30 g, 23.2 mmol), in MeOH (70 mL) at 0 °C was added benzyl (2*S*)-2-amino-3-methylbutanoate (7.22 g, 34.8 mmol) and $ZnCl_2$ (4.75 g, 34.8 mmol). The mixture was warmed to room temperature and stirred for 30 min, then cooled to 0 °C and $NaCNBH_3$ (2.92 g, 46.4 mmol) was added in portions. The mixture was warmed to room temperature and stirred for 2 h, then cooled to 0 °C and saturated aqueous NH_4Cl added. The mixture was extracted with EtOAc (3 x 200 mL) and the combined organic layers were washed with brine (150 mL), dried over anhydrous Na_2SO_4 and filtered. The filtrate was concentrated under reduced pressure and the residue was purified by silica gel column chromatography to give 1-(*tert*-butyl) 3-methyl 3-(2-(((S)-1-(benzyloxy)-3-methyl-1-oxobutan-2-yl)amino)ethyl)pyrrolidine-1,3-dicarboxylate (6.4 g, 54% yield) as an oil. ^{1}H NMR (300 MHz, DMSO-d_6) δ 7.40 – 7.32 (m, 5H), 5.13 (s, 2H), 3.76 – 3.62 (m, 1H), 3.59 (s, 3H), 3.32 – 3.23 (m, 2H), 3.18 – 3.00 (m, 2H), 2.96 – 2.84 (m, 1H), 2.49 – 2.41 (m, 1H), 2.29 – 2.09 (m, 2H), 1.87 – 1.70 (m, 4H), 1.38 (2s, J = 1.1 Hz, 9H), 0.88 – 0.79 (m, 6H); ^{13}C NMR (101 MHz, DMSO) δ 175.2 (2C), 174.7, 153.9, 153.8, 136.6, 128.8, 128.6, 128.5, 78.8, 67.5, 67.3 (2C), 67.2, 65.9, 54.0, 53.9, 53.5, 53.2, 52.4, 52.2, 52.0, 51.2, 51.1, 45.1, 44.8, 36.5, 31.4, 28.6, 19.5, 19.0; LCMS (ESI): m/z [M+H] calc'd for $C_{25}H_{38}N_2O_6$ 462.3; found 463.4.

tert-butyl (R)-7-((S)-1-(benzyloxy)-3-methyl-1-oxobutan-2-yl)-6-oxo-2,7-diazaspiro[4.4]nonane-2-carboxylate (**T24**) To a mixture of 1-(*tert*-butyl) 3-methyl 3-(2-(((*S*)-1-(benzyloxy)-3-methyl-1-oxobutan-2-yl)amino)ethyl)pyrrolidine-1,3-dicarboxylate (4.50 g, 9.7 mmol) in toluene (50 mL) was added DIPEA (12.57 g, 97.3 mmol) and DMAP (1.19 g, 9.7 mmol). The resulting mixture was heated to 80 °C and stirred for 24 h, then concentrated under reduced pressure and the residue was purified by preparative-HPLC, then by chiral-HPLC to give *tert*-butyl (*R*)-7-((S)-1-(benzyloxy)-3-methyl-1-oxobutan-2-yl)-6-oxo-2,7-diazaspiro[4.4]nonane-2-carboxylate (1.0 g, 32% yield) and *tert*-butyl (*S*)-7-((*S*)-1-(benzyloxy)-3-methyl-1-oxobutan-2-yl)-6-oxo-2,7-diazaspiro[4.4]nonane-2-carboxylate (1.0 g, 32% yield) and as a an oil. ^{1}H NMR (400 MHz, DMSO-d_6) δ 7.42 – 7.30 (m, 5H), 5.18, 5.15 (ABq, J = 12.4 Hz, 2H), 4.32 (d, J = 9.9 Hz, 1H), 3.48 – 3.18 (m, 6H), 2.26 – 2.11 (m, 1H), 2.02 – 1.79 (m, 3H), 1.73 – 1.62 (m, 1H), 1.40 (s, 9H), 0.91 (d, J = 6.5 Hz, 3H), 0.81 (d, J = 6.7 Hz, 3H); ^{13}C NMR (101 MHz, DMSO) δ 176.2, 170.0, 153.8, 153.8, 136.2, 128.9, 128.6 (2C), 78.8, 66.5, 60.5, 54.0, 53.8, 50.1, 49.2, 45.4, 45.2, 41.4, 34.2, 33.4, 31.0, 28.6, 27.6, 27.5, 19.6, 19.3;LCMS (ESI): m/z [M+H] calc'd for $C_{24}H_{34}N_2O_5$ 430.5; found 431.2 and LCMS (ESI): m/z [M+H] calc'd for $C_{24}H_{34}N_2O_5$ 430.3; found 431.2.

(S)-2-((R)-7-(tert-butoxycarbonyl)-1-oxo-2,7-diazaspiro[4.4]nonan-2-yl)-3-methylbutanoic acid (**T25**) A mixture of *tert*-butyl (*R*)-7-((S)-1-(benzyloxy)-3-methyl-1-oxobutan-2-yl)-6-oxo-2,7-diazaspiro[4.4]nonane-2-carboxylate (4.0 g) and 10% Pd/C (1 g) in MeOH (40 mL) was stirred at room temperature under an atmosphere of H_2. The mixture was

filtered through a pad of Celite pad and the filtrate was concentrated under reduced pressure to give (*S*)-2-((*R*)-7-(*tert*-butoxycarbonyl)-1-oxo-2,7-diazaspiro[4.4]nonan-2-yl)-3-methylbutanoic acid (4.9 g) as a solid. ^{1}H NMR (400 MHz, DMSO-d_6) δ 4.17 (d, J = 9.7 Hz, 1H), 3.51 – 3.41 (m, 2H), 3.38 – 3.17 (m, 4H), 2.20 – 2.07 (m, 1H), 2.05 – 1.87 (m, 3H), 1.82 – 1.69 (m, 1H), 1.39 (s, 9H), 0.94 (d, J = 6.5 Hz, 3H), 0.81 (d, J = 6.6 Hz, 3H); ^{13}C NMR (101 MHz, DMSO) δ 176.1, 171.8, 153.9, 153.8, 78.8, 60.6, 54.1, 53.9, 50.1, 49.2, 45.5, 45.3, 41.5, 40.5, 40.3, 40.1, 39.9, 39.6, 39.4, 39.2, 34.2, 33.4, 31.1, 28.5, 27.6, 27.5, 19.8, 19.4; ^{13}C NMR (101 MHz, DMSO) δ 176.1, 171.8, 153.9, 153.8, 78.8, 60.6, 54.1, 53.9, 50.1, 49.2, 45.5, 45.3, 41.5, 34.2, 33.4, 31.1, 28.5, 27.6, 27.5, 19.8, 19.4 LCMS (ESI): m/z [M+H] calc'd for $C_{17}H_{28}N_2O_5$ 340.2; found 339.3.

tert-butyl (5R)-7-((2S)-1-(((6^{3}S,4S)-1^1-ethyl-1^2-(2-((S)-1-methoxyethyl)pyridin-3-yl)-10,10-dimethyl-5,7-dioxo-6^1,6^2,6^3,6^4,6^5,6^6-hexahydro-1^{1}H-8-oxa-1(5,3)-indola-6(1,3)-pyridazina-2(1,3)-benzenacycloundecaphane-4-yl)amino)-3-methyl-1-oxobutan-2-yl)-6-oxo-2,7-diazaspiro[4.4]nonane-2-carboxylate (**T26**) To a mixture of (6^3*S*,4*S*)-4-amino-1^1-ethyl-1^2-(2-((S)-1-methoxyethyl)pyridin-3-yl)-10,10-dimethyl-6^1,6^2,6^3,6^4,6^5,6^6-hexahydro-1^1*H*-8-oxa-1(5,3)-indola-6(1,3)-pyridazina-2(1,3)-benzenacycloundecaphane-5,7-dione (500 mg, 0.8 mmol) in DCM at 0 °C were added DIPEA (829 mg, 6.4 mmol), ((S)-2-((*R*)-7-(*tert*-butoxycarbonyl)-1-oxo-2,7-diazaspiro[4.4]nonan-2-yl)-3-methylbutanoic acid (273 mg, 0.8 mmol) and HATU (396 mg, 1.0 mmol) in portions over 1 min. The mixture was allowed to warm to room temperature and stirred 2 h, then concentrated under reduced pressure and the residue was purified by preparative-TLC to give *tert*-butyl (5*R*)-7-((2*S*)-1-(((6^3*S*,4*S*)-1^1-ethyl-1^2-(2-((*S*)-1-methoxyethyl)pyridin-3-yl)-10,10-dimethyl-5,7-dioxo-6^1,6^2,6^3,6^4,6^5,6^6-hexahydro-1^1*H*-8-oxa-1(5,3)-indola-6(1,3)-pyridazina-2(1,3)-benzenacycloundecaphane-4-yl)amino)-3-methyl-1-oxobutan-2-yl)-6-oxo-2,7-diazaspiro[4.4]nonane-2-carboxylate (500 mg, 64% yield) as an oil. ^{1}H NMR (400 MHz, DMSO-d_6) δ 8.82 – 8.73 (m, 1H), 8.53 (d, J = 7.7 Hz, 1H), 8.03 (s, 1H), 7.87 (s, 1H), 7.81 (d, J = 7.6 Hz, 1H), 7.72 (d, J = 8.6 Hz, 1H), 7.67 (d, J = 7.7 Hz, 1H), 7.60 (d, J = 8.6 Hz, 1H), 7.56 – 7.50 (m, 1H), 7.26 (t, J = 7.5 Hz, 1H), 7.17 (d, J = 7.5 Hz, 1H), 5.48 – 5.17 (m, 2H), 4.38 – 4.22 (m, 4H), 4.13 – 3.92 (m, 2H), 3.77 – 3.50 (m, 3H), 3.45 – 3.29 (m, 4H), 3.29 – 3.18 (m, 2H), 3.15 (s, 3H), 3.00 – 2.74 (m, 4H), 2.11 – 1.58 (m, 9H), 1.46 – 1.35 (m, 12H), 0.97 – 0.91 (m, 6H), 0.80 – 0.74 (m, 6H), 0.52 (s, 3H); ^{13}C NMR (101 MHz, DMSO) δ 175.7, 172.5, 172.0, 169.4, 159.4, 153.9, 150.2, 141.1, 140.6, 140.2, 136.9, 135.8, 130.4, 130.2, 129.0, 127.2, 126.8, 125.7, 123.8, 123.4, 120.1, 116.0, 111.5, 111.2, 78.8, 76.1, 70.9, 61.0, 59.2, 56.1, 54.2, 52.1, 50.4, 49.4, 45.6, 45.4, 41.3, 40.6, 40.4, 40.2, 40.0, 39.8, 39.5, 39.3, 38.7, 38.4, 35.9, 34.5, 33.7, 32.7, 31.0, 29.2, 28.6, 27.2, 26.1, 25.1, 23.4, 19.7, 19.3, 16.9, 15.1; LCMS (ESI): m/z [M+H] calc'd for $C_{54}H_{71}N_7O_8$ 945.5; found 946.5.

Step 7

(2S)-N-((6^{3}S,4S)-1^1-ethyl-1^2-(2-((S)-1-methoxyethyl)pyridin-3-yl)-10,10-dimethyl-5,7-dioxo-6^1,6^2,6^3,6^4,6^5,6^6-hexahydro-1^{1}H-8-oxa-1(5,3)-indola-6(1,3)-pyridazina-2(1,3)-benzenacycloundecaphane-4-yl)-3-methyl-2-((S)-1-oxo-2,7-diazaspiro[4.4]nonan-2-yl)butanamide (**T27**) To a mixture of *tert*-butyl (5*R*)-7-((2*S*)-1-(((6^3*S*,4*S*)-1^1-ethyl-1^2-(2-((*S*)-1-methoxyethyl)pyridin-3-yl)-10,10-dimethyl-5,7-dioxo-6^1,6^2,6^3,6^4,6^5,6^6-hexahydro-1^1*H*-8-oxa-1(5,3)-indola-6(1,3)-pyridazina-2(1,3)-benzenacycloundecaphane-4-yl)amino)-3-methyl-1-oxobutan-2-yl)-6-oxo-2,7-diazaspiro[4.4]nonane-2-carboxylate (1.0 g, 1.06 mmol) in DCM (10 mL) at 0 °C was added TFA (3 mL) dropwise. The mixture was warmed to room temperature and

stirred for 1 h, then concentrated under reduced pressure to give (2*S*)-*N*-((6^3*S*,4*S*)-1^1-ethyl-1^2-(2-((*S*)-1-methoxyethyl)pyridin-3-yl)-10,10-dimethyl-5,7-dioxo-6^1,6^2,6^3,6^4,6^5,6^6-hexahydro-1^1*H*-8-oxa-1(5,3)-indola-6(1,3)-pyridazina-2(1,3)-benzenacycloundecaphane-4-yl)-3-methyl-2-((*S*)-1-oxo-2,7-diazaspiro[4.4]nonan-2-yl)butanamide (1.3 g). ^{1}H NMR (400 MHz, DMSO-d_6) δ 8.82 – 8.73 (m, 1H), 8.55 (s, 1H), 8.05 (s, 1H), 7.89 (s, 1H), 7.80 (d, *J* = 6.8 Hz, 1H), 7.73 (d, *J* = 8.3 Hz, 1H), 7.68 (d, *J* = 7.5 Hz, 1H), 7.59 (d, *J* = 8.7 Hz, 1H), 7.54 – 7.47 (m, 1H), 7.32 – 7.17 (m, 2H), 5.56 – 5.20 (m, 2H), 4.45 – 4.19 (m, 4H), 4.14 – 3.92 (m, 2H), 3.78 – 3.54 (m, 4H), 3.41 (s, 1H), 3.22 – 3.08 (m, 4H), 3.01 – 2.74 (m, 7H), 2.15 – 1.56 (m, 9H), 1.42 (d, *J* = 5.6 Hz, 3H), 1.01 – 0.87 (m, 6H), 0.85 – 0.70 (m, 6H), 0.52 (s, 3H); ^{13}C NMR (101 MHz, DMSO) δ 177.9, 172.6, 172.0, 169.6, 159.4, 150.3, 141.1, 140.6, 140.3, 136.9, 135.8, 130.4, 130.2, 129.0, 127.2, 125.8, 123.9, 123.4, 120.1, 116.0, 111.5, 111.1, 76.1, 70.9, 61.0, 59.2, 56.5, 56.1, 52.1, 51.7, 47.3, 41.5, 38.3, 37.3, 35.9, 32.8, 29.2, 27.2, 26.1, 25.1, 19.7, 19.3, 16.9, 15.1; LCMS (ESI): m/z [M+H] calc'd for $C_{49}H_{63}N_7O_6$ 846.1; found 845.5.

Step 8

(2S)-2-((S)-7-(4-(dimethylamino)-4-methylpent-2-ynoyl)-1-oxo-2,7-diazaspiro[4.4]nonan-2-yl)-N-((6^{3}S,4S)-1^1-ethyl-1^2-(2-((S)-1-methoxyethyl)pyridin-3-yl)-10,10-dimethyl-5,7-dioxo-6^1,6^2,6^3,6^4,6^5,6^6-hexahydro-1^{1}H-8-oxa-1(5,3)-indola-6(1,3)-pyridazina-2(1,3)-benzenacycloundecaphane-4-yl)-3-methylbutanamide (**RMC-4998**) To a mixture of (2*S*)-*N*-((6^3*S*,4*S*)-1^1-ethyl-1^2-(2-((*S*)-1-methoxyethyl)pyridin-3-yl)-10,10-dimethyl-5,7-dioxo-6^1,6^2,6^3,6^4,6^5,6^6-hexahydro-1^1*H*-8-oxa-1(5,3)-indola-6(1,3)-pyridazina-2(1,3)-benzenacycloundecaphane-4-yl)-3-methyl-2-((*S*)-1-oxo-2,7-diazaspiro[4.4]nonan-2-yl)butanamide (500 mg, 0.59 mmol) and DIPEA (764 mg, 5.9 mmol) in DMF (5 mL) at 0 °C were added 4-(dimethylamino)-4-methylpent-2-ynoic acid (110 mg, 0.71 mmol) and HATU (292 mg, 0.77 mmol) in portions. The mixture was warmed to room temperature and stirred for 1 h, then H_2O (10 mL) was added and the mixture extracted with EtOAc (10 mL x 3). The combined organic layers were washed with brine (10 mL), dried over anhydrous Na_2SO_4 and filtered. The filtrate was concentrated under reduced pressure and the residue was purified by preparative-HPLC to give (**RMC-4998**) (177 mg, 28.94% yield) as a white solid. ^{1}H NMR (300 MHz, DMSO-d_6) δ 8.77 (dd, *J* = 4.7, 1.8 Hz, 1H), 8.59 – 8.46 (m, 1H), 8.00 (s, 1H), 7.90 – 7.79 (m, 2H), 7.74 – 7.59 (m, 3H), 7.53 (dd, *J* = 7.7, 4.7 Hz, 1H), 7.25 (t, *J* = 7.6 Hz, 1H), 7.13 (d, *J* = 7.5 Hz, 1H), 5.38 – 5.22 (m, 2H), 4.37 – 4.20 (m, 4H), 4.12 – 3.80 (m, 3H), 3.75 – 3.53 (m, 4H), 3.43 – 3.35 (m, 2H), 3.27 – 3.18 (m, 1H), 3.14 (d, *J* = 2.0 Hz, 3H), 2.94 – 2.59 (m, 5H), 2.24 (s, 3H), 2.18 (s, 3H), 2.11 – 1.77 (m, 7H), 1.73 – 1.51 (m, 2H), 1.39 (d, *J* = 6.0 Hz, 3H), 1.38 (s, 3H), 1.34 (s, 3H), 1.00 – 0.88 (m, 6H), 0.81 – 0.71 (m, 6H), 0.52 (s, 3H); ^{13}C NMR (101 MHz, DMSO-d_6) δ 173.5, 173.2, 170.5, 169.9, 167.4, 167.3, 157.3, 149.8, 149.7, 148.2, 139.1, 139.0, 138.6, 138.2, 134.8, 133.7, 128.2, 128.1, 126.9, 125.1, 124.8, 123.6, 121.7, 121.3, 118.0, 113.9, 109.4, 109.1, 89.7 (2C), 76.5, 76.4, 74.0, 68.8, 58.9, 57.1, 54.0, 53.8, 52.7 (2C), 51.1, 50.1, 47.9, 47.2, 45.6, 42.8, 39.3, 38.3, 38.2, 36.3, 33.9, 31.9, 31.2, 30.6, 28.6, 28.4, 27.2, 26.1 (2C), 25.2, 24.0, 23.1, 21.4, 17.6, 17.3, 17.1, 14.9, 13.0; HRMS(ESI$^+$, m/z) calc'd for $(C_{57}H_{75}N_8O_7)^+$: 983.57532 $[M+H]^+$, found 983.57190

Synthesis of **Intermediate 2**

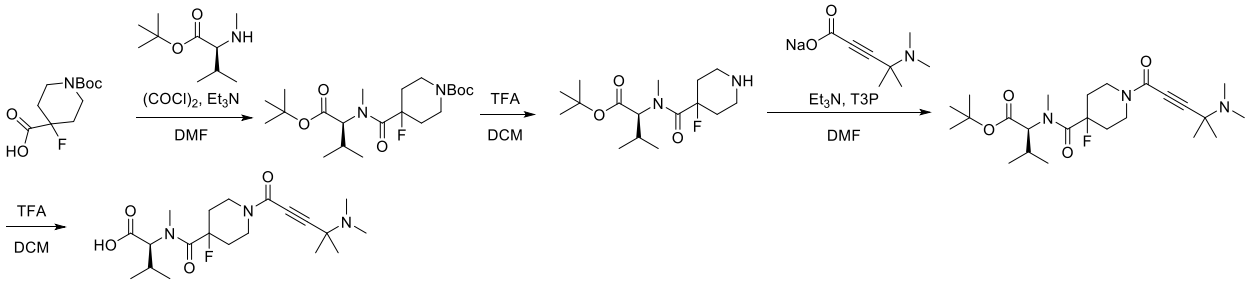

tert-butyl (S)-4-((1-(tert-butoxy)-3-methyl-1-oxobutan-2-yl)(methyl)carbamoyl)-4-fluoropiperidine-1-carboxylate (**T28**) To a mixture of 1-[(*tert*-butoxy)carbonyl]-4-fluoropiperidine-4-carboxylic acid (2.0 g, 8.1 mmol) in DCM (20 mL) was added oxalic dichloride (1.34 g, 10.5 mmol) and DMF (30 mg, 0.4 mmol). The resulting solution was stirred at room temperature for 1 h. Et_3N (3.2 g, 3.2 mmol) and (2*S*)-3-methyl-2-(methylamino)butanoic acid (1.25 g, 9.5 mmol) were added and the mixture was stirred at room temperature for 1 h. H_2O (100 mL) was added and the mixture was extracted with EtOAc (50 mL x 3). The combined organic layers were concentrated under reduced pressure and the residue was purified by silica gel column chromatography to give *tert*-butyl (*S*)-4-((1-(*tert*-butoxy)-3-methyl-1-oxobutan-2-yl)(methyl)carbamoyl)-4-fluoropiperidine-1-carboxylate (1.34 g, 45% yield) as a solid. ^{1}H NMR (400 MHz, DMSO-d_6) δ 4.37 (d, J = 10.3 Hz, 1H), 3.82 (d, J = 13.5 Hz, 2H), 3.11 – 3.01 (m, 3H), 2.73 (s, 1H), 2.28 – 2.10 (m, 2H), 2.00 – 1.80 (m, 4H), 1.40 (d, J = 6.3 Hz, 18H), 0.97 (d, J = 6.6 Hz, 3H), 0.80 (dd, J = 24.0, 6.7 Hz, 3H). ^{13}C NMR (101 MHz, DMSO) δ 170.68, 170.27, 170.06, 169.52, 169.38, 154.16, 96.79, 94.92, 82.04, 81.09, 79.37, 65.52, 65.38, 64.92, 60.16, 55.31, 40.63, 40.42, 40.22, 40.01, 39.80, 39.59, 39.38, 33.31, 33.14, 30.54, 28.43, 28.00, 27.21, 26.74, 21.15, 20.53, 20.05, 19.05, 18.81, 14.50. LCMS (ESI): m/z [M+Na] calc'd for $C_{21}H_{37}FN_2O_5Na$ 439.3; found 439.3.

*N-(4-fluoropiperidine-4-carbonyl)-N-methyl-L-valine (***T29**) A mixture of *tert*-butyl (*S*)-4-((1-(*tert*-butoxy)-3-methyl-1-oxobutan-2-yl)(methyl)carbamoyl)-4-fluoropiperidine-1-carboxylate (290 mg, 0.70 mmol) in DCM (4 mL) and TFA (2 mL) was stirred at room temperature for 2 h, then concentrated under reduced pressure to give *N*-(4-fluoropiperidine-4-carbonyl)-*N*-methyl-*L*-valine, which was used directly in the next step without further purification. ^{1}H NMR (400 MHz, DMSO-d_6) δ 4.29 (d, J = 10.1 Hz, 1H), 3.08 (dt, J = 12.9, 4.0 Hz, 2H), 3.00 (d, J = 5.0 Hz, 2H), 2.91 (td, J = 12.3, 3.8 Hz, 2H), 2.67 (s, 1H), 2.14 (ddd, J = 16.5, 8.0, 4.1 Hz, 3H), 2.05 – 1.94 (m, 2H), 1.34 (d, J = 8.6 Hz, 9H), 0.92 (d, J = 6.6 Hz, 3H), 0.74 (dd, J = 22.0, 6.7 Hz, 3H). ^{13}C NMR (101 MHz, $CDCl_3$) δ 171.58, 171.38, 170.86, 170.65, 169.42, 169.06, 97.43, 96.70, 95.56, 94.83, 81.45, 80.69, 77.71, 77.59, 77.39, 77.07, 65.29, 65.13, 64.05, 41.42, 41.30, 41.24, 41.09, 34.14, 33.93, 33.59, 33.38, 33.18, 32.20, 32.03, 29.94, 29.32, 27.61, 27.55, 26.90, 26.46, 19.88, 19.48, 18.49, 18.12. LCMS (ESI): m/z [M+H] calc'd for $C_{12}H_{21}FN_2O_3$ 260.2; found 261.2.

N-(1-(4-(dimethylamino)-4-methylpent-2-ynoyl)-4-fluoropiperidine-4-carbonyl)-N-methyl-L-valinate (**T30**) To a solution of the *tert*-butyl *N*-(4-fluoropiperidine-4-carbonyl)-*N*-methyl-L-valinate (1.7 g, 5.3 mmol), sodium 4-(dimethylamino)-4-methylpent-2-ynoate (1.67 g, 9.4 mmol) and Et_3N (2.73 g, 36.9 mmol) in DMF (20 mL) stirred at 5 °C was added T3P (4.11 g, 10.7 mmol, 50wt% in EtOAc). The reaction mixture was stirred at 5 °C for 1 h. The resulting

mixture was quenched with H_2O (100 mL) and extracted with EtOAc (50 mL x 3). The combined organic layers were concentrated and purified by silica gel column chromatography to give *tert*-butyl *N*-(1-(4-(dimethylamino)-4-methylpent-2-ynoyl)-4-fluoropiperidine-4-carbonyl)-*N*-methyl-L-valinate (1.6 g, 74.0% yield) as a solid. ^{1}H NMR (400 MHz, DMSO-d_6) δ 4.45 – 4.32 (m, 1H), 4.25 – 4.13 (m, 2H), 3.59 – 3.36 (m, 2H), 3.08 (d, J = 5.0 Hz, 3H), 2.73 (d, J = 2.3 Hz, 1H), 2.21 (s, 6H), 2.14 – 1.99 (m, 3H), 1.94 – 1.83 (m, 1H), 1.40 (d, J = 9.2 Hz, 9H), 1.35 (s, 6H), 0.98 (d, J = 6.6 Hz, 3H), 0.81 (dd, J = 24.0, 6.8 Hz, 3H). ^{13}C NMR (101 MHz, $CDCl_3$) δ 170.58, 170.39, 170.05, 169.85, 169.32, 168.88, 168.78, 152.40, 152.31, 97.06, 96.99, 96.35, 95.18, 94.46, 93.32, 93.27, 93.24, 93.10, 81.92, 81.82, 81.02, 77.69, 77.37, 77.05, 76.50, 76.47, 65.61, 65.44, 65.28, 64.36, 64.15, 54.66, 42.63, 42.51, 42.49, 42.39, 42.23, 40.06, 36.61, 36.36, 36.27, 36.13, 33.86, 33.77, 33.63, 33.33, 33.11, 33.02, 32.88, 32.66, 32.49, 32.33, 32.21, 32.13, 32.04, 31.91, 30.09, 30.05, 27.73, 27.67, 27.63, 26.91, 26.83, 26.67, 26.53, 19.96, 19.91, 19.56, 18.72, 18.68, 18.22, 18.09, 1.48. LCMS (ESI): m/z [M+H] calc'd for $C_{24}H_{40}FN_3O_4$ 453.3; found 454.2.

N-(1-(4-(dimethylamino)-4-methylpent-2-ynoyl)-4-fluoropiperidine-4-carbonyl)-N-methyl-L-valine (**T31**) To a solution of *tert*-butyl *N*-(1-(4-(dimethylamino)-4-methylpent-2-ynoyl)-4-fluoropiperidine-4-carbonyl)-*N*-methyl-L-valinate (50 mg, 0.11 mmol) in DCM (2 mL) was added TFA (1 mL). The reaction mixture was stirred at 20 °C for 2 h, then concentrated under reduced pressure to afford crude *N*-(1-(4-(dimethylamino)-4-methylpent-2-ynoyl)-4-fluoropiperidine-4-carbonyl)-*N*-methyl-L-valine. It was used for the next step directly without further purification. ^{1}H NMR (400 MHz, Chloroform-d) δ 10.77 – 10.15 (m, 1H), 4.57 – 3.82 (m, 3H), 3.31 (d, J = 13.2 Hz, 1H), 2.93 (d, J = 17.1 Hz, 3H), 2.67 (s, 2H), 2.32 (s, 6H), 1.95 (d, J = 71.0 Hz, 4H), 1.36 (s, 6H), 0.95 – 0.51 (m, 6H). ^{13}C NMR (101 MHz, CDCl3) δ 170.55, 170.36, 169.96, 169.83, 151.76, 96.80, 96.30, 94.92, 94.41, 90.42, 90.28, 77.75, 77.42, 77.10, 56.42, 42.78, 42.54, 39.16, 36.59, 33.91, 33.69, 33.46, 33.15, 32.93, 32.78, 32.39, 32.19, 31.67, 30.47, 29.41, 29.10, 27.36, 27.21, 26.90, 26.31, 26.28, 26.24, 26.21, 26.17, 22.46, 20.20, 19.92, 18.88, 18.79, 18.63, 18.50, 13.97. LCMS (ESI): m/z [M+H] calc'd for $C_{20}H_{32}FN_3O_4$ 397.2; found 398.3.

Synthesis of **RMC-6291**

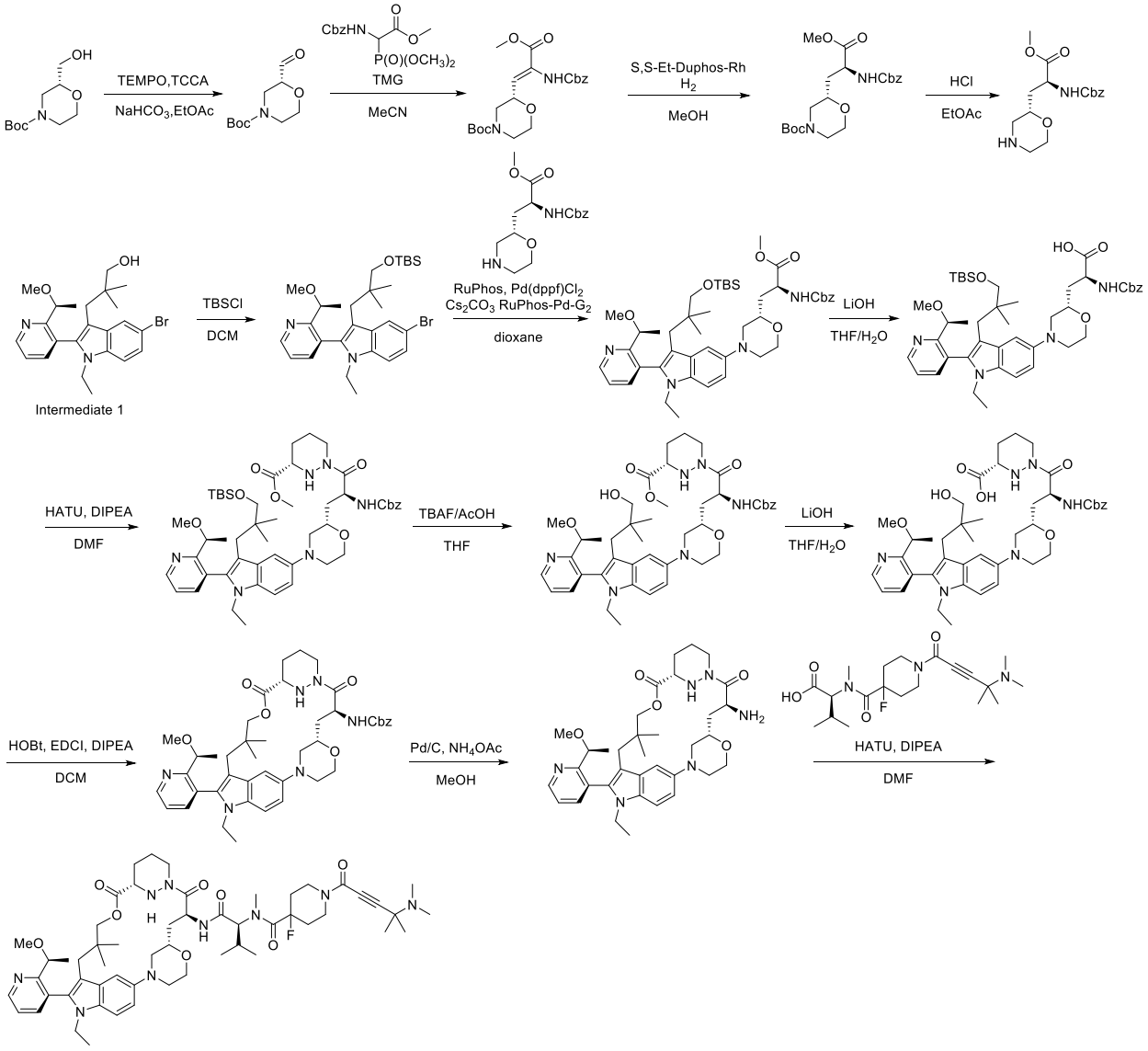

tert-butyl (2R)-2-formylmorpholin-4-yl formate (**T32**) To a solution of *tert*-butyl (2*R*)-2-(hydroxymethyl)morpholin-4-yl formate (50 g, 230 mmol) in EtOAc (1 L) was added TEMPO (715 mg, 4.6 mmol) and $NaHCO_3$ (58 g, 690 mmol) at 20 °C. The mixture was cooled to -50 °C, then TCCA (56 g, 241mmol) in EtOAc (100 mL) was added dropwise over 30 min. The reaction mixture was warmed to 5 °C for 2 h, then quenched with 10% $Na_2S_2O_3$ (200 mL) and stirred for 20 min. The resulting mixture was filtered and the organic phase was separated from filtrate. The aqueous phase was extracted with EtOAc (100 mL x 2). The combined organic layers were washed with H_2O (100 mL) and brine (100 mL), and dried over anhydrous Na_2SO_4. The organic layer was concentrated under reduced pressure to afford *tert*-butyl (2*R*)-2-formylmorpholin-4-yl formate (50 g, crude) as an oil. ^{1}H NMR (400 MHz, DMSO-d_6) δ 6.28 (dd, J = 12.5, 7.4 Hz, 1H), 4.41 – 4.25 (m, 1H), 3.95 – 3.72 (m, 2H), 3.68 (d, J = 12.7 Hz, 1H), 3.60 – 3.27 (m, 2H), 3.22 – 3.00 (m, 1H), 2.73 (d, J = 71.0 Hz, 1H), 1.40 (d, J = 3.1 Hz, 9H). ^{13}C NMR (76 MHz, DMSO) δ 149.94, 92.33, 92.19, 75.23, 72.97, 72.54, 72.15, 72.11, 61.68, 61.39, 50.18, 50.01, 23.46.

(S,Z)-2-(2-(((benzyloxy)carbonyl)amino)-3-methoxy-3-oxoprop-1-en-1-yl)morpholine-4-carboxylate (**T33**) To a solution of *tert*-butyl (2*R*)-2-formylmorpholin-4-yl formate (49 g, 153 mmol) and methyl 2-{[(benzyloxy)carbonyl]amino}-2-(dimethoxyphosphoryl)acetate (60 g, 183 mmol) in CAN (300 mL) was added tetramethylguanidine (35 g, 306 mmol) at 0~10 °C. The reaction mixture was stirred at 10 °C for 30 min then warmed to 20 °C for 2 h. The reaction mixture was diluted with DCM (200 mL) and washed with Citric acid (10%, 200 mL) and 10% $NaHCO_3$ aqueous solution (200 mL). The organic phase was concentrated under reduced pressure, and purified by silica gel column chromatography to afford *tert*-butyl (*S*,*Z*)-2-(2-(((benzyloxy)carbonyl)amino)-3-methoxy-3-oxoprop-1-en-1-yl)morpholine-4-carboxylate (36 g, 90% yield) as solid. ^{1}H NMR (400 MHz, DMSO-d_6) δ 9.11 (s, 1H), 7.27 (dd, J = 19.5, 4.9 Hz, 5H), 6.02 (d, J = 7.9 Hz, 1H), 5.02 (s, 2H), 4.16 (ddd, J = 10.6, 7.7, 2.8 Hz, 1H), 3.85 – 3.67 (m, 2H), 3.67 – 3.61 (m, 1H), 3.58 (s, 3H), 3.32 (td, J = 11.2, 2.6 Hz, 1H), 2.81 (t, J = 11.4 Hz, 1H), 2.71 – 2.47 (m, 1H), 1.33 (s, 9H). ^{13}C NMR (76 MHz, DMSO) δ 164.92, 154.75, 154.29, 136.86, 129.66, 128.82, 128.42, 128.27, 79.63, 71.68, 66.62, 65.75, 52.63, 40.77, 40.49, 40.21, 39.93, 39.66, 39.38, 39.10, 28.41. LCMS (ESI): m/z [M+Na] calc'd for $C_{21}H_{28}N_2O_4$ 420.2; found: 443.1

tert-butyl (S)-2-((S)-2-(((benzyloxy)carbonyl)amino)-3-methoxy-3-oxopropyl)morpholine-4-carboxylate (**T34**) To a solution of *tert*-butyl (*S*,*Z*)-2-(2-(((benzyloxy)carbonyl)amino)-3-methoxy-3-oxoprop-1-en-1-yl)morpholine-4-carboxylate (49 g, 0.12 mol) in MeOH (500 mL) was added (*S*,*S*)-Et-DUPHOS-Rh (500 mg, 0.7 mmol). The mixture was stirred at 25 °C under an H_2 (60 psi) atmosphere for 48 h. The reaction was concentrated and purified by chromatography to give *tert*-butyl (*S*)-2-((*S*)-2-(((benzyloxy)carbonyl)amino)-3-methoxy-3-oxopropyl)morpholine-4-carboxylate (44 g, 89.8% yield) as solid. ^{1}H NMR (400 MHz, Chloroform-*d*) δ 7.40 – 7.18 (m, 5H), 6.16 (d, J = 8.7 Hz, 1H), 5.09 (s, 2H), 4.55 (td, J = 8.4, 3.9 Hz, 1H), 3.94 – 3.73 (m, 3H), 3.69 (s, 3H), 3.41 (qd, J = 9.1, 7.7, 4.5 Hz, 2H), 2.86 (s, 1H), 2.55 (s, 1H), 1.96 – 1.75 (m, 2H), 1.45 (s, 9H). ^{13}C NMR (101 MHz, $CDCl_3$) δ 172.47, 171.11, 156.10, 154.51, 136.34, 128.50, 128.17, 128.14, 80.17, 77.44, 77.12, 76.81, 66.95, 66.44, 64.33, 60.37, 52.43, 51.64, 34.80, 30.63, 29.68, 28.36, 21.03, 19.11, 14.20, 13.71, 0.01. LCMS (ESI): m/z [M+Na] calc'd for $C_{21}H_{30}N_2O_7$ 422.2; found: 445.2.

methyl (S)-2-(((benzyloxy)carbonyl)amino)-3-((S)-morpholin-2-yl)propanoate (**T35**) To a stirred solution of *tert*-butyl (*S*)-2-((*S*)-2-(((benzyloxy)carbonyl)amino)-3-methoxy-3-oxopropyl)morpholine-4-carboxylate (2.2 g, 5.2 mmol) in EtOAc (2 mL) was added HCl/EtOAc (25 mL) at 15 °C. The reaction was stirred at 15 °C for 2 h, then concentrated under reduced pressure to afford methyl (*S*)-2-(((benzyloxy)carbonyl)amino)-3-((*S*)-morpholin-2-yl)propanoate (1.51 g, 90.4% yield) as an oil. ^{1}H NMR (400 MHz, Chloroform-*d*) δ 7.40 – 7.28 (m, 5H), 6.13 (d, J = 8.7 Hz, 1H), 5.19 – 5.03 (m, 2H), 4.53 (ddd, J = 9.0, 6.9, 4.2 Hz, 1H), 3.85 – 3.76 (m, 1H), 3.72 (s, 3H), 3.49 (dddd, J = 12.5, 9.9, 8.1, 2.9 Hz, 2H), 2.84 – 2.70 (m, 3H), 2.53 (dd, J = 12.1, 10.1 Hz, 1H), 1.84 (td, J = 9.1, 8.5, 3.6 Hz, 2H). ^{13}C NMR (101 MHz, $CDCl_3$) δ 172.73, 156.18, 155.56, 136.42, 128.40, 128.04, 128.01, 127.61, 77.74, 77.62, 77.42, 77.10, 73.92, 67.76, 66.69, 53.58, 52.20, 51.65, 50.96, 45.46. LCMS (ESI): m/z [M+H] calc'd for $C_{16}H_{22}N_2O_5$ 322.1; found 323.2.

(S)-5-bromo-3-(3-((tert-butyldimethylsilyl)oxy)-2,2-dimethylpropyl)-1-ethyl-2-(2-(1-methoxyethyl)pyridin-3-yl)-1H-indole (**T36**) To a solution of 3-(5-bromo-1-ethyl-2-{2-[(1*S*)-1-

methoxyethyl]pyridin-3-yl}indol-3-yl)-2,2-dimethylpropan-1-ol(100 g, 0.22 mol) and 1H-imidazole(30.6 g, 0.45 mol) in DCM (800 mL) was added TBSCl (50.7 g, 0.34 mol) in DCM (200 mL) at 0 °C. The reaction was stirred at 25 °C for 2 h. The resulting solution was washed with H_2O (300 mL x 3) and brine (200 mL x 2), dried over anhydrous sodium sulfate, filtered and concentrated under reduced pressure. The residue was purified with silica gel column chromatography to give (*S*)-5-bromo-3-(3-((*tert*-butyldimethylsilyl)oxy)-2,2-dimethylpropyl)-1-ethyl-2-(2-(1-methoxyethyl)pyridin-3-yl)-1*H*-indole (138 g, 90% yield) as an solid. ^{1}H NMR (400 MHz, DMSO-d_6) δ 8.73 (dd, *J* = 4.7, 1.8 Hz, 1H), 7.88 – 7.79 (m, 2H), 7.54 – 7.44 (m, 2H), 7.27 (dd, *J* = 8.7, 1.9 Hz, 1H), 4.13 – 4.02 (m, 2H), 3.78 (ddd, *J* = 14.7, 7.3, 2.2 Hz, 1H), 3.16 (ddd, *J* = 60.7, 9.6, 2.2 Hz, 2H), 2.82 (d, *J* = 2.1 Hz, 3H), 2.66 (d, *J* = 14.0 Hz, 1H), 2.16 (dd, *J* = 14.1, 2.2 Hz, 1H), 1.37 (dd, *J* = 6.3, 2.1 Hz, 3H), 1.11 (td, *J* = 7.1, 2.2 Hz, 3H), 0.86 – 0.81 (m, 11H), 0.58 (dd, *J* = 11.4, 2.2 Hz, 5H), -0.00 (d, *J* = 2.2 Hz, 3H), -0.03 (d, *J* = 2.2 Hz, 3H).^{13}C NMR (101 MHz, $CDCl_3$) δ 160.67, 150.50, 140.21, 135.58, 134.47, 130.93, 126.79, 124.56, 122.99, 121.92, 112.63, 112.13, 110.86, 77.61, 77.29, 76.97, 75.84, 71.31, 56.42, 38.72, 38.05, 32.84, 26.09, 25.78, 25.20, 24.90, 18.60, 18.29, 18.27, 18.04, 15.12, 14.24, -4.93, -5.21, -5.44. LCMS (ESI): m/z [M+H] calc'd for $C_{29}H_{43}BrN_2O_2Si$ 558.2; found 559.2.

methyl (2S)-2-{[(benzyloxy)carbonyl]amino}-3-[(2S)-4-(3-{3-[(tert-butyldimethylsilyl)oxy]-2,2-dimethylpropyl}-1-ethyl-2-{2-[(1S)-1-methoxyethyl]pyridin-3-yl}indol-5-yl)morpholin-2-yl]propanoate (**T37**) To a stirred solution of Intermediate 1 (50 g, 89.3 mmol) in dioxane (500 mL) was added methyl (2*S*)-2-{[(benzyloxy)carbonyl]amino}-3-[(2*S*)-morpholin-2-yl]propanoate from step 1 (31.7 g, 98.2 mmol), RuPhos (16.7 g, 35.7 mmol), Di-mu-chlorobis(2-amino-1,1-biphenyl-2-yl-C,N)dipalladium(II) (2.8 g, 4.4 mmol) and cesium carbonate (96 g, 295 mmol) followed by RuPhos-Pd-G2 (3.5 g, 4.4 mmol) at 105 °C under an N_2 atmosphere. The reaction mixture was stirred for 6 h at 105 °C under an N_2 atmosphere. The resulting mixture was filtered, and the filtrate was concentrated under reduced pressure. The residue was purified by prep-TLC chromatography to afford methyl (2*S*)-2-{[(benzyloxy)carbonyl]amino}-3-[(2*S*)-4-(3-{3-[(*tert*-butyldimethylsilyl)oxy]-2,2-dimethylpropyl}-1-ethyl-2-{2-[(1*S*)-1-methoxyethyl]pyridin-3-yl}indol-5-yl)morpholin-2-yl]propanoate (55 g, 73% yield) as a solid. ^{1}H NMR (400 MHz, Chloroform-*d*) δ 8.82 (dd, *J* = 4.8, 1.8 Hz, 1H), 7.68 (dd, *J* = 7.7, 1.8 Hz, 1H), 7.44 – 7.27 (m, 8H), 7.06 – 6.98 (m, 1H), 6.06 (d, *J* = 8.9 Hz, 1H), 5.23 – 5.09 (m, 2H), 4.72 – 4.53 (m, 1H), 4.17 (q, *J* = 6.2 Hz, 1H), 4.11 – 3.95 (m, 2H), 3.93 – 3.74 (m, 6H), 3.46 – 3.24 (m, 3H), 3.19 (d, *J* = 9.3 Hz, 1H), 3.11 (d, *J* = 2.8 Hz, 3H), 2.92 (td, *J* = 11.5, 3.0 Hz, 1H), 2.68 (dd, *J* = 15.3, 12.5 Hz, 2H), 2.31 (d, *J* = 14.2 Hz, 1H), 2.12 – 1.99 (m, 2H), 1.48 (d, *J* = 6.2 Hz, 3H), 1.20 (q, *J* = 9.6, 8.3 Hz, 3H), 0.86 (d, *J* = 2.7 Hz, 9H), 0.78 (d, *J* = 5.5 Hz, 3H), 0.68 (s, 3H). ^{13}C NMR (101 MHz, $CDCl_3$) δ 172.55, 160.75, 156.20, 150.42, 140.26, 136.44, 134.99, 132.02, 129.55, 128.52, 128.19, 128.14, 127.20, 121.81, 114.79, 112.20, 110.07, 108.33, 77.52, 77.20, 76.88, 75.74, 73.54, 72.52, 67.01, 66.95, 57.00, 56.41, 52.45, 52.09, 51.77, 38.62, 38.57, 35.10, 33.27, 25.95, 24.94, 24.55, 18.60, 18.22, 15.32, -5.33, -5.41. LCMS (ESI): m/z [M+H] calc'd for $C_{45}H_{64}N_4O_7Si$ 800.5; found 801.5.

(2S)-2-{[(benzyloxy)carbonyl]amino}-3-[(2S)-4-(3-{3-[(tert-butyldimethylsilyl)oxy]-2,2-dimethylpropyl}-1-ethyl-2-{2-[(1S)-1-methoxyethyl]pyridin-3-yl}indol-5-yl)morpholin-2-yl]propanoic acid (**T38**) To a solution of methyl (2*S*)-2-{[(benzyloxy)carbonyl]amino}-3-[(2*S*)-4-(3-{3-[(*tert*-butyldimethylsilyl)oxy]-2,2-dimethylpropyl}-1-ethyl-2-{2-[(1*S*)-1-methoxyethyl]pyridin-3-yl}indol-5-yl)morpholin-2-yl]propanoate (10 g, 12 mmol) in THF (270

mL) was added LiOH (1.3 g, 31 mmol) in H_2O (45 mL) at 20 °C. The reaction was stirred at 20 °C for 2 h, then treated with 1N HCl to adjust pH to 4~5 at 0~5 °C. The resulting mixture was extracted with EtOAc (50 mL x 2). The combined organic layers were washed with brine and dried over anhydrous Na_2SO_4. The organic phase was then concentrated under reduced pressure to afford (2*S*)-2-{[(benzyloxy)carbonyl]amino}-3-[(2*S*)-4-(3-{3-[(*tert*-butyldimethylsilyl)oxy]-2,2-dimethylpropyl}-1-ethyl-2-{2-[(1*S*)-1-methoxyethyl]pyridin-3-yl}indol-5-yl)morpholin-2-yl]propanoic acid (9.5 g, 97% yield) as a solid. ^{1}H NMR (400 MHz, Chloroform-*d*) δ 8.87 (d, *J* = 5.6 Hz, 1H), 7.78 – 7.56 (m, 1H), 7.53 – 7.02 (m, 9H), 6.28 – 6.08 (m, 1H), 5.15 (dd, *J* = 26.4, 8.9 Hz, 2H), 4.84 – 4.50 (m, 1H), 4.23 – 3.81 (m, 6H), 3.54 (t, *J* = 13.1 Hz, 2H), 3.33 – 2.90 (m, 6H), 2.87 – 2.55 (m, 2H), 2.35 (d, *J* = 15.0 Hz, 2H), 2.17 – 1.84 (m, 2H), 1.44 (s, 3H), 1.26 (dt, *J* = 23.4, 7.0 Hz, 4H), 0.94 – 0.54 (m, 15H), 0.12 – -0.17 (m, 6H). ^{13}C NMR (101 MHz, $CDCl_3$) δ 174.31, 173.84, 170.98, 160.59, 156.27, 150.26, 142.16, 140.55, 136.66, 135.09, 133.17, 129.32, 128.41, 128.07, 127.94, 127.14, 122.00, 115.26, 112.61, 110.41, 109.84, 77.79, 77.47, 77.15, 75.70, 73.82, 72.56, 67.81, 66.66, 66.20, 60.29, 57.52, 56.40, 52.34, 38.67, 38.53, 34.99, 33.21, 29.65, 25.91, 25.01, 24.35, 20.96, 18.70, 18.15, 15.28, 14.20, -5.34, -5.42. LCMS (ESI): m/z [M+H] calc'd for $C_{44}H_{62}N_4O_7Si$ 786.4; found 787.4.

methyl (S)-1-((S)-2-(((benzyloxy)carbonyl)amino)-3-((S)-4-(3-(3-((tert-butyldimethylsilyl)oxy)-2,2-dimethylpropyl)-1-ethyl-2-(2-((S)-1-methoxyethyl)pyridin-3-yl)-1H-indol-5-yl)morpholin-2-yl)propanoyl)hexahydropyridazine-3-carboxylate (**T39**) To a stirred solution of (2*S*)-2-{[(benzyloxy)carbonyl]amino}-3-[(2*S*)-4-(3-{3-[(*tert*-butyldimethylsilyl)oxy]-2,2-dimethylpropyl}-1-ethyl-2-{2-[(1*S*)-1-methoxyethyl]pyridin-3-yl}indol-5-yl)morpholin-2-yl]propanoic acid (10 g, 12.7 mmol) in DMF (150 mL), was added methyl (*S*)-hexahydropyridazine-3-carboxylate (2 g, 14 mmol), then cooled to 0 °C, DIPEA (32.8 g, 254 mmol) was added followed by HATU (9.7 g, 25.4 mmol) at 0~5 °C. The reaction mixture was stirred at 0~5 °C for 1 h. The resulting mixture was diluted with EtOAc (500 mL) and H_2O (200 mL). The organic layer was separated and washed with H_2O (100 mL x 2) and brine (100 mL), dried over anhydrous sodium sulfate. The solution was filtered and concentrated under reduced pressure, and the residue was purified by silica gel column chromatography to afford methyl (*S*)-1-((*S*)-2-(((benzyloxy)carbonyl)amino)-3-((*S*)-4-(3-(3-((*tert*-butyldimethylsilyl)oxy)-2,2-dimethylpropyl)-1-ethyl-2-(2-((*S*)-1-methoxyethyl)pyridin-3-yl)-1*H*-indol-5-yl)morpholin-2-yl)propanoyl)hexahydropyridazine-3-carboxylate (8 g, 70% yield) as a solid. ^{1}H NMR (400 MHz, Chloroform-*d*) δ 8.83 (dd, *J* = 4.8, 1.8 Hz, 1H), 7.69 (dd, *J* = 7.7, 1.8 Hz, 1H), 7.44 – 7.31 (m, 7H), 7.21 (d, *J* = 2.2 Hz, 1H), 7.03 (dd, *J* = 8.8, 2.1 Hz, 1H), 5.94 (d, *J* = 9.2 Hz, 1H), 5.47 (ddd, *J* = 9.3, 6.7, 4.5 Hz, 1H), 5.21 – 5.06 (m, 2H), 4.41 – 4.30 (m, 1H), 4.19 (d, *J* = 6.5 Hz, 1H), 4.02 (dq, *J* = 14.2, 6.9 Hz, 2H), 3.97 – 3.81 (m, 4H), 3.77 (d, *J* = 8.8 Hz, 3H), 3.58 (dt, *J* = 10.3, 5.2 Hz, 1H), 3.35 (d, *J* = 11.6 Hz, 2H), 3.31 – 3.17 (m, 2H), 3.13 (s, 3H), 2.99 (s, 2H), 2.92 (d, *J* = 0.6 Hz, 2H), 2.69 (d, *J* = 14.0 Hz, 2H), 2.33 (d, *J* = 14.1 Hz, 1H), 2.08 (s, 2H), 2.05 (d, *J* = 8.3 Hz, 1H), 1.96 – 1.78 (m, 2H), 1.71 (q, *J* = 12.0, 9.8 Hz, 2H), 1.48 (d, *J* = 6.3 Hz, 3H), 1.21 (t, *J* = 7.1 Hz, 3H), 0.86 (s, 9H), 0.81 (s, 3H), 0.69 (s, 3H), 0.00 (d, *J* = 3.5 Hz, 6H). ^{13}C NMR (101 MHz, $CDCl_3$) δ 173.07, 171.75, 171.04, 168.79, 162.91, 160.73, 156.15, 150.39, 145.21, 140.35, 136.61, 136.41, 134.48, 131.76, 129.42, 128.38, 127.95, 127.89, 127.12, 121.86, 114.80, 112.10, 109.98, 107.96, 77.77, 77.45, 77.13, 75.79, 73.22, 72.49, 66.55, 60.27, 58.63, 56.83, 56.41, 55.12, 52.31, 52.15, 51.63, 49.01, 41.68, 38.48, 36.41, 36.15, 33.28, 31.27, 27.94, 25.87, 24.96, 24.42, 22.52, 20.93, 18.83, 18.11, 15.23, 14.14, 12.65, -5.41, -5.49. LCMS (ESI): m/z [M+H] calc'd for $C_{50}H_{72}N_6O_8Si$ 912.5; found 913.4.

methyl (S)-1-((S)-2-(((benzyloxy)carbonyl)amino)-3-((S)-4-(1-ethyl-3-(3-hydroxy-2,2-dimethylpropyl)-2-(2-((S)-1-methoxyethyl)pyridin-3-yl)-1H-indol-5-yl)morpholin-2-yl)propanoyl)hexahydropyridazine-3-carboxylate (**T40**) A solution of methyl (*S*)-1-((*S*)-2-(((benzyloxy)carbonyl)amino)-3-((*S*)-4-(3-(3-((*tert*-butyldimethylsilyl)oxy)-2,2-dimethylpropyl)-1-ethyl-2-(2-((*S*)-1-methoxyethyl)pyridin-3-yl)-1*H*-indol-5-yl)morpholin-2-yl)propanoyl)hexahydropyridazine-3-carboxylate (8.5 g, 9 mmol) in THF (8 mL) was added a mixture of tetrabutylammonium fluoride (1M in THF, 180 mL, 180 mmol) and AcOH (11 g, 200 mmol) at 20 °C. The reaction mixture was stirred at 75 °C for 3 h. The resulting mixture was diluted with EtOAc (150 mL) and washed with H_2O (20 mL x 6). The organic phase was concentrated under reduced pressure to give methyl (*S*)-1-((*S*)-2-(((benzyloxy)carbonyl)amino)-3-((*S*)-4-(1-ethyl-3-(3-hydroxy-2,2-dimethylpropyl)-2-(2-((*S*)-1-methoxyethyl)pyridin-3-yl)-1*H*-indol-5-yl)morpholin-2-yl)propanoyl)hexahydropyridazine-3-carboxylate (7.4 g, 100% yield) as solid. ^{1}H NMR (400 MHz, Chloroform-*d*) δ 8.80 (dd, *J* = 4.7, 1.8 Hz, 1H), 7.67 (dd, *J* = 7.7, 1.8 Hz, 1H), 7.42 – 7.24 (m, 8H), 7.00 (dd, *J* = 8.9, 2.2 Hz, 1H), 5.95 (dd, *J* = 23.2, 8.9 Hz, 1H), 5.41 (dd, *J* = 9.4, 5.1 Hz, 1H), 5.10 (d, *J* = 3.7 Hz, 2H), 4.32 (d, *J* = 12.4 Hz, 1H), 4.18 – 4.13 (m, 1H), 4.04 – 3.91 (m, 3H), 3.89 – 3.77 (m, 3H), 3.71 (d, *J* = 17.3 Hz, 3H), 3.60 – 3.47 (m, 1H), 3.41 (d, *J* = 11.9 Hz, 2H), 3.32 (dd, *J* = 10.4, 3.5 Hz, 1H), 3.25 – 3.15 (m, 1H), 3.09 (d, *J* = 1.1 Hz, 3H), 2.95 – 2.84 (m, 2H), 2.80 (d, *J* = 14.1 Hz, 1H), 2.65 (t, *J* = 10.3 Hz, 1H), 2.39 – 2.26 (m, 1H), 2.24 – 2.08 (m, 2H), 2.01 (d, *J* = 14.0 Hz, 2H), 1.84 (td, *J* = 10.5, 4.6 Hz, 2H), 1.66 (d, *J* = 9.9 Hz, 2H), 1.46 (d, *J* = 6.2 Hz, 3H), 1.18 (t, *J* = 7.1 Hz, 3H), 0.78 (d, *J* = 6.0 Hz, 3H), 0.72 (d, *J* = 4.2 Hz, 3H). ^{13}C NMR (101 MHz, $CDCl_3$) δ 173.07, 171.53, 171.15, 170.99, 167.08, 160.77, 160.74, 156.31, 156.06, 150.42, 145.13, 140.24, 136.63, 136.34, 134.71, 131.54, 129.51, 129.47, 128.49, 128.43, 128.07, 127.95, 127.17, 121.89, 114.72, 114.58, 111.93, 111.84, 110.00, 109.93, 107.50, 77.58, 77.26, 76.94, 75.68, 73.11, 72.13, 71.13, 70.96, 66.95, 66.72, 66.67, 60.39, 58.89, 58.34, 56.40, 56.30, 52.24, 52.16, 51.69, 51.55, 49.02, 47.43, 45.60, 41.88, 38.58, 38.03, 37.99, 37.10, 36.44, 33.29, 28.37, 26.54, 25.32, 25.22, 24.90, 23.88, 22.69, 21.04, 18.67, 15.30, 14.20, 0.03. LCMS (ESI): m/z [M+H] calc'd for $C_{44}H_{58}N_6O_8$ 799.4; found 798.4.

(S)-1-((S)-2-(((benzyloxy)carbonyl)amino)-3-((S)-4-(1-ethyl-3-(3-hydroxy-2,2-dimethylpropyl)-2-(2-((S)-1-methoxyethyl)pyridin-3-yl)-1H-indol-5-yl)morpholin-2-yl)propanoyl)hexahydropyridazine-3-carboxylic acid (**T41**) To a solution of methyl (*S*)-1-((*S*)-2-(((benzyloxy)carbonyl)amino)-3-((*S*)-4-(1-ethyl-3-(3-hydroxy-2,2-dimethylpropyl)-2-(2-((*S*)-1-methoxyethyl)pyridin-3-yl)-1*H*-indol-5-yl)morpholin-2-yl)propanoyl)hexahydropyridazine-3-carboxylate (8 g, 10 mmol) in THF (200 mL) was added lithium hydroxide (600 mg, 25 mmol) in H_2O (30 mL). The reaction mixture was stirred at 20 °C for 1 h, then treated with 1N HCl to adjust pH to 4~5 at 0~5 °C, and extracted with EtOAc (500 mL x 2). The organic phase was washed with brine, and concentrated under reduced pressure to afford (*S*)-1-((*S*)-2-(((benzyloxy)carbonyl)amino)-3-((*S*)-4-(1-ethyl-3-(3-hydroxy-2,2-dimethylpropyl)-2-(2-((*S*)-1-methoxyethyl)pyridin-3-yl)-1*H*-indol-5-yl)morpholin-2-yl)propanoyl)hexahydropyridazine-3-carboxylic acid (8 g, crude) as a solid. ^{1}H NMR (400 MHz, Chloroform-*d*) δ 8.84 (dt, *J* = 4.2, 2.1 Hz, 1H), 7.67 (dd, *J* = 7.7, 1.9 Hz, 1H), 7.40 – 7.10 (m, 8H), 6.00 (d, *J* = 8.8 Hz, 1H), 5.42 (s, 1H), 5.06 (q, *J* = 11.8 Hz, 2H), 4.20 – 3.90 (m, 5H), 3.88 – 3.54 (m, 3H), 3.47 (s, 1H), 3.35 (d, *J* = 10.5 Hz, 1H), 3.24 – 2.96 (m, 5H), 2.86 (d, *J* = 14.3 Hz, 2H), 2.19 – 1.97 (m, 4H), 1.95 – 1.74 (m, 2H), 1.66 (s, 2H), 1.45 (dd, *J* = 6.3, 1.7 Hz, 3H), 1.26 (td, *J* = 7.2, 1.6 Hz, 1H), 1.18 (dd, *J* = 9.1, 4.3 Hz, 3H), 0.78 (d, *J* = 7.5 Hz, 3H), 0.64 (s, 3H). ^{13}C NMR (101 MHz, $CDCl_3$) δ 174.67,

173.96, 172.82, 171.25, 160.61, 156.33, 156.17, 150.35, 140.56, 136.54, 135.50, 129.47, 128.43, 128.04, 127.96, 127.92, 126.90, 122.11, 114.23, 112.81, 110.32, 77.53, 77.21, 76.89, 75.70, 72.23, 70.07, 67.90, 66.71, 65.37, 60.42, 58.78, 58.29, 56.44, 56.41, 53.51, 48.70, 42.10, 38.75, 37.82, 37.72, 36.48, 33.00, 31.90, 29.67, 27.84, 25.72, 25.57, 25.49, 24.80, 22.67, 21.04, 20.93, 18.68, 15.26, 14.19, 14.13, 0.02. LCMS (ESI): m/z [M+H] calc'd for $C_{43}H_{56}N_6O_8$ 784.4; found 785.4.

((2²S,6³S,4S)-1¹-ethyl-1²-(2-((S)-1-methoxyethyl)pyridin-3-yl)-10,10-dimethyl-5,7-dioxo-6¹,6²,6³,6⁴,6⁵,6⁶-hexahydro-1¹H-8-oxa-2(4,2)-morpholina-1(5,3)-indola-6(1,3)-pyridazinacycloundecaphane-4-yl)carbamate (**T42**) To a stirred solution of (*S*)-1-((*S*)-2-(((benzyloxy)carbonyl)amino)-3-((*S*)-4-(1-ethyl-3-(3-hydroxy-2,2-dimethylpropyl)-2-(2-((*S*)-1-methoxyethyl)pyridin-3-yl)-1*H*-indol-5-yl)morpholin-2-yl)propanoyl)hexahydropyridazine-3-carboxylic acid (8 g, 10.2 mmol) and DIPEA (59 g, 459 mmol) in DCM (800 mL) was added EDCI (88 g, 458 mmol) and HOBT (27.6 g, 204 mmol) at 25 °C under an argon atmosphere. The reaction mixture was stirred at 25 °C for 16 h. The resulting mixture was concentrated under reduced pressure, and the residue was purified by silica gel column chromatography to afford benzyl ((2²*S*,6³*S*,4*S*)-1¹-ethyl-1²-(2-((*S*)-1-methoxyethyl)pyridin-3-yl)-10,10-dimethyl-5,7-dioxo-6¹,6²,6³,6⁴,6⁵,6⁶-hexahydro-1¹*H*-8-oxa-2(4,2)-morpholina-1(5,3)-indola-6(1,3)-pyridazinacycloundecaphane-4-yl)carbamate (5 g, 66% yield) as a solid; ^{1}H NMR (400 MHz, Chloroform-*d*) δ 8.79 (dd, *J* = 4.8, 1.9 Hz, 1H), 7.61 (dt, *J* = 8.5, 4.3 Hz, 1H), 7.40 – 7.11 (m, 8H), 7.10 – 6.93 (m, 1H), 5.53 (t, *J* = 6.5 Hz, 1H), 5.38 (d, *J* = 6.9 Hz, 1H), 5.20 – 4.84 (m, 2H), 4.68 (d, *J* = 13.4 Hz, 1H), 4.31 (d, *J* = 6.4 Hz, 1H), 4.17 – 3.84 (m, 5H), 3.85 – 3.58 (m, 4H), 3.27 (d, *J* = 20.8 Hz, 4H), 3.01 – 2.82 (m, 2H), 2.81 – 2.53 (m, 2H), 2.19 (d, *J* = 12.9 Hz, 1H), 2.12 – 2.01 (m, 2H), 2.00 – 1.92 (m, 1H), 1.81 (t, *J* = 19.1 Hz, 2H), 1.68 – 1.54 (m, 1H), 1.47 (t, *J* = 5.1 Hz, 3H), 1.26 (t, *J* = 7.1 Hz, 3H), 0.81 (s, 3H), 0.52 (s, 3H). ^{13}C NMR (101 MHz, $CDCl_3$) δ 173.68, 171.19, 171.07, 159.98, 155.77, 150.12, 145.30, 144.81, 140.33, 139.91, 136.62, 135.69, 131.78, 130.02, 128.89, 128.37, 127.95, 127.88, 127.33, 125.21, 122.46, 121.71, 120.21, 114.54, 110.95, 110.42, 109.38, 85.14, 77.53, 77.21, 76.89, 75.87, 72.97, 71.65, 71.19, 67.11, 66.85, 66.54, 63.73, 60.33, 60.18, 59.46, 56.39, 56.24, 54.73, 51.66, 50.28, 47.49, 46.66, 45.15, 41.66, 39.38, 38.67, 38.28, 37.68, 36.52, 35.81, 32.83, 31.87, 29.64, 29.32, 27.56, 25.88, 25.03, 23.46, 23.16, 22.65, 21.01, 20.29, 17.06, 15.29, 14.83, 14.18, 9.11, 0.00. LCMS (ESI): m/z [M+H] calc'd for $C_{43}H_{54}N_6O_7$ 766.4; found 767.4.

(2²S,6³S,4S)-4-amino-1¹-ethyl-1²-(2-((S)-1-methoxyethyl)pyridin-3-yl)-10,10-dimethyl-6¹,6²,6³,6⁴,6⁵,6⁶-hexahydro-1¹H-8-oxa-2(4,2)-morpholina-1(5,3)-indola-6(1,3)-pyridazinacycloundecaphane-5,7-dione (**T43**) To a solution of benzyl ((2²*S*,6³*S*,4*S*)-1¹-ethyl-1²-(2-((*S*)-1-methoxyethyl)pyridin-3-yl)-10,10-dimethyl-5,7-dioxo-6¹,6²,6³,6⁴,6⁵,6⁶-hexahydro-1¹*H*-8-oxa-2(4,2)-morpholina-1(5,3)-indola-6(1,3)-pyridazinacycloundecaphane-4-yl)carbamate (400 mg, 0.5 mmol) in MeOH (20 mL) was added Pd/C (200 mg) and ammonium acetate (834 mg, 16 mmol) at 20 °C under an H_2 atmosphere and the mixture was stirred for 2 h. Then resulting mixture was filtered and concentrated under reduced pressure. The residue was redissolved in DCM (20 mL) and washed with H_2O (5 mL x 2), then concentrated under reduced pressure to afford (2²*S*,6³*S*,4*S*)-4-amino-1¹-ethyl-1²-(2-((*S*)-1-methoxyethyl)pyridin-3-yl)-10,10-dimethyl-6¹,6²,6³,6⁴,6⁵,6⁶-hexahydro-1¹*H*-8-oxa-2(4,2)-morpholina-1(5,3)-indola-6(1,3)-pyridazinacycloundecaphane-5,7-dione (320 mg, 97% yield) as a solid. ^{1}H NMR (400 MHz, Chloroform-*d*) δ 8.79 (d, *J* = 4.7 Hz, 1H), 7.61 (d, *J* = 7.8 Hz, 1H), 7.33 (dd, *J* = 14.3, 6.1 Hz,

2H), 7.05 (d, *J* = 6.9 Hz, 2H), 4.82 (s, 1H), 4.68 (d, *J* = 13.2 Hz, 1H), 4.33 (q, *J* = 6.0 Hz, 1H), 4.24 – 3.98 (m, 3H), 3.95 – 3.61 (m, 5H), 3.50 (d, *J* = 12.0 Hz, 1H), 3.33 (s, 2H), 3.18 (d, *J* = 11.4 Hz, 1H), 2.89 (q, *J* = 12.1 Hz, 2H), 2.72 – 2.46 (m, 2H), 2.38 – 2.10 (m, 3H), 1.98 (d, *J* = 47.7 Hz, 2H), 1.87 – 1.70 (m, 2H), 1.66 – 1.49 (m, 2H), 1.45 (d, *J* = 6.2 Hz, 2H), 1.26 (t, *J* = 6.6 Hz, 5H), 1.05 – 0.77 (m, 6H), 0.47 (s, 2H). ^{13}C NMR (101 MHz, $CDCl_3$) δ 176.23, 171.59, 159.89, 156.83, 150.12, 145.27, 140.00, 135.99, 132.67, 131.41, 130.14, 128.63, 127.32, 122.58, 114.41, 110.99, 110.63, 107.45, 104.78, 77.45, 77.13, 76.81, 75.93, 73.79, 71.38, 71.18, 67.36, 59.29, 56.35, 53.48, 51.68, 46.66, 41.55, 38.26, 37.32, 36.67, 35.83, 32.66, 31.91, 29.69, 29.38, 26.74, 26.62, 25.98, 25.61, 24.82, 23.20, 22.68, 22.56, 21.93, 16.84, 14.78, 14.13. LCMS (ESI): m/z [M+H] calc'd for $C_{35}H_{48}N_6O_5$ 632.4; found 633.3.

1-(4-(dimethylamino)-4-methylpent-2-ynoyl)-N-((2S)-1-(((2^{2}S,6^{3}S,4S)-1^1-ethyl-1^2-(2-((S)-1-methoxyethyl)pyridin-3-yl)-10,10-dimethyl-5,7-dioxo-6^1,6^2,6^3,6^4,6^5,6^6-hexahydro-1^{1}H-8-oxa-2(4,2)-morpholina-1(5,3)-indola-6(1,3)-pyridazinacycloundecaphane-4-yl)amino)-3-methyl-1-oxobutan-2-yl)-4-fluoro-N-methylpiperidine-4-carboxamide (**RMC-6291**) To a solution of the (2^2*S*,6^3*S*,4*S*)-4-amino-1^1-ethyl-1^2-(2-((*S*)-1-methoxyethyl)pyridin-3-yl)-10,10-dimethyl-6^1,6^2,6^3,6^4,6^5,6^6-hexahydro-1^1*H*-8-oxa-2(4,2)-morpholina-1(5,3)-indola-6(1,3)-pyridazinacycloundecaphane-5,7-dione (50 mg, 0.079 mmol), *N*-(1-(4-(dimethylamino)-4-methylpent-2-ynoyl)-4-fluoropiperidine-4-carbonyl)-*N*-methyl-L-valine (47 mg, 0.12 mmol) in DMF (2 mL) stirred at 0 °C was added HATU (36 mg, 0.09 mmol) and DIPEA (153 mg, 1.2 mmol) dropwise. The reaction was stirred at 0 °C for 1 h. The resulting mixture was purified by reverse phase to afford 1-(4-(dimethylamino)-4-methylpent-2-ynoyl)-*N*-((2*S*)-1-(((2^2*S*,6^3*S*,4*S*)-1^1-ethyl-1^2-(2-((*S*)-1-methoxyethyl)pyridin-3-yl)-10,10-dimethyl-5,7-dioxo-6^1,6^2,6^3,6^4,6^5,6^6-hexahydro-1^1*H*-8-oxa-2(4,2)-morpholina-1(5,3)-indola-6(1,3)-pyridazinacycloundecaphane-4-yl)amino)-3-methyl-1-oxobutan-2-yl)-4-fluoro-*N*-methylpiperidine-4-carboxamide (11.9 mg, 13.9% yield) as a solid. ^{1}H NMR (400 MHz, CD_3OD) δ 8.71 (dd, *J* = 4.8, 1.7 Hz, 1H), 7.86 (d, *J* = 7.8 Hz, 1H), 7.51 (dd, *J* = 7.8, 4.8 Hz, 1H), 7.39 (d, *J* = 8.9 Hz, 1H), 7.15 – 7.04 (m, 2H), 5.67 (d, *J* = 8.8 Hz, 1H), 4.62 (d, *J* = 11.2 Hz, 1H), 4.46 (d, *J* = 12.4 Hz, 1H), 4.39 – 4.27 (m, 2H), 4.23 (d, *J* = 6.1 Hz, 1H), 4.17 – 4.08 (m, 1H), 3.93 (s, 2H), 3.86 (s, 1H), 3.84 – 3.76 (m, 2H), 3.74 – 3.65 (m, 2H), 3.63 – 3.51 (m, 2H), 3.27 – 3.23 (m, 1H), 3.22 – 3.11 (m, 6H), 3.0 – 2.89 (m, 2H), 2.85 – 2.75 (m, 2H), 2.74 – 2.55 (m, 2H), 2.36 (d, *J* = 8.2 Hz, 6H), 2.32 – 2.21 (m, 2H), 2.20 – 2.02 (m, 5H), 1.92 (d, *J* = 12.5 Hz, 2H), 1.69 (dd, *J* = 43.8, 12.6 Hz, 2H), 1.46 (dt, *J* = 8.0, 4.9 Hz, 9H), 1.03 (d, *J* = 3.5 Hz, 3H), 0.90 (dd, *J* = 48.3, 6.5 Hz, 6H), 0.77 (d, *J* = 3.0 Hz, 3H), 0.69 (s, 3H). LCMS (ESI): m/z [M+H] calc'd for $C_{55}H_{78}FN_9O_8$ 1012.60302; found 1012.59882.

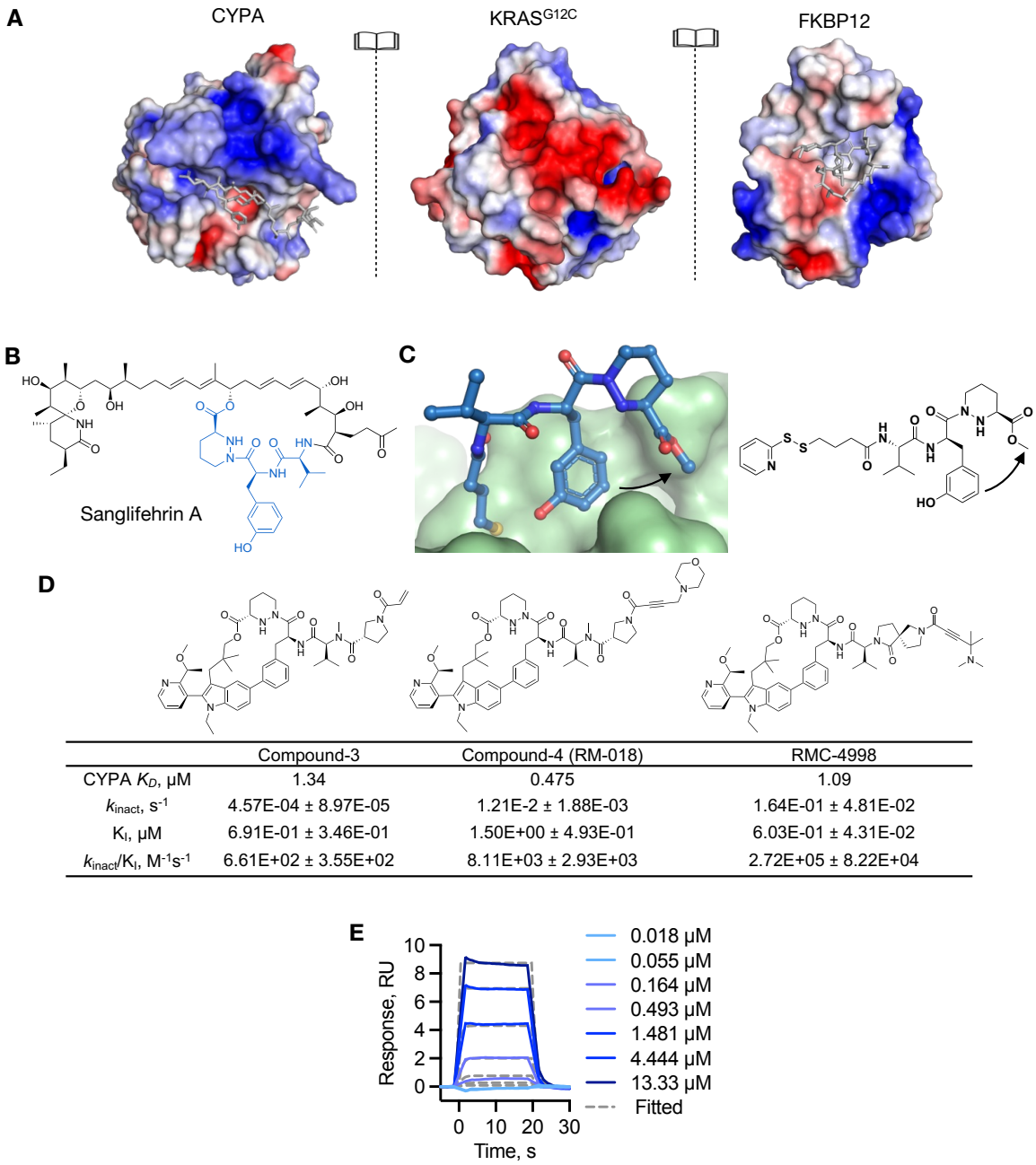

	Compound-3	Compound-4 (RM-018)	RMC-4998
CYPA K_D, μM	1.34	0.475	1.09
k_{inact}, s^{-1}	4.57E-04 ± 8.97E-05	1.21E-2 ± 1.88E-03	1.64E-01 ± 4.81E-02
K_I, μM	6.91E-01 ± 3.46E-01	1.50E+00 ± 4.93E-01	6.03E-01 ± 4.31E-02
k_{inact}/K_I, $M^{-1}s^{-1}$	6.61E+02 ± 3.55E+02	8.11E+03 ± 2.93E+03	2.72E+05 ± 8.22E+04

Fig. S1. CYPA as a chaperone enabling tri-complex inhibitors of KRAS^{G12C}. (**A**) Comparisons of APBS surface electrostatic charge between the effector binding interface of KRAS^{G12C}, the rapamycin-binding region of FKBP12 (PDB: 2PPN) (*39*), and the sanglifehrin binding region of CYPA (PDB: 3K0N) *(30)*. (**B**) The chemical structure of the natural product sanglifehrin A with the minimal CYPA binding motif depicted in blue. (**C**) The conformation of Compound-1 from the tri-complex crystal structure (left) with the chemical structure (right). The vector for macrocyclization is indicated with the arrow on both panels. (**A**) Chemical structures of the tricomplex inhibitors Compound-3, Compound-4 (RM-018) *(13)*, and RMC-4998 along with their CYPA binding affinity and KRAS^{G12C} covalent engagement kinetics (mean ± SD, N=3). (**E**) Surface plasmon resonance sensograms depicting the reversible binding of RMC-4998 to immobilized CYPA, representative of N=9

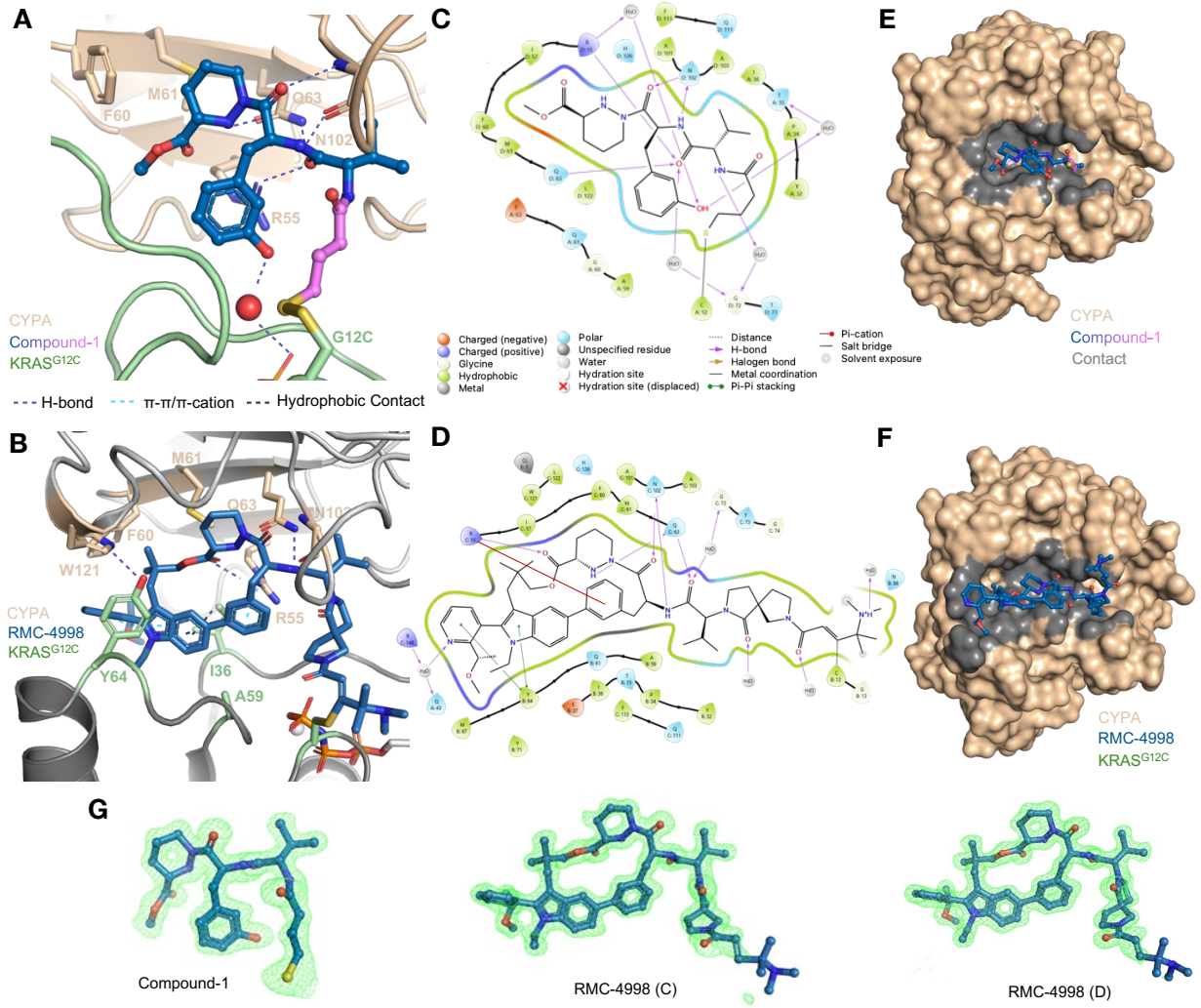

Fig. S2. Tricomplex inhibitors with improved engagement of the KRAS^{G12C} active state. The binding interface between KRAS, CYPA, and Compound-1 (**A**) or KRAS, CYPA, and RMC-4998 (**B**) from the tri-complex crystal structures. Ligand interaction diagrams are shown for Compound-1 (**C**) and RMC-4998 (**D**) to indicate the contacts with KRAS and CYPA (chain A/B is KRAS^{G12C} and chain C/D is CYPA). Atomic contacts between CYPA and Compound-1 (**E**) or between CYPA and RMC-4998 (**F**) are depicted in grey on the surface of CYPA. **(G)** The unbiased omit maps for Compound-1 and RMC-4998 from their respective x-ray crystal structures.

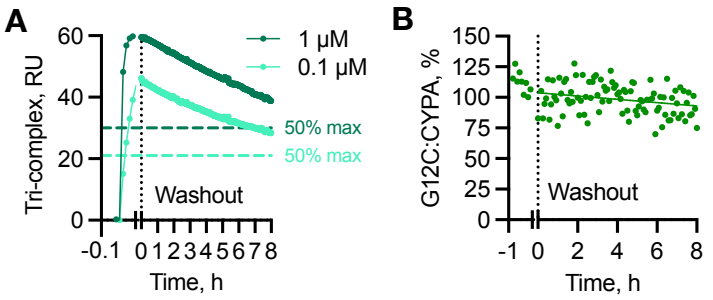

Fig. S3. RMC-4998 forms a long-lived tri-complex with KRAS^{G12C} and CYPA. (**A**) GMPPNP-loaded KRAS^{G12C} was immobilized on a streptavidin SPR chip then CYPA (25 µM), free GMPPNP (10 µM), and RMC-4998 (0.1 or 1 µM) were flowed for 180s to form the tri-complex. At the indicated time, buffer washout was initiated, and the presence of the tri-complex was monitored over time by SPR. Results are representative of N=2. (**B**) Nanoluciferase-tagged KRAS^{G12C} and HaloTag-CYPA were transfected into CYPA knockout U2OS cells. RMC-4998 (100 nM) was added for one hour, then media was washed out and replaced with one containing cyclosporin A (100 µM, which acts as a competitive inhibitor to block any residual binding of RMC-4998 to CYPA). The cellular KRAS^{G12C}-CYPA interaction was monitored using intracellular BRET signal. Results are representative of N=3.

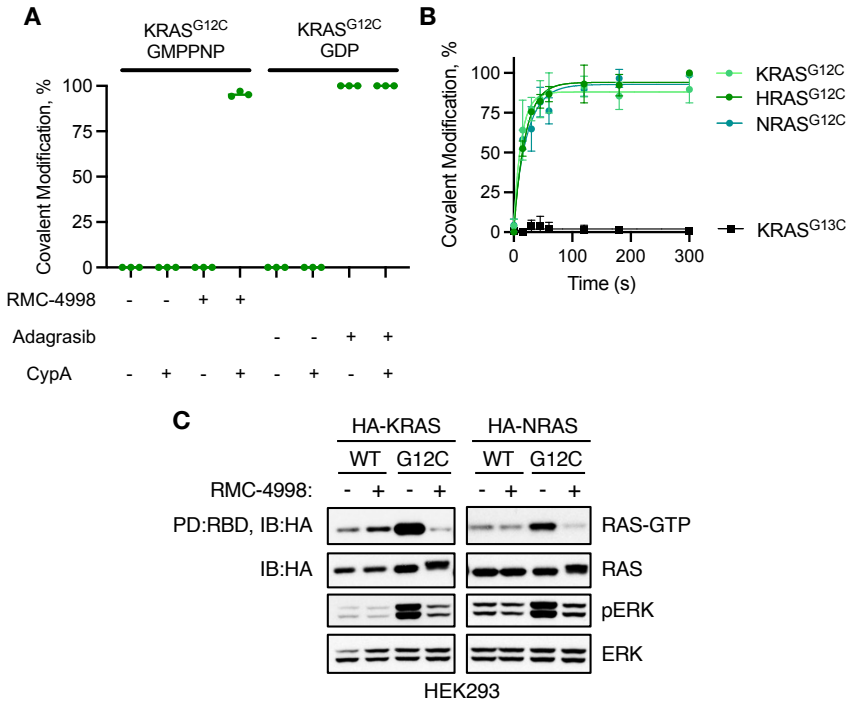

Fig. S4. Covalent modification of RAS by RMC-4998. (A) RMC-4998 (4 μM) was incubated with GMPPNP-loaded KRAS^{G12C} (1 μM) in the presence or absence of CYPA (25 μM). Adagrasib (4 μM) was incubated with GDP-loaded KRAS^{G12C} (1 μM) in the presence or absence of CYPA (25 μM) as a control reaction that is not CYPA-dependent. The covalent modification of KRAS^{G12C} was determined by mass spectrometry following a 24-hour incubation (n=3). **(B)** RMC-4998 (4 μM) was incubated with GMPPNP-loaded KRAS^{G12C}, HRAS^{G12C}, NRAS^{G12C}, or KRAS^{G13C} (1 μM) in the presence of CYPA (25 μM). Reactions were quenched at the indicated time point, and the covalent modification of KRAS^{G12C} was determined by mass spectrometry (mean ± SD, n=3). (**C**) HEK293 cells were transfected with HA-tagged KRAS or NRAS and subjected to RMC-4998 treatment (100 nM, 2 h). The cells were lysed and the levels of pERK and ERK were assessed by immunoblotting. The amount of active HA-tagged RAS proteins (HA-GTP) were assessed by pulldown using the RBD of RAF followed by detection of HA tag.

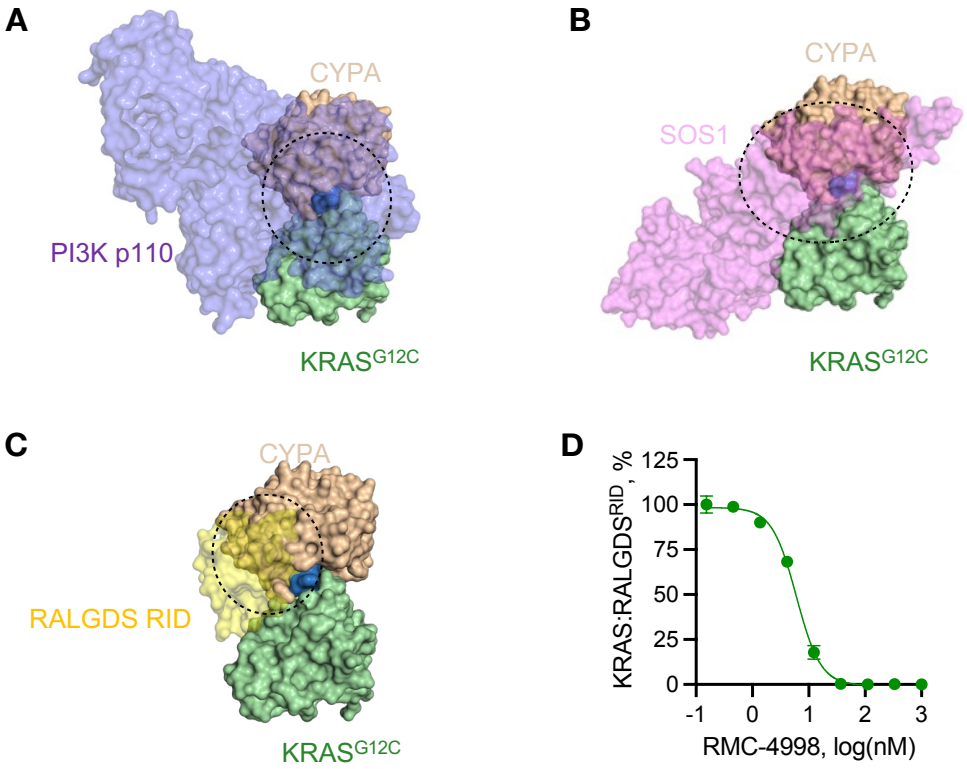

Fig. S5. Tri-complex formation sterically occludes the RAS effector binding interface. Superimposition of the CYPA:RMC-4998:KRAS^{G12C} tri-complex structure with that of (**A**) HRAS:PIK3CD (PDB: 1HE8) *(40),* or (B) KRAS:SOS$^{REM-CDC25}$ (PDB: 1XD2) (*41*), or (**C**) HRAS:RALGDS (PDB: 1LFD, A) (*42*). Note the steric clashes (dashed circle) caused by CYPA occupying the Switch I and II motif of KRAS. (**D**) Disruption of the interaction between KRAS^{G12C} (12.5 nM) and the RID of RALGDS (50 nM) by RMC-4998 in the presence of CYPA (25 μM) was assessed by TR-FRET (mean ± SD, n = 3).

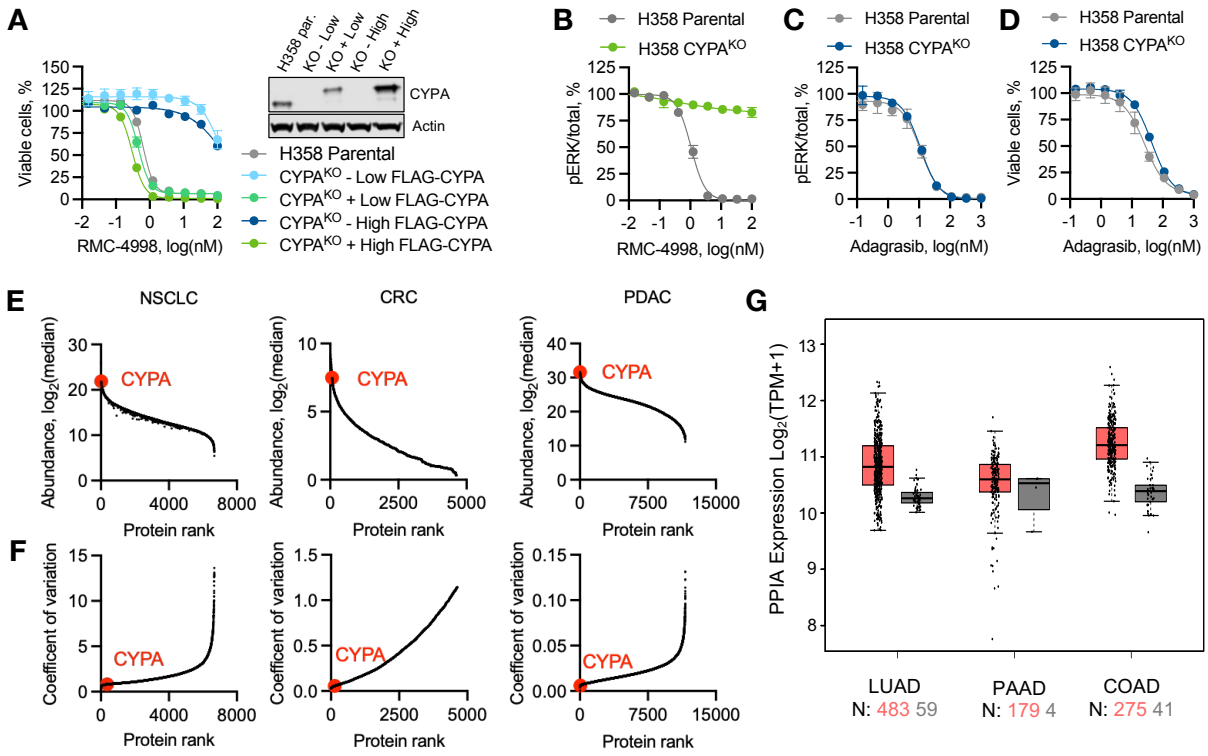

Fig. S6. Tri-complex inhibitors require intact CYPA expression. (**A**) Parental, CYPA knock-out (KO), and low- or high-expressing FLAG-CYPA add-back H358 cells were treated as shown for 120 h to determine the effect on cell viability (mean ± range, n=2, representative of N=2). Inset: The indicated cell extracts were evaluated by immunoblotting to determine the expression of CYPA. Data are representative of N=2. Parental or CYPA knockout cells were treated with (**B**) RMC-4998 or (**C**) adagrasib for 4 hours and the levels of of ERK phosphorylation were measured relative to the untreated condition (mean ± SEM, n=2, N=2-4). (**D**) Parental or CYPA KO cells were treated with adagrasib for 120 h to determine the effect on cell viability (mean ± SEM, n = 2, N=2-5). Clinical proteomic data from the CPTAC consortium were mined to determine the (**E**) relative abundance of CYPA protein expression and (**F**) the coefficient of variation in CYPA protein expression across RAS-mutant cancer histotypes. (**G**) mRNA expression data from the TCGA were used to determine the relative expression of CYPA in tumor (red bars) or normal tissue (grey bars). *(43)*

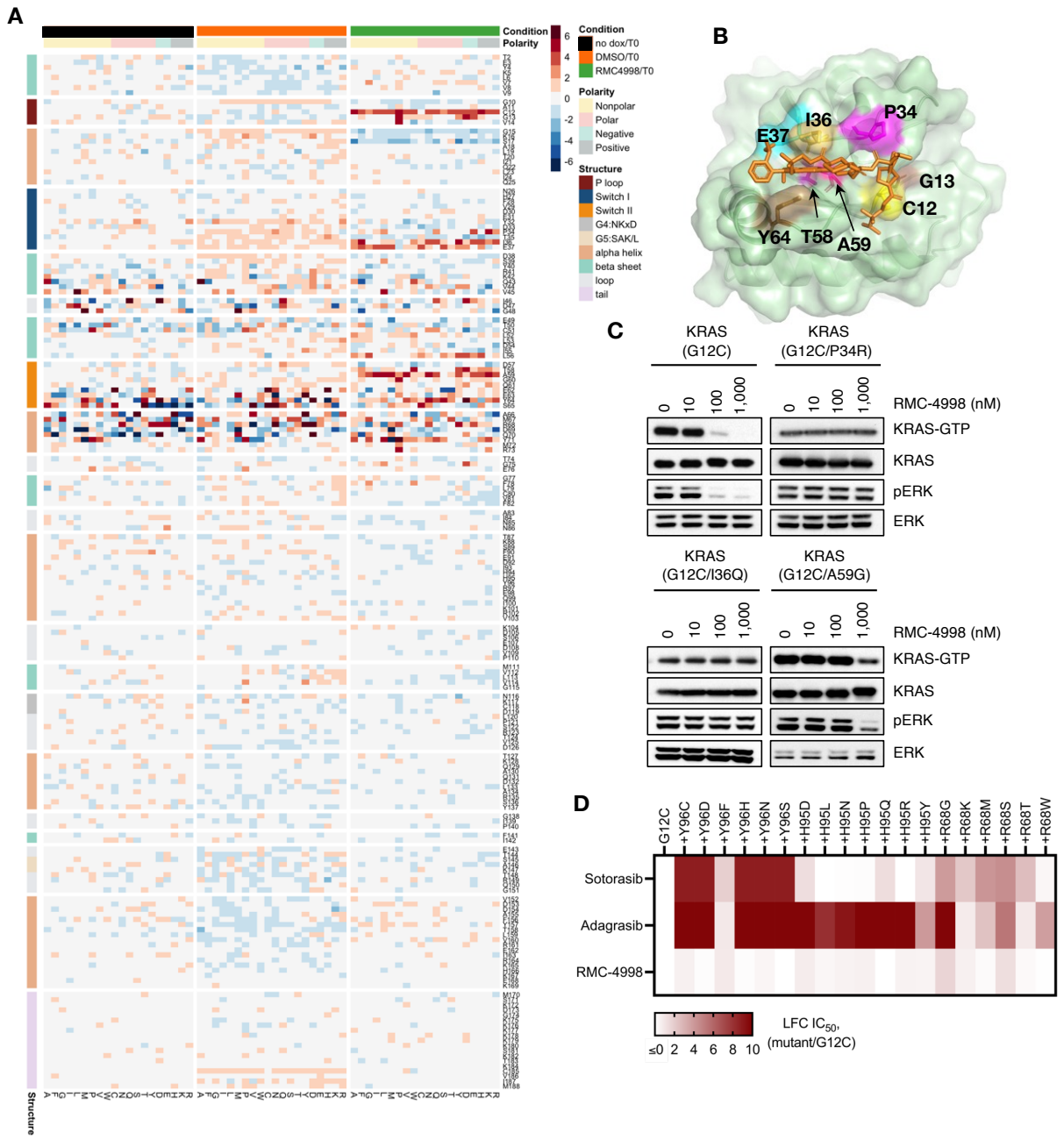

Fig. S7. Saturation mutagenesis screen reveals residues necessary for inhibition. (A) A heat map showing the scaled log fold-change vs. T0 for all variants present in the library (mean, n=3). **(B)** Prominent resistance mutations from A were projected on the tri-complex binding interface. **(C)** NCI-H358 cells were transduced with the indicated mutant KRAS proteins and subjected to RMC-4998 treatment for 2 h before being subjected immunoblotting. **(D)** Independent evaluation using a cellular RAS-RAF disruption assay of all key substitutions at R68, H95 and Y96 amino acids in KRAS, residues that are known to confer clinical resistance to inactive state selective inhibitors such as adagrasib and/or sotorasib. The $\log_2$(fold-change) (LFC) in IC_{50} is represented as a heat map (N=2).

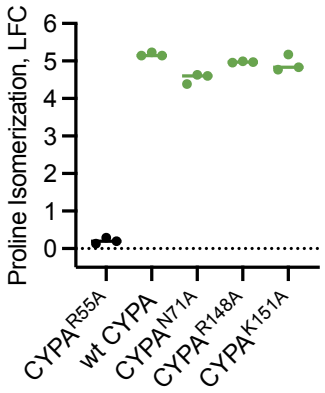

Fig. S8. Peptide proline isomerization of CYPA mutants. The rate constant for isomerization of a Suc-AAPF-pNA substrate was determined for each mutant and plotted as the $\log_2$(fold-change) (LFC) as compared with the spontaneous isomerization rate. $CYPA^{R55A}$ is a known catalytically dead mutant (*44*) that was included as a control (line at mean, n=3).

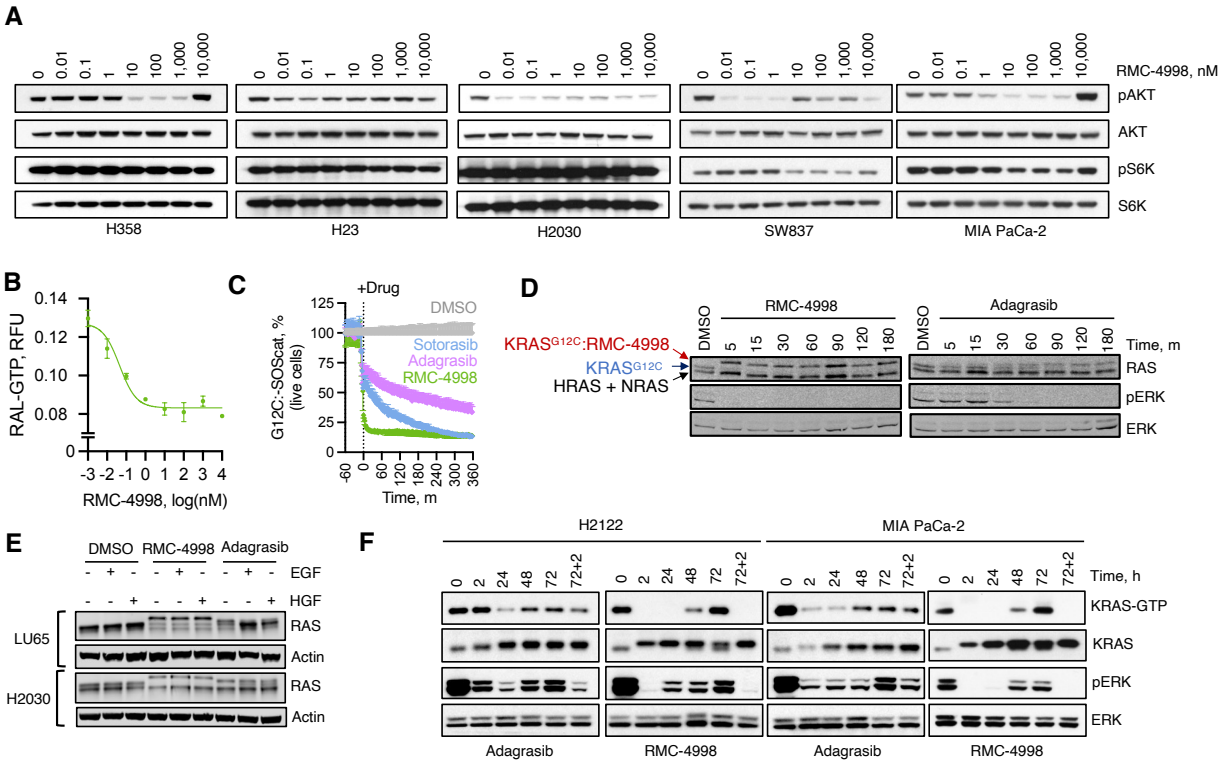

Fig. S9. Signaling Effects of RMC-4998. (A) The indicated cell lines were treated with RMC-4998 for 2 h before being lysed and subjected to immunoblotting to assess effects on AKT/mTOR signaling. **(B)** MIA PaCa-2 cells were treated as shown for 2 h and their extracts were subjected to a RAL activation GLISA assay (mean ± SEM, n=3). **(C)** The effect of RMC-4998 on the interaction between $KRAS^{G12C}$and SOS1 was assessed using a live-cell biosensor (mean ± SEM, n=3). **(D)** Extracts from MIA PaCa-2 cells were treated with RMC-4998 (20 nM) or adagrasib (100 nM) as shown were subjected to immunoblotting to determine the effect on the electrophoretic motility of KRAS or that on ERK phosphorylation. Results are representative of N=3. **(E)** As in D but the cells were treated with the indicated inhibitors for 3 hours with or without concurrent growth factor stimulation (EGF or HGF, 100 ng/mL, added immediately prior to the drug). Results are representative of N=3. **(F)** NCI-H2122 or MIA PaCa-2 cells were treated with 100 nM of adagrasib or RMC-4998 and cell extracts were prepared and subjected to immunoblotting at the indicated time post-treatment. For the 72+2 h treatment, cells were treated with compound for 72 h and the medium was refreshed with fresh compound at 2 h pre-lysis.

A

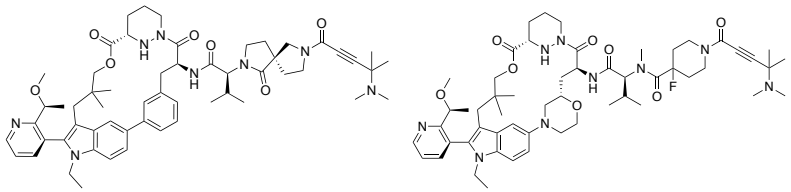

	RMC-4998	RMC-6291
CYPA K_D, μM	1.09 ± 0.38	1.81 ± 0.21
k_{inact}, s^{-1}	1.64E-01 ± 4.81E-02	1.35E-1 ± 4.18E-02
K_I, μM	6.03E-01 ± 4.31E-02	5.04E-1 ± 2.59E-01
k_{inact}/K_I, $M^{-1}s^{-1}$	2.72E+05 ± 8.22E+04	2.99E+05 ± 8.30E+04

B

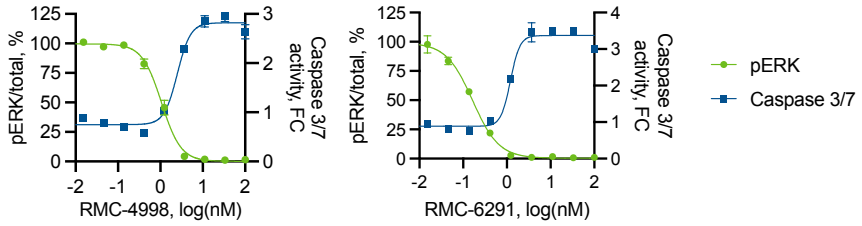

Fig. S10. Comparison of preclinical (RMC-4998) and clinical (RMC-6291) tri-complex inhibitors. (**A**) Chemical structures of the tricomplex inhibitor series along with their CYPA binding affinity and $KRAS^{G12C}$ covalent engagement kinetics (mean ± SEM, n=3). (**B**) H358 cells were treated with either RMC-4998 (left) or RMC-6291 (right) to determine the effect on ERK signaling (pERK/total ERK relative to untreated) and on apoptosis as determined by measuring caspase 3/7 activity (mean ± range, n=2, N=2-3).

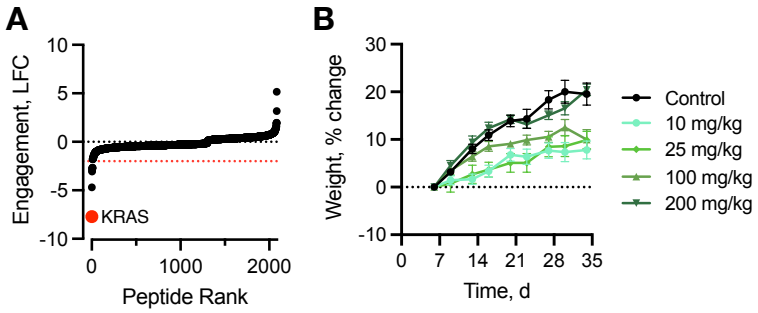

Fig. S11. In vitro selectivity and in vivo tolerability of the clinical tri-complex inhibitor. (**A**) Extracts from H358 cells treated with RMC-6291 (1 μM) were subjected to proteome-wide cysteine reactivity. (**B**) Mice bearing H358 xenografts were treated with RMC-6291, administered orally once a day, to determine the effect on animal weight (mean ± SEM, n=6 for control, n=8 for treatment). LFC: $\log_2$ fold-change

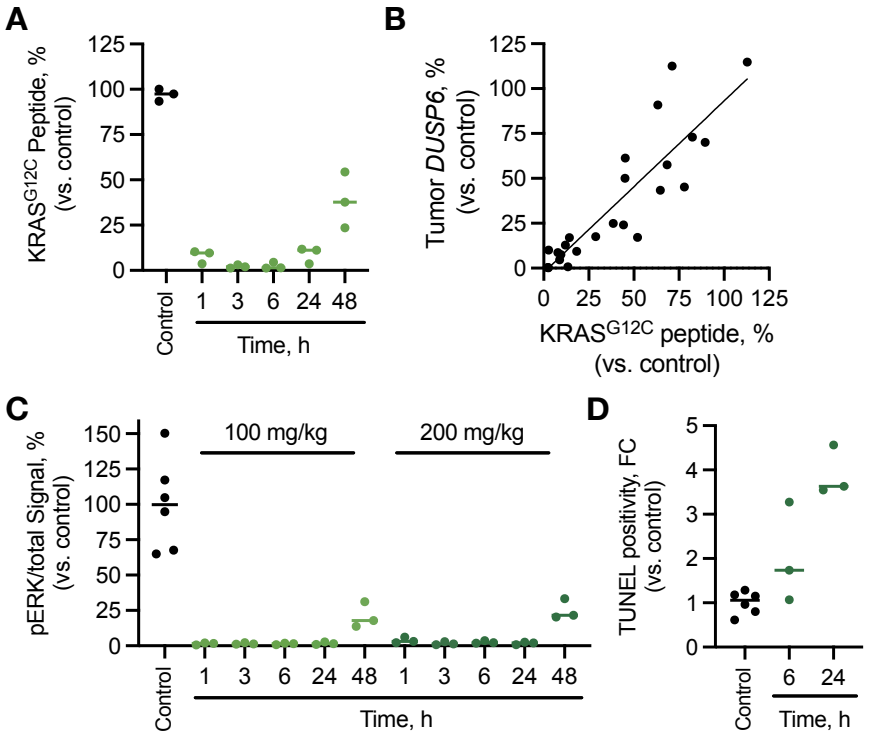

Fig. S12. In vivo pharmacodynamic characteristics of RMC-6291. (**A**) H358 xenograft tumors excised at various times after a single 100 mg/kg dose of RMC-6291 were subjected to LC/MS to determine the covalent modification of $KRAS^{G12C}$. (**B**) The correlation between $KRAS^{G12C}$ covalent engagement and DUSP6 expression (a marker of ERK-dependent transcriptional output). (**C**) As in A, but two different doses were used to determine the effect on pERK by IHC. (**D**) Effect of a single dose of RMC-6291 (200 mg/kg) on the induction of apoptosis in vivo by using TUNEL staining (fold-change in TUNEL-positive cells)

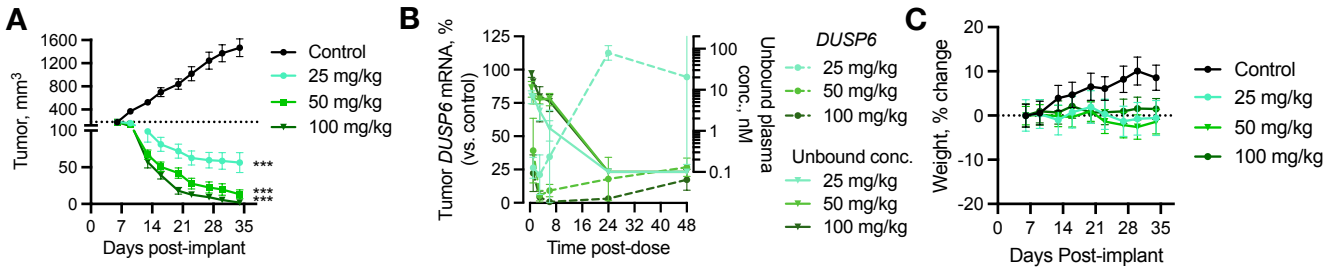

Fig. S13. Antitumor activity of the preclinical tri-complex inhibitor RMC-4998. (**A**) Mice bearing H358 xenograft tumors were treated as shown with RMC-4998, administered orally once a day, to determine the effect on tumor volume. ***adj.p<0.001 for RMC-4998 (all dose groups) vs control, using repeated measures 2-way ANOVA (n=9/group for control, n=10/group for RMC-4998); adjusted p-value (adj.p) based on multiple comparison via Dunnett's test on the final tumor measurement. (**B**) Effect of a single oral dose of RMC-4998 model on the level of *DUSP6* in the H358 xenograft model (mean± SEM, n=3). (**C**) Effect of RMC-4998 treatment on animal weight (mean± SEM, n=9 for control, n=10 for treatment).

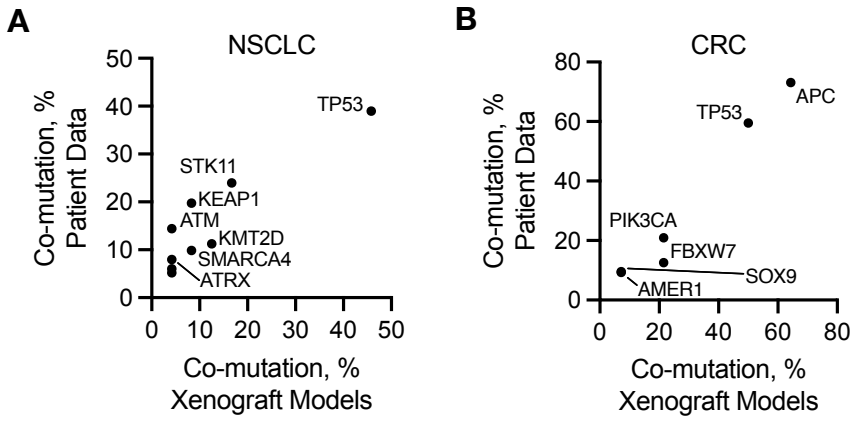

Fig. S14. Baseline alterations in xenograft models and their fidelity to patients with lung or colorectal cancer. Correlation in prevalence of co-occurring mutations observed in patients with $KRAS^{G12C}$ tumors and in cohort of NSCLC (**A**) or CRC (**B**) xenograft models evaluated here. Data are from project GENIE (public release 12.00, June 28, 2021) *(45)*. Only variants described as "oncogenic" or "likely oncogenic" by OncoKB were included *(46)*.

Table S1. Refinement statistics for the tri-complex crystal structures

	$KRAS^{G12C}$:Compound-1:CYPA	**$KRAS^{G12C}$:RMC-4998:CYPA**
PDB entry code	8G9Q	8G9P
Wavelength (Å)	0.97946	1.03317
Resolution range	36.31 - 1.4 (1.45 - 1.4)	43.43 - 1.5 (1.554 - 1.5)
Space group	P 2_1 2_1 2	P 1 2_1 1
Unit Cell		
a, b, c (Å)	67.159, 100.689, 47.776	48.03, 101.76, 66.36
α, β, γ (°)	90, 90, 90	90, 91.04, 90
Total reflections	420894 (38356)	387699 (33787)
Unique reflections	63310 (6055)	94582 (8308)
Multiplicity	6.6 (6.3)	4.1 (4.1)
Completeness (%)	98.0 (95.2)	93.0 (82.4)
Mean I/sigma(I)	9.3 (1.0)	12.6 (3.4)
Wilson B-factor	19	16
R-merge	0.075 (1.026)	0.059 (0.328)
R-meas	0.081 (1.117)	0.068 (0.377)
R-pim	0.031 (0.434)	0.033 (0.183)
CC1/2	0.998 (0.749)	0.998 (0.918)
CC*	1 (0.925)	1 (0.978)
Reflections used in refinement	63256 (6050)	94572 (8305)
Reflections used for R-free	3191 (292)	4754 (408)
R-work	0.186 (0.368)	0.155 (0.181)
R-free	0.214 (0.408)	0.186 (0.229)
CC(work)	0.964 (0.818)	0.970 (0.943)
CC(free)	0.958 (0.769)	0.960 (0.890)
Number of non-hydrogen atoms	3098	6658
macromolecules	2670	5421
ligands	68	212
solvent	360	1025
Protein residues	334	670
RMS (bonds)	0.005	0.009
RMS (angles)	0.76	1.07
Ramachandran favored (%)	96.97	96.53
Ramachandran allowed (%)	3.03	3.47
Ramachandran outliers (%)	0.00	0.00
Rotamer outliers (%)	1.03	1.02
Clashscore	1.49	1.09
Average B-factor	27	20
macromolecules	26	18
RVMD Compounds	18	17
solvent	34	29
Number of TLS groups	2	4

Table S2. Antiproliferative potency of RMC-4998, RMC-6291 and adagrasib

	Cell Line	Cancer type	Mutation	RMC-4998 EC_{50} (nM)	RMC-6291 EC_{50} (nM)	Adagrasib EC_{50} (nM)
KRAS^{G12C}	MIA Paca-2	Pancreas	*KRAS*^{G12C}	0.180	0.0661	0.324
	NCI-H1373	Lung	*KRAS*^{G12C}	0.179	0.0708	8.91
	NCI-H2030	Lung	*KRAS*^{G12C}	0.266	0.123	3.16
	NCI-H2122	Lung	*KRAS*^{G12C}	0.319	0.145	8.71
	SW1463	Intestine/ Colorectum	*KRAS*^{G12C}	0.470	0.219	17.4
	SW1573	Lung	*KRAS*^{G12C}	> 302	> 302	> 302
	UMUC3	Urinary/ Bladder	*KRAS*^{G12C}	0.0618	0.0355	1.23
	Calu1	Lung	*KRAS*^{G12C}	0.263	0.0891	8.13
	NCI-H1792	Lung	*KRAS*^{G12C}	0.141	0.0631	2.63
	NCI-H23	Lung	*KRAS*^{G12C}	0.304	0.178	3.47
	NCI-H358	Lung	*KRAS*^{G12C}	0.278	0.107	1.51
	SW837	Intestine/ Colorectum	*KRAS*^{G12C}	0.293	0.102	3.16
	HCC-44	Lung	*KRAS*^{G12C}	0.230	0.0813	19.1
	IA-LM	Lung	*KRAS*^{G12C}	0.556	0.251	3.98
	KYSE-410	Esophageal	*KRAS*^{G12C}	> 302	> 302	> 302
	LU65	Lung	*KRAS*^{G12C}	0.184	0.0813	5.75
	OV56	Ovarian	*KRAS*^{G12C}	> 302	> 302	> 302
			Median EC_{50}	**0.278**	**0.107**	**5.75**
Non-*KRAS*^{G12C}	HCC827	Lung	*EGFR*$^{E746\_A750del}$	730	1450	2290
	NCI-H1975	Lung	*EGFR*$^{L858R/T790M}$	1600	4370	4900
	AsPC1	Pancreas	*KRAS*^{G12D}	998	2340	1450
	A427	Lung	*KRAS*^{G12D}	217	562	1320
	SW480	Intestine/ Colorectum	*KRAS*^{G12V}	387	813	1230
	A549	Lung	*KRAS*^{G12S}	604	1660	1820
	MeWo	Skin	*NF1*^{LOF}	401	891	2090
	HCT116	Intestine/ Colorectum	*KRAS*^{G13D}	356	603	1860
	NCI-H1299	Lung	*NRAS*^{Q61K}	1600	4370	4900
	COLO205	Intestine/ Colorectum	*BRAF*^{V600E}	393	2880	871
	A375	Skin	*BRAF*^{V600E}	339	912	1290
			Median EC_{50}	**401**	**1450**	**1820**
			Fold selectivity*	**1450**	**13500**	**316**

*Fold selectivity was calculated by (median EC_{50} non-$KRAS^{G12C}$)/(median EC_{50} $KRAS^{G12C}$) and rounded to 3 significant figures

Table S3. Anti-tumor activity in a panel of human $KRAS^{G12C}$ xenograft models

Models	Cancer type	Tumor volume, % change (mean ± sem)[†]
LXFA-592	NSCLC	-99 ± 1; n=3
NCI-H358[*]		-96 ± 1; n=8
CTG-1680		-94 ± 3; n=3
CTG-2539		-89 ± 3; n=3
LUN055		-87 ± 7; n=3
LXFA-983		-84 ± 6; n=3
LXFA-923		-82 ± 8; n=3
CTG-2011		-80 ± 4; n=3
LXFL-1072		-76 ± 7; n=3
CTG-0192		-73 ± 6; n=3
CTG-0828		-71 ± 4; n=3
LXFE-2324		-68 ± 11; n=3
CTG-2210		-68 ± 1; n=3
LXFA-2155		-64 ± 5; n=3
CTG-2579		-63 ± 3; n=3
CTG-2487		-58 ± 4; n=3
CTG-2751		-37 ± 12; n=3
LUN092		-37 ± 5; n=10
NCI-H2030[*]		-23 ± 8; n=3
ST2972		-9 ± 13; n=10
LXFA-1335		2 ± 9; n=3
LXFE-1022		20 ± 18; n=3
CTG-2536		176 ± 46; n=17
NCI-H2122[*]		240 ± 41; n=3
CTG-2026		418 ± 84; n=3
ST1384	CRC	-79 ± 12; n=5
CXF-2163		-75 ± 4; n=3
SW837[*]		-60 ± 6; n=5
CRC024		-33 ± 5; n=8
CTG-0387		-25 ± 13; n=2
ST4859		-12 ± 14; n=5
ST230		-7 ± 7; n=5
STF167		47 ± 20; n=5
CRC022		56 ± 30; n=8
ST3235		59 ± 17; n=5
ST046		63 ± 61; n=3
ST094		102 ± 27; n=5
CTG-1489		113 ± 49; n=3
ST4368		187 ± 68; n=3
ST026		403 ± 159; n=3

[*]Cell line-derived xenograft models. All others are models derived from patients.
[†]Percentage of tumor volume change from baseline was calculated as described in Materials and Methods. RMC-6291 was administered orally daily at 200 mg/kg

Movie S1. Morph of the CYPA surface changes induced by tri-complex formation with RMC-4998 and KRAS^{G12C}. Changes in the surface of the CYPA protein when comparing the apo form (PDB: 3K0N) and the CYPA:RMC-4998:KRAS^{G12C} tri-complex (PDB: 8G9P).

Data S1. Cysteine depletion profiling of H358 cells treated with 1 µM RMC-6291. The list of protein targets with associated abundance fold-changes and statistics in the cysteinome profiling of RMC-6291 (corresponds to fig. S11A).

References

32. W. Kabsch, Xds. *Acta Crystallogr D Biol Crystallogr* **66**, 125-132 (2010).
33. A. J. McCoy *et al.*, Phaser crystallographic software. *J Appl Crystallogr* **40**, 658-674 (2007).
34. F. Long *et al.*, AceDRG: a stereochemical description generator for ligands. *Acta Crystallogr D Struct Biol* **73**, 112-122 (2017).
35. P. Emsley, B. Lohkamp, W. G. Scott, K. Cowtan, Features and development of Coot. *Acta Crystallogr D Biol Crystallogr* **66**, 486-501 (2010).
36. G. N. Murshudov *et al.*, REFMAC5 for the refinement of macromolecular crystal structures. *Acta Crystallogr D Biol Crystallogr* **67**, 355-367 (2011).
37. D. Liebschner *et al.*, Macromolecular structure determination using X-rays, neutrons and electrons: recent developments in Phenix. *Acta Crystallogr D Struct Biol* **75**, 861-877 (2019).
38. J. Dornan *et al.*, Biochemical and structural characterization of a divergent loop cyclophilin from Caenorhabditis elegans. *J Biol Chem* **274**, 34877-34883 (1999).
39. S. Szep, S. Park, E. T. Boder, G. D. Van Duyne, J. G. Saven, Structural coupling between FKBP12 and buried water. *Proteins* **74**, 603-611 (2009).
40. M. E. Pacold *et al.*, Crystal structure and functional analysis of Ras binding to its effector phosphoinositide 3-kinase gamma. *Cell* **103**, 931-943 (2000).
41. H. Sondermann *et al.*, Structural analysis of autoinhibition in the Ras activator Son of sevenless. *Cell* **119**, 393-405 (2004).
42. L. Huang, F. Hofer, G. S. Martin, S. H. Kim, Structural basis for the interaction of Ras with RalGDS. *Nat Struct Biol* **5**, 422-426 (1998).
43. Z. Tang *et al.*, GEPIA: a web server for cancer and normal gene expression profiling and interactive analyses. *Nucleic Acids Res* **45**, W98-W102 (2017).
44. L. D. Zydowsky *et al.*, Active site mutants of human cyclophilin A separate peptidyl-prolyl isomerase activity from cyclosporin A binding and calcineurin inhibition. *Protein Sci* **1**, 1092-1099 (1992).
45. A. P. G. Consortium, AACR Project GENIE: Powering Precision Medicine through an International Consortium. *Cancer Discov* **7**, 818-831 (2017).
46. D. Chakravarty *et al.*, OncoKB: A Precision Oncology Knowledge Base. *JCO Precis Oncol* **2017**, (2017).